

1978

The Self-assembly Of Papaya Mosaic Virus

John Waite Erikson

Follow this and additional works at: <https://ir.lib.uwo.ca/digitizedtheses>

Recommended Citation

Erikson, John Waite, "The Self-assembly Of Papaya Mosaic Virus" (1978). *Digitized Theses*. 2706.
<https://ir.lib.uwo.ca/digitizedtheses/2706>

This Dissertation is brought to you for free and open access by the Digitized Special Collections at Scholarship@Western. It has been accepted for inclusion in Digitized Theses by an authorized administrator of Scholarship@Western. For more information, please contact tadam@uwo.ca, wlsadmin@uwo.ca.

THE SELF-ASSEMBLY
OF
PAPAYA MOSAIC VIRUS

by

John Waite Erickson
Department of Plant Sciences

/

Submitted in partial fulfillment
of the requirements for the degree of
Doctor of Philosophy

Faculty of Graduate Studies
The University of Western Ontario
London, Ontario
June, 1978

© John Waite Erickson 1978

ABSTRACT

Papaya mosaic virus (PMV) is a flexuous, rod-shaped plant virus belonging to the potato virus X group. The in vitro reconstitution of PMV from its isolated coat protein and nucleic acid is described and related to the self-assembly of the coat protein into a variety of polymers, including a nucleic acid-free tube whose surface structure is indistinguishable from that of the native virus. The protein rods are formed within minutes at pH 4.0 at 25°C. In contrast, the virus reconstitutes best with 5% (w/w) RNA to form infectious particles at pH 8.0 at 25°C. NaCl inhibits virus assembly and reconstitution is routinely done in 0.01 M tris. Under reconstitution conditions, PMV coat protein exists in a dynamic equilibrium among several polymorphic species, most notably the 14S and 25S polymers. The equilibrium is sensitive to pH, ionic strength, temperature and protein concentration. Evidence is presented to suggest that PMV assembly is regulated predominantly by entropic forces similar to those which govern the 14S - 25S equilibrium.

PMV is assembled in two energetically and kinetically distinct steps. There is a rapid, temperature-independent initiation phase followed by a slower elongation phase which proceeds best at 25°C. The kinetics of the elongation phase can be satisfactorily described by a second-order

reaction mechanism in which the rate-limiting step is the productive collision of coat protein, in some form, with the growing end of the helix. Particle formation is complete by about 20 min in stoichiometric mixtures (protein:RNA = 20:1). The rate of elongation may be influenced by localized regions on the RNA.

The in vitro assembly of PMV is highly specific, being regulated by a pH-controlled switch. PMV protein reconstitutes specifically with its own RNA or that from at least one other related virus at pH 8.0, but it forms thin, extended particles with RNAs from unrelated viruses under the same conditions. From pH 6.0 - 7.5, the coat protein assembles with either homologous or heterologous RNA to form particles with discontinuities along their length, resulting in a "kinked" appearance. Polyadenylic acid and polycytidylic acid are also recognized by PMV protein at pH 8.0, whereas polyuridylic acid and polyinosinic acid are not. PMV-RNA whose cytosine residues have been chemically transformed into uracil is no longer recognized at pH 8.0. DNA is encapsidated at pH 6.0, but not at pH 8.0.

ACKNOWLEDGEMENTS

I am deeply indebted to Dr. John B. Bancroft, my thesis supervisor, for his effort, time and patience, and for his continued advice and encouragement throughout my research. My association with Dr. Bancroft was a most enriching experience for which I am grateful.

I wish to thank my friends and colleagues Drs. Gary G. Altman and Mounir AbouHaidar for rewarding associations and also for their many critical and stimulating discussions.

I am grateful to Drs. M. A. Lauffer, A. C. H. Durham and W. P. Alford for their helpful discussions on certain aspects of this work.

I thank Drs. W. G. Hopkins, R. B. van Huystee, D. B. Smith, and P. Kaesberg for sacrificing their time in order to serve on my examining committee.

I wish to express my sincere appreciation to Messrs. Reg Johnston and D. Muirhead, for providing excellent technical assistance; to Mr. Ron Smith for his patient direction and aid in the use of the electron microscope; to Mr. Alan Noon, for his expert advice and assistance with the photography; and to Mrs. Sharon Willis, who performed an excellent job in the typing of this manuscript.

I gratefully acknowledge financial support
from a National Research Council grant to Dr. John B. Bancroft.

Finally, I wish to pay a special tribute to my
parents, Russell and Patricia Erickson, for their contin-
ued love, encouragement and support throughout my life.
They are the very finest people and I dedicate this thesis
to them.

TABLE OF CONTENTS

CERTIFICATE OF EXAMINATION	ii
ABSTRACT	iii
ACKNOWLEDGEMENTS	v
TABLE OF CONTENTS	vii
LIST OF TABLES	xi
LIST OF FIGURES	xii
CHAPTER 1: INTRODUCTION	1
1.1 Self-assembly processes in biology	1
1.1.1 Why and how self-assembly processes are studied	1
1.1.2 Driving forces behind self-assembly processes	2
1.2 Self-assembly of plant viruses	3
1.2.1 Structural principles	5
1.2.2 Physical-chemical principles	5
1.3 Assembly studies with rod-shaped plant viruses	8
1.3.1 Environmental parameters	10
1.3.2 Mechanics	12
1.3.3 Specificity	13
1.4 Goals of this research	15
CHAPTER 2: MATERIALS AND METHODS	16
2.1 Virus purification	16
2.2 Preparation of PMV coat protein	17
2.3 Preparation of PMV-RNA	18
2.4 Purification of other viral RNAs	19

2.4.1	Clover Yellow Mosaic Virus (CYMV)	19
2.4.2	Tobacco Mosaic Virus (TMV)	19
2.4.3	Brome Mosaic Virus (BMV)	19
2.5	Other nucleic acids	20
2.6	Cytosine modification of PMV-RNA	20
2.7	Protein assembly	20
2.8	Analytical ultracentrifugation	21
2.9	Molecular weight determinations of the PMV coat protein	21
2.9.1	Polyacrylamide gel electrophoresis	21
2.9.2	Sedimentation equilibrium	23
2.10	Virus reconstitution	24
2.11	Infectivity assays	25
2.12	Turbidimetry	25
2.13	Electron microscopy	26
2.14	Particle length measurements	27
CHAPTER 3: THE PMV COAT PROTEIN SUBUNIT AND ITS POLYMERIZATION INTO HELICAL RODS		29
3.1	Introduction	29
3.2	The protein subunit.....	30
3.3	Environmental requirements for polymerization	31
3.3.1	pH	31
3.3.2	Temperature	35
3.3.3	pH reversibility	40
3.3.4	Control of the extent of polymerization	43

3.3.5	Ionic strength	53
3.3.6	Cation effects	53
2.4	Discussion	58
CHAPTER 4: THE SELF-ASSEMBLY OF PMV FROM ITS COAT PROTEIN AND RNA		64
4.1	Introduction	64
4.2	Experimental results	64
4.2.1	The effect of pH	64
4.2.2	The effect of temperature	77
4.2.3	The effect of protein concentration..	95
4.2.4	The effect of NaCl	101
4.2.5	Stoichiometry	115
4.3	Discussion	115
CHAPTER 5: KINETICS OF PMV ASSEMBLY		129
5.1	Introduction	129
5.2	Experimental results	129
5.2.1	Assembly kinetics in stoichiometric (20:1) conditions	129
5.2.2	Low temperature assembly	137
5.2.3	Assembly kinetics in protein excess (80:1)	138
5.3	Kinetic model of assembly: theoretical analysis	146
5.3.1	Correcting for the time-dependent distribution of growing ends	149
5.3.2	Kinetic parameters for elongation ...	150
5.4	Discussion	154

CHAPTER 6: SPECIFICITY OF PMV ASSEMBLY	159
6.1 Introduction	159
6.2 Experimental results	159
6.2.1 Assembly with plant virus RNAs	159
6.2.2 Assembly with DNA	165
6.2.3 Assembly with synthetic poly- ribonucleotides	166
6.2.4 Assembly with chemically modified PMV-RNA	170
6.3 Discussion	170
 CHAPTER 7: THE FORMATION OF 25S COAT PROTEIN IS ENTROPY-DRIVEN	 178
7.1 Introduction	178
7.2 Theoretical analysis	179
7.3 Discussion	182
 APPENDIX	 190
 REFERENCES	 199
 VITA	 211

LIST OF TABLES

Table	Description	Page
1	Sedimentation coefficients of PMV protein at different concentrations and temperatures	87
2	Some properties of non-specific and specific assembly reactions with PMV protein	174
3	Apparent percentages of polymorphic forms of PMV protein at different concentrations and temperatures at pH 8	181
4	Calculated K_{app} values for the 14S - 25S equilibrium of PMV protein at various temperatures and concentrations at pH 8	183
5	Thermodynamic parameters for the 14S - 25S equilibrium of PMV protein	186

LIST OF FIGURES

Figure	Description	Page
1	Schlieren diagrams of papaya mosaic virus protein after various treatments	34
2	Electron micrographs and diffraction patterns of papaya mosaic virus protein and virus	37
3	Schlieren patterns of PMV protein polymerized under various conditions	39
4	Schlieren patterns of PMV protein polymerized for various incubation periods at pH 4.0	42
5	pH reversal of rod formation	45
6	Scheme used in the rod elongation experiments	47
7	Effect of addition of cold 14S protein to protein rods	50
8	Effect of addition of warm 14S protein to protein rods	52
9	Effect of NaCl concentration on PMV protein polymerization	55

10	Cation effects on protein rod formation	57
11	The effect of pH level on the reconstit- ution of PMV	66
12	Electron micrographs of nucleoprotein assembled at pH 6.0 and pH 8.0	69
13	Sedimentation of PMV assembled at pH 6.0 and pH 8.0	71
14	Schlieren patterns of PMV protein at 3 mg/ml at various pH levels	73
15	Kinetics of 14S - 25S interconversion in response to pH	76
16	The effect of temperature on the re- constitution of PMV	79
17	Arrhenius plot of the effect of temper- ature on the relative rate, k, of elonga- tion for PMV assembly at pH 8.0 in 0.01 <u>M</u> tris	81
18	Electron micrographs of PMV assembly products obtained from 1 mg/ml protein and 0.05 mg/ml RNA at pH 8.0 (0.01 <u>M</u> tris) after various temperature treat- ments	83

19	The effects of temperature and concentration on the 14S - 25S equilibrium of PMV protein at pH 8.0	86
20	Effect of temperature on the turbidity of PMV protein	90
21	Extent of formation of the 25S aggregate of PMV protein as a function of temperature	92
22	Kinetics of the 14S - 25S interconversion in response to temperature	94
23	Fractionation of PMV protein by sedimentation in sucrose	97
24	The effect of protein concentration on the assembly of PMV at 25°C	100
25	Effect of NaCl concentration on the assembly of PMV as measured by infectivity	103
26	Electron micrographs showing the effects of NaCl on PMV assembly	105
27	The effect of NaCl on assembly	107
28	The effect of NaCl concentration on the 14S - 25S equilibrium of PMV protein at pH 8.0	110

29	Effect of NaCl concentration on the turbidity of PMV protein at pH 8.0	112
30	Kinetics of NaCl-induced disassembly of 25S protein at pH 8.0	114
31	Effect of protein:RNA ratio on PMV at pH 8.0	117
32	Kinetics of PMV assembly as measured by infectivity and turbidity	132
33	Histograms of particle length distri- butions for PMV assembly products after various times	134
34	Number and weight average rod lengths measured during the course of the PMV self-assembly reaction	136
35	Histograms of particle length distri- butions for PMV assembly products after various times	140
36	Histograms of particle length distri- butions for PMV assembly products after various times	143
37	Number and weight average rod lengths measured during the course of the 80:1 PMV assembly reaction	145

38	Interpretation of the data for the 20:1 and 80:1 experiments according to equation (9)	153
39	Specificity of the assembly reaction of PMV protein with various plant virus RNAs as a function of pH: sedimentation analysis	161
40	Specificity of the assembly reaction of PMV protein with various plant virus RNAs as a function of pH: particle morphology	163
41	Electron micrograph of salmon-sperm DNA reacted with PMV protein at pH 6.0	167
42	Electron micrographs of polynucleo- tides reacted with PMV protein at pH 6.0 and pH 8.0	169
43	Electron micrographs of C → U trans- formed PMV-RNA reacted with PMV pro- tein at pH 6.0 and pH 8.0	172
44	Dependence of K_{app} on temperature for the equilibrium $2\ 14S \rightleftharpoons 25S$	185

LIST OF ABBREVIATIONS

BMV	brome (grass) mosaic virus
BSMV	barley stripe mosaic virus
C	strain designation for tobacco rattle virus
CAM	strain designation for tobacco rattle virus
CYMV	clover yellow mosaic virus
DNA	deoxyribonucleic acid
EDTA	ethylene diamine tetracetic acid
MES	2-(N-morpholino) ethane sulfonate
poly A	polyadenylic acid
poly C	polycytidylic acid
poly I	polyinosinic acid
poly U	polyuridylic acid
PMV	papaya mosaic virus
PVX	potato virus X
PVY	potato virus Y
RNA	ribonucleic acid
S	Svedberg unit (10^{-13} sec)
SDS	sodium dodecyl sulfate
TMV	tobacco mosaic virus
TRV	tobacco rattle virus

The author of this thesis has granted The University of Western Ontario a non-exclusive license to reproduce and distribute copies of this thesis to users of Western Libraries. Copyright remains with the author.

Electronic theses and dissertations available in The University of Western Ontario's institutional repository (Scholarship@Western) are solely for the purpose of private study and research. They may not be copied or reproduced, except as permitted by copyright laws, without written authority of the copyright owner. Any commercial use or publication is strictly prohibited.

The original copyright license attesting to these terms and signed by the author of this thesis may be found in the original print version of the thesis, held by Western Libraries.

The thesis approval page signed by the examining committee may also be found in the original print version of the thesis held in Western Libraries.

Please contact Western Libraries for further information:

E-mail: libadmin@uwo.ca

Telephone: (519) 661-2111 Ext. 84796

Web site: <http://www.lib.uwo.ca/>

CHAPTER 1
INTRODUCTION

1.1 Self-assembly processes in biology

1.1.1 Why and how self-assembly processes are studied

Studies of self-assembling systems of macromolecules are important to our understanding of how biological structures at a sub-cellular level are constructed and maintained. Enzyme complexes, microtubules and microfilaments, flagella and pili, chromosomes, ribosomes, membranes and cell walls, to name a few, are all examples of such systems. Kushner (1969) has presented a general review of self-assembly processes.

The factors which govern self-assembly are most easily studied in vitro. The basic operations required are as follows: the biological structure is isolated; it is dissociated into its components, which are in turn separated from each other; and the components are re-mixed in such a way as to produce the original biological structure with functional integrity restored. This last step is the most difficult to achieve and often reflects the dissociation procedure.

Assuming the isolated components are functionally competent to participate in a self-assembly reaction, the elucidation of the environmental conditions required for

proper assembly to occur is critical. Indeed, the definition of such conditions usually reveals the nature of the physical forces which regulate the self-assembly process.

1.1.2 Driving forces behind self-assembly processes

The ability of macromolecules to self-assemble depends on the net free energy change which the overall system incurs upon assembly; this change must be negative for a spontaneous self-assembly reaction to take place. The overall system includes not only the self-assembling macromolecules, but also all other molecular species in the immediate surroundings, including buffer and salt constituents, and although often neglected, the solvent (usually water). The free energy change of the system is given by

$$\Delta G = \Delta H - T\Delta S \quad (1).$$

Equation (1) simply states that the free energy change of the system is the difference between the enthalpy (H) and entropy (S) changes which the system incurs during the self-assembly reaction.

The enthalpy (or heat content) component of the free energy of biochemical reactions is generally attributed to changes in interaction energies between components. These changes are usually manifested in terms of alterations in numbers and types of chemical bonds which characterize the system under study. For self-assembly processes, these are usually non-covalent. The entropy component, on

the other hand, is concerned with changes in the relative "randomness" of the system. These are caused by differences in the way in which the system components are ordered, or put together. For self-assembly processes, "ordering" is usually brought about via changes in the degree of surface exposure of macromolecules with the solvent. Lauffer (1975), in his treatise on the importance of entropy as a driving force for many biological self-assembly reactions, pointed to water (i.e. solvent molecules) as an important regulatory factor in assembly reactions. Macromolecules must release much of their "bound" water upon self-association. The resulting change in the proportion of $\frac{\text{bound}}{\text{free}}$ water can often result in large entropy gains.

Environmental variables which can affect the thermodynamic components of the system free energy would be expected to exert considerable control over the self-assembly reaction itself. Typical environmental factors which should have in vivo relevance for biological self-assembly reactions are pH, ionic strength, ionic composition, temperature, and the concentrations, both absolute and relative, of the assembly components. By studying the effects of changing the environmental variables upon a self-assembly process, the physical-chemical driving forces for the process may be revealed.

1.2 Self-assembly of plant viruses

Viruses occupy a special position among self-

assembly systems. Firstly, many of the basic rules of biological self-assembly were elucidated through the study of viruses. Secondly, unlike other sub-cellular systems, viruses are able to utilize the principles of self-assembly for the purpose of replication at the expense of their hosts.

The capsids of most bacterial and animal viruses consist of several different species of proteins. Most of these function as structural components of the capsid; in the case of the more complex viruses, some of these proteins may give rise to viral organelles such as attachment fibers, or they may possess certain enzymatic functions required by the virus for successful infection of the host. Additionally, many animal viruses are surrounded by a membranous structure, much of which may be derived from the host. Assembly studies concerning the complex bacterial and animal viruses have been reviewed recently by Casjens and King (1975).

Most simple plant viruses are constructed from identical protein subunits and a single piece of single-stranded ribonucleic acid (RNA). Because of their simplicity they are ideally suited structures for the study of basic principles governing virus self-assembly in particular, and protein-protein and protein-nucleic acid interactions in general.

1.2.1 Structural principles

The geometrical principles for the assembly of viruses were advanced by Caspar and Klug (1962). Energetically, the most stable structures that can be built from identical building blocks are those in which each building block has an equivalent environment. Spheres and regular helices, or tubes, (excepting the ends) best satisfy this requirement. Caspar and Klug supposed that these same principles extend to virus assembly. However, since the fundamental building block in the virus capsid, the protein subunit, is highly asymmetric, they postulated the principle of quasi-equivalence of inter-subunit bonds for all viruses containing certain restricted numbers of identical subunits greater than 60. The utility of this principle has been demonstrated many times for the construction of simple viruses; indeed, the principle of quasi-equivalence can even be seen in the construction of the more complex virus capsids, such as the T-bacteriophage heads, and has architectural advantages as well.

1.2.2 Physical-chemical principles

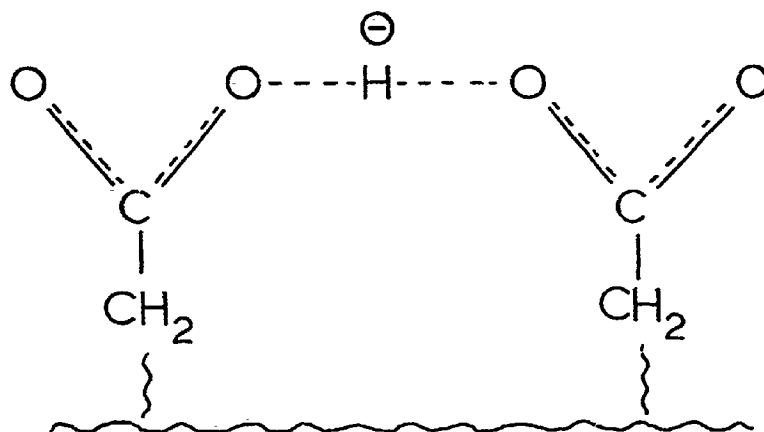
The physical-chemical principles which govern virus assembly are more difficult to grasp precisely; this is partly due to the fact that different viruses assemble by energetically different pathways, and partly because our understanding of the physical chemistry of macromolecular

interactions is limited. This limitation is perhaps most acutely revealed by our inability to define precisely the causes of the effects of simple salt solutions upon virus association and dissociation (for review, see Kaper, 1975). Such complications notwithstanding, the simple plant viruses are exceedingly useful subjects for the study of the physical chemistry of virus assembly.

The first virus to be functionally self-assembled, or reconstituted, in vitro was tobacco mosaic virus (TMV) (Fraenkel-Conrat and Williams, 1955). TMV is a rigid, rod-shaped virus and consists of a helical assembly of identical protein subunits within which a single-stranded molecule of RNA is helically wound. TMV is the only virus whose physical chemistry is well-defined, largely due to the efforts of Lauffer and co-workers (for review, see Lauffer, 1975). Many basic theoretical concepts for TMV assembly were prophesied by Caspar (1963) far in advance of experimental verification. For the most recent review of TMV assembly, Butler and Durham (1977) should be consulted.

A particularly interesting feature of TMV assembly, from a physical principles standpoint, is that the TMV coat protein spontaneously forms helical rods which are indistinguishable in external structure to the native virus (Franklin, 1955). This suggested that protein-protein interactions are particularly important in TMV, and provided an experimental system for focusing separately on

this issue. The environmental conditions for the assembly of the coat protein helix and the virus helix are different, most significantly with regard to pH. The virus assembles at pH 7.0 - 7.5, whereas the protein helix will form only at an acidic pH. The formation of protein helices and reconstituted virus, however, both result in the appearance of at least two anomalously titrating carboxyl residues in the protein with pK's near 7. This discovery led Caspar (1963) to hypothesize that in both these structures carboxyl residues are brought into such proximity that they are forced to form carboxyl-carboxylate hydrogen bonds of the form



This situation results in one of the residues having an abnormally high pK. Only in the presence of nucleic acid can the protein form a helix at elevated pH. This hypothetical control mechanism has been substantiated recently with the elucidation of the atomic structure of TMV at 4.0 Å resolution (Stubbs *et al.*, 1977).

The self-assembly of simple plant viruses with

spherical, or icosahedral, symmetry was accomplished by Bancroft and co-workers for the bromoviruses (for review, see Bancroft, 1970). The coat proteins of these viruses also form nucleic acid-free capsids spontaneously, and again do so at pH levels lower than those required for optimal reconstitution of these viruses. This fact, coupled with the discovery that these native viruses "swell" hydrodynamically at high pH, led Bancroft et al. (1967) to postulate a role for carboxyl-carboxylate pairs in controlling the assembly of the bromoviruses.

It appears, then, that the existence of some sort of negative switch is required for the proper regulation of virus assembly when protein-protein interactions supply a predominate share of the driving force. Ionizable amino acid residues, being sensitive to small changes in pH, are ideally suited to serve as the components of such a switch.

1.3 Assembly studies with rod-shaped plant viruses

Rod-shaped viruses fall into two main structural categories, rigid and flexuous. Papaya mosaic virus (PMV), the virus used in this thesis, falls into the latter category. In this section, some important aspects of the assembly of the rod-shaped plant viruses and their proteins are summarized.

The spontaneous assembly of an infectious virus from its isolated coat protein and nucleic acid was first demonstrated over 20 years ago for TMV by Fraenkel-Conrat and Williams (1955). Since that time relatively few rod-shaped viruses have been successfully reconstituted, namely one other rigid rod virus, tobacco rattle virus (TRV) (Morris and Semancik, 1973; AbouHaidar et al., 1973), and a flexuous rod virus, potato virus X (PVX) (Goodman et al., 1976). Barley stripe mosaic virus (BSMV) (Atabekov et al., 1970) and potato virus Y (PVY) (McDonald and Bancroft, 1977) can be assembled to form virus-like rods which are uninfective.

The ability of TMV protein to polymerize spontaneously into nucleic acid-free rods having the same structure as the virus has been known for over 30 years (Schramm, 1947; Franklin, 1955). Other coat proteins from rigid rod viruses have shown a tendency to polymerize to form virus-like capsids, notably TRV protein (Morris and Semancik, 1973; Fritsch et al., 1973b) and BSMV protein (Atabekov et al., 1968). Despite attempts, none of the flexuous rod virus coat proteins, except for the PMV protein (Erickson et al., 1976), have been assembled into capsids with a viral geometry. Rod-shaped structures with anomalous geometries, however, have been observed in preparations of PVY protein (McDonald et al., 1976) and, occasionally, with PVX protein (Kaftanova et al., 1975; Goodman et al., 1976), indicating that proteins from flexuous viruses also tend to aggregate to form rods.

Out of these studies, as well as others concerned with different classes of viruses (see Casjens and King (1975) for review), several important questions have arisen. One concerns the relationship between the types of interactions (protein-protein) which predominate in the polymerization of coat protein into virus-like structures with those (protein-protein and protein-nucleic acid) which serve to stabilize the functional virus particle. Another question deals with the specificities of these interactions, especially with respect to virus assembly. A third related problem concerns the mechanics and controls involved in the assembly processes.

1.3.1 Environmental parameters

Definition of the optimal conditions for virus reconstitution and for coat protein polymerization is important in establishing the predominant types of interactions. TMV is reconstituted from purified RNA and coat protein most efficiently near neutrality (pH 7.25) in 0.1 M phosphate buffer at 30°C (Fraenkel-Conrat and Williams, 1955). BSMV also reconstitutes near pH 7 and at 30°C, but at lower ionic strength (0.01 M Tris-HCl buffer) (Atabekov et al., 1970). PVX reconstitutes best under slightly acidic conditions (pH 6.0 - 6.2) at 20°C and 0.01 M buffer (Goodman et al., 1975). Two strains of TRV have been reconstituted: the C strain assembles best at pH 7.5 - 8.0 in 0.25 M

glycine (Morris and Semancik, 1973) whereas the CAM strain prefers acidic conditions (pH 4.7) in 0.5 M phosphate buffer (Abou Haidar et al., 1973). Curiously, both strains require low temperature (1 - 4°C) for optimal reconstitution. The in vivo significance of this is unclear. Thus, while TRV reconstitution in vitro is apparently exothermic, the other rod-shaped viruses all appear to assemble by entropy-driven mechanisms since they all require heat.

Polymerization of coat protein into rod-shaped virus-like structures occurs under conditions which differ from those in which virus assembly occurs optimally. TMV coat protein polymerization is favored by moderate temperature (30°C) and ionic strength (0.1 M phosphate buffer) similar to TMV reconstitution conditions; however, as mentioned earlier, it requires an acidic environment, pH 6.5 or below (see Lauffer and Stevens, 1968). BSMV coat protein polymerizes into long rods only after prolonged storage at low temperature and alkaline pH, and it has a peculiar requirement for a divalent metal cation such as Ca^{2+} (Atabekov et al., 1968). Polymerization of TRV coat protein from the C strain is favored by high temperature (in contrast to TRV reconstitution), alkaline pH and low ionic strength (0.01 M phosphate buffer) (Morris and Semancik, 1973). The formation of stacked-disc rods from PVY coat protein takes place from pH 6.0 - 9.0 in 0.01 - 0.10 M

phosphate buffer at 0 - 4°C (McDonald et al., 1976). It is clear that the environmental requirements of virus reconstitution and coat protein polymerization vary widely from virus to virus. It can be assumed that the predominant types of interactions involved in these processes also vary.

1.3.2 Mechanics

The mechanics of the assembly processes which the coat proteins of rod-shaped plant viruses undergo appear to share some general features. Coat protein polymerization and virus reconstitution for TMV (Durham et al., 1971; Butler and Klug, 1971), TRV (Morris and Semancik, 1973), BSMV (Atabekov et al., 1968) and PVY (J. G. McDonald, personal communication) seem to require, at some stage of assembly, disc-like polymers of protein. While the number and arrangement of subunits in these discs, the functional state of aggregation of discs (single vs. double discs, for example), and the conditions favoring disc formation vary from one virus to another, it seems clear that discs are required at least for the initiation of virus assembly, and possibly for the initiation of protein polymerization as well. The current model for the initiation of TMV assembly employs a double layer lock-washer arrangement of protein subunits which envelops a special recognition sequence of over 100 nucleotides in TMV-RNA (see Butler and Durham, 1977).

1.3.3 Specificity

The specificity of the protein-protein and protein-nucleic acid interactions involved in virus assembly is a subject of major importance. That such specificity exists in vivo is strongly implied by the homogeneity of RNA extracted from purified virus particles and the lack of pseudovirions. Viral assembly inside the cell might be grossly inefficient were such specificities not exerted. The proper packaging of viral nucleic acid might be aided by intracellular compartmentalization, resulting in enhanced accessibility of viral RNA to its coat protein.

Studies of BSMV and PVX reconstitutions have shown that the coat proteins of these viruses do not prefer homologous over heterologous RNAs under the conditions used (Atabekov et al., 1970, 1972). The coat proteins of the spherical bromoviruses also assemble into virus-like particles in the presence of a variety of nucleic acids (RNA and DNA), as well as with several polyanions (see Bancroft, 1970). On the other hand, the relative specificity of TMV protein for its own RNA has been documented many times (see Atabekov et al., (1972) for a recent review). In the few instances where foreign nucleating agents (such as poly A) have been encapsidated, the efficiency was low. Since it is not unreasonable to expect that specificity should occur, the argument has been made that TMV is the only

properly reconstituted plant virus.

There is another consideration to be made concerning the recognition of nucleic acid by coat protein. Such proteins are designed by nature to associate with nucleic acid and, since the entire nucleotide sequence of a viral RNA clearly cannot contain site-specific recognition characteristics, it is not too surprising that in vitro specificity is difficult to demonstrate. TMV reconstitution is known to initiate on a special sequence of nucleotides, about 1000 nucleotides in from the 3'-end of the TMV-RNA molecule, with the double-disc aggregate of TMV protein (Zimmern, 1976). The formation of double-discs is critically dependent upon pH, ionic strength and temperature. Once initiation is complete, the elongation phase of TMV rod formation can be mediated by less highly ordered forms of TMV protein (Okada, 1975). The above evidence suggests that specificity of coat protein-RNA recognition is exerted, in terms of functional significance, at the level of initiation, in which highly ordered protein structures are required; whereas, elongation is a less stringent, and therefore probably a less specific, process. This might serve to explain the lack of specificity found in the reconstitution experiment; for those viruses whose protein sub-assembly intermediates have not been well-defined.

In summary, while the self-assembly processes of viruses and their coat proteins may share certain general

features, the details of the processes may vary with individual viruses. As in so many other instances of virology, different viruses appear to attain the same end differently. A result of this variability is that we are provided with an immense diversity of macromolecular interactions, the continued study of which should lead to the development of fundamental rules relating these interactions to the structure and function of viruses and other complex biological structures.

1.4 Goals of this research

PMV is a flexuous, rod-shaped virus (Purcifull and Hiebert, 1971) and belongs to the PVX family (Harrison et al., 1971). It is obtainable in high yields, is easily purified and assayed, and can be disassembled by standard methods. Further, its protein assumes a variety of polymeric structures. PMV is ideal for the detailed study of the self-assembly processes of a flexuous virus and its coat protein.

The goals of this research are the following:

- to characterize the polymerization of PMV coat protein;
- to characterize the reconstitution of PMV from its RNA and protein;
- to characterize the specificity of the protein-nucleic acid interactions involved in the self-assembly of PMV.

CHAPTER 2
MATERIALS AND METHODS

2.1 Virus purification

PMV was grown in and purified from Carica papaya L. Upper leaves from greenhouse-grown papaya trees, infected for several months to years, were harvested in 100g lots and either homogenized directly or stored at -20°C prior to use. Tissue was homogenized at 4°C with 2 vol (w/v) of 0.05 M sodium phosphate buffer, pH 8.0, containing 0.01 M ethylene diamine tetraacetic acid (EDTA). In some purifications, a 10% aqueous solution of Triton X-100 (Baker Chemicals) was blended in gradually (over about 1 minute) with the homogenized tissue to yield a final concentration of 1%. If Triton was used, several drops of a 1:1 mixture of butanol-chloroform were added at the start of the blending to prevent excessive foaming. For clarification, 1/2 vol (w/v) of a 1:1 butanol-chloroform mixture was added to the blender. The emulsion was separated by centrifugation in a GSA rotor (Sorvall) at 10,000 rpm for 10 min. The virus-containing upper aqueous phase was decanted and centrifuged in an SS-34 rotor (Sorvall) at 17,000 rpm for 30 min. The supernatant fluid was overlaid onto 7 ml of a 30% (w/v) sucrose solution containing 5×10^{-3} M EDTA, pH 8.0 and was then centrifuged in a Beckman 30 rotor at 27,000 rpm for 3 1/2 hr. The pellets

were suspended to about 10 mg/ml in 5×10^{-3} M Tris, pH 8.0, and several crystals of sodium azide were added as preservative. PMV prepared in this manner was usually free of plant pigments, had an A_{260}/A_{280} ratio of about 1.4 and sedimented as a single species in the analytical centrifuge. If further cycles of differential centrifugation were required, PMV suspensions were first diluted to 1 - 2 mg/ml. Yields without Triton were about 1.5 to 2 mg/g fresh weight tissue and with Triton 2 to 2.5 mg/g tissue. PMV concentrations were estimated taking $E_{260 \text{ nm}}^{0.1\%} = 2.85$ (Hiebert, 1970). Protein from fresh virus prepared as described usually gave a single band migrating at the rate of coat protein (MW ca. 22,000) in dodecyl sulfate polyacrylamide gels.

2.2 Preparation of PMV coat protein

PMV coat protein was prepared by acetic acid degradation (Fraenkel-Conrat, 1957). Two vol of glacial acetic acid were added to concentrated virus on ice. Insoluble RNA was removed after 1 hour by centrifugation in an SS-34 rotor (Sorvall) at 10,000 rpm for 30 min. The supernatant liquid was dialyzed overnight against 20 vol of distilled water to a final concentration of about 3% acetic acid and then centrifuged at 27,000 rpm for 5 hr in a Beckman 30 rotor to remove any residual virus. The supernatant solution was then dialyzed for 48 hr against several changes of

distilled water to remove the acetic acid completely. The protein solution was then titrated slowly with 0.1 N NaOH to pH 9.5 to be certain that helices, which form during the long-term dialysis as the solution pH goes through pH 4.0, are disassembled. The resulting preparations were devoid of virus-like particles as judged by electron microscopy and had typical protein spectra with $A_{280 \text{ nm}}/A_{250 \text{ nm}}$ between 2.0 and 2.5. Protein concentrations were estimated assuming $E_{280 \text{ nm}}^{0.1\%} = 1.0$.

In some early protein polymerization experiments, PMV protein was dialyzed for 48 hr against several changes of 0.01 M glycine, pH 3.0, or 0.01 M Tris-HCl buffer, pH 8.0.

2.3 Preparation of PMV-RNA

PMV-RNA was prepared by the guanidine hydrochloride method (Reichmann and Stace-Smith, 1959). One vol of 5 M guanidine HCl containing 1×10^{-3} M EDTA, pH 8.0, was added to concentrated virus in ice. The RNA precipitate was collected by centrifugation at 5,000 rpm for 1 min and was then dissolved in sterilized, distilled water. Several water washings were usually required for quantitative recovery (about 5 mg RNA/100 mg virus). Successive washings were pooled and the RNA was precipitated with 2 vol of cold 95% ethanol to which a drop of 5 M NaCl was added to aid precipitation. PMV-RNA preparations gave typical nucleic acid spectra with $A_{260 \text{ nm}}/A_{280 \text{ nm}}$ ratios of 2.0 and purified

PMV-RNA migrated as a single band (MW ca. 2.2×10^6) in SDS acrylamide gels. RNA concentrations were estimated assuming $E_{260 \text{ nm}}^{0.1\%} = 25.0$.

2.4 Purification of other viral RNAs

2.4.1 Clover Yellow Mosaic Virus (CYMV) RNA

CYMV was grown in Pisum sativum L. var Little Marvel and was purified as for PMV except that butanol-chloroform was not used and Triton X-100 was always added to 0.5% (v/v) to the supernatant liquid obtained after the first low speed centrifugation. CYMV-RNA was extracted as for PMV-RNA.

2.4.2 Tobacco Mosaic Virus (TMV) RNA

TMV was grown in Nicotiana tabacum L. var Burley, clarified with butanol-chloroform and purified by differential ultracentrifugation according to standard procedures. TMV-RNA was obtained by phenol extraction.

2.4.3 Brome Mosaic Virus (BMV) RNA

BMV was grown in Hordeum vulgare L. var Herta, clarified at pH 4.8 and purified by differential ultracentrifugation according to standard procedures. BMV-RNA was obtained by phenol extraction.

All the above viral RNAs were assumed to have an $E_{260 \text{ nm}}^{0.1\%} = 25.0$.

2.5 Other nucleic acids

Salmon-sperm DNA was obtained from Sigma and an $E_{260 \text{ nm}}^{0.1\%} = 22.0$ was used. The polynucleotides were all A grade obtained from Calbiochem. Extinctions of $E_{257 \text{ nm}}^{0.1\%} = 29.6$, $E_{269 \text{ nm}}^{0.1\%} = 20.6$, $E_{260 \text{ nm}}^{0.1\%} = 29.5$ and $E_{246 \text{ nm}}^{0.1\%} = 30.9$ were used for poly A, poly C, poly U and poly I, respectively.

2.6 Cytosine modification of PMV-RNA

PMV-RNA at 5 - 6 mg/ml in water was treated with 2 M sodium sulfite, pH 5.8, for 24 hr at 25°C (Hayatsu et al., 1970). Under these conditions, cytosine is changed to 5,6-dihydrouracil sulfonate which is converted into uracil by dialysis against 0.01 M borate buffer, pH 8.5 after 24 hr at 5°C. Transformed RNA was precipitated by 2 vol of ethanol before use. The reaction converted 50 to 75% of PMV-RNA cytosine into uracil as measured by paper chromatography.

2.7 Protein assembly

The protein assembly experiments reported in Chapter 3 employed starting protein at pH 3.0 (0.01 M glycine-HCl buffer) or pH 8.0 (0.01 M Tris-HCl buffer) (see also section 2.3, this chapter). Assembly experiments

were performed by adjusting the ionic conditions by 48 hour dialysis at 4°C prior to analysis. Assembly products were assayed by electron microscopy and by analytical ultracentrifugation, as described below.

2.8 Analytical ultracentrifugation

A Beckman Model E analytical ultracentrifuge equipped with Schlieren optics was employed to analyze the polymorphism of PMV coat protein under a variety of experimental conditions. Sedimentation coefficients are reported in Svedberg units S after correction to water at 20°C. At low protein concentrations S values were sometimes determined using UV absorption optics. In this case, scans of the cell image were taken at 280 nm and the radial positions r_i of the inflection points (mid-points of the sedimenting boundary) of the concentration distributions were estimated graphically. A plot of the $\log r_i$ vs time directly yields S .

2.9 Molecular weight determinations of the PMV coat protein

2.9.1 Polyacrylamide gel electrophoresis

Molecular weight determination of the PMV coat protein subunit was performed essentially according to the method of Weber and Osborne (1969). Purified virus, protein and protein standards were dissolved in dissociation medium,

0.1 M phosphate buffer, pH 7.0, containing 1% 2-mercaptoethanol (2-ME) and 1% sodium dodecyl sulfate (SDS), at 200-300 ug/ml and were dissociated by heating for one minute in a boiling water bath. The densities of the samples were increased for layering by the addition of 1 - 2 drops of sterile glycerol. Usually about 25 ul of sample was layered per gel. Gels were 7.5% acrylamide (monomer:bis ratio = 37.1) and contained the same buffer-SDS composition as the running buffer: 0.1 M phosphate buffer, pH 7.0, 0.1% SDS. Gels were typically run at 8 mA/gel for 3 1/2 hrs (5 hrs at 5 mA/gel gave indistinguishable results). 5 ul of 0.05% bromophenol blue, diluted 1:1 in dissociation medium, was added to each gel along with the sample. At the end of electrophoresis gels were removed and scanned with a Joyce-Loebl UV densitometer, and the peak positions of the protein bands relative to that of the marker dye were used to calculate relative mobilities. Alternatively, gels were sliced at the position of the marker band, stained in 0.25% Coomassie Brilliant Blue R (methanol:distilled water:acetic acid = 227:227:46), destained (methanol:water:acetic acid = 50:875:75), and the positions of the stained protein bands relative to the total gel length (after slicing) were used to calculate relative mobilities. The results from both procedures were indistinguishable.

Cytochrome c (13,400 daltons), cowpea chlorotic mottle virus coat protein (19,600 daltons) and aldolase (37,500 daltons) were employed as protein standards. The relative mobilities of the standards were plotted vs log molecular weight and, using a linear least-squares routine to derive the slope and intercept for the empirical plot, the molecular weight of the PMV protein subunit was estimated from its relative mobility.

2.9.2 Sedimentation equilibrium

Molecular weight determinations of the PMV coat protein subunit were performed by sedimentation equilibrium using a Model E ultracentrifuge equipped with split-beam UV absorption scanning capabilities. Standard procedures for centrifugation and data handling were employed (Chervenka, 1969). Sedimentation was performed in a model An-F rotor equipped with double sector cells. $0.04 A_{280}$ units/ml of PMV protein in $0.01 M$ glycine-HCl buffer, pH 3.0, was centrifuged in one-half of a double sector cell at 15,220 rpm, $15^{\circ}C$, for 48 hrs, by which time a stable concentration distribution had formed. The other half of the cell contained an equal volume of $0.01 M$ glycine-HCl buffer and this provided an internal correction for any absorbance due to the buffer system.

Once a stable distribution had formed a UV scan of the cell image was taken at 280 nm and was used to

determine the radial dependency of protein concentration. Molecular weight values were calculated from the equation

$$M = \frac{2RT}{(1-\bar{v}\rho)\omega^2} \cdot \frac{d \ln c}{dr^2}$$

where M = molecular weight

R = gas constant (8.313×10^7 ergs/deg mole)

T = absolute temperature (deg Kelvin)

\bar{v} = partial specific volume (ml/gm)

ρ = solution density (gm/ml)

ω = angular velocity (radians/sec)

c = concentration (A_{280} units)

r = distance from the axis of rotation (cm)

The \bar{v} of PMV protein was calculated from its amino acid composition to be 0.727 ml/gm.

2.10 Virus reconstitution

All solutions employed for reconstitution studies were prepared with sterile, de-ionized, glass-distilled H₂O. PMV-RNA, stored in ethanol at -20°C, was collected by centrifugation at 1,500 g for 5 min in a clinical centrifuge and was dissolved in water and adjusted to 1 mg/ml. PMV coat protein, stored in water at 4°C, was diluted to the appropriate concentration in water and equilibrated at the desired temperature in a water bath. The pH of the reaction was pre-adjusted by addition, to the protein in water, of the appropriate 1.0 M buffer to a final concentration of 0.01 M and reconstitution was initiated immediately thereafter by addition of a small aliquot of RNA to the

buffered protein solution. Protein and RNA concentrations of 1 mg/ml and 0.05 mg/ml, respectively, in 1 ml of 0.01 M Tris, pH 8.0 and 25°C were usually used. For the reconstitutions in NaCl, the zero time salt adjustments were made just prior to the pH adjustments by addition, to the protein in water, of the appropriate volume of 2.0 M NaCl. Reconstitution reactions were usually stopped after 30 min by the addition of 4 M NaCl to a final concentration of 0.2 M prior to assay.

For the kinetics experiments reconstitution reactions were stopped by the addition, at the desired times, of NaCl to a final concentration of 0.2 M.

2.11 Infectivity assays

The infectivities of reconstitution mixtures, incubated after the NaCl treatment with 1 unit ribonuclease T₁ (Calbiochem) per 50 µg RNA for 30 min at 37°C, were assayed on Gomphrena globosa L., a local lesion host for PMV (Purcifull and Hiebert, 1971). The assays were arranged so that 8 - 10 half-leaf comparisons were made for each treatment against a suitable control. Infectivities are expressed as percent of control infectivity.

2.12 Turbidimetry

A Pye Unicam SP 1800 recording spectrophotometer was employed to measure turbidity at 310 nm. For kinetic studies, solution additions to the cuvettes were made in the dark. Cuvette temperatures were controlled by means

of a variable temperature, circulating water bath connected to a water-jacketed cuvette block. For the temperature-jump kinetics, the sample temperature was measured indirectly by a thermistor placed in a cuvette immediately adjacent to the sample.

The appropriate blanks are indicated in the figure legends. For the reconstitution kinetics, the blank was always a solution of protein, NaCl and Tris-HCl buffer, all at the same final concentrations as contained in the sample. PMV-RNA, at the low concentration employed (50 $\mu\text{g/ml}$), has no measurable turbidity at 310 nm.

2.13 Electron microscopy

Reconstitution mixtures were examined for morphology in the electron microscope both before and after the addition of salt. Samples treated with NaCl were diluted as required and pipetted onto carbon-coated Formvar grids and stained with 1% uranyl acetate. Untreated samples were pipetted directly, without dilution, onto grids and stained. The products of protein assembly were examined in a similar manner but without prior salt addition or dilution.

2.14 Particle length measurements

Nucleoprotein particles, formed after various assembly times, were stained with 1% uranyl acetate on copper grids covered with a support film of carbon-coated Formvar. These were examined in a Phillips 200 electron microscope for areas with suitable particle density and staining quality. Several times throughout the course of photographing at a given magnification setting, micrographs of a copper diffraction grating, employed as an external standard, were taken for calibration. Negatives were projected, using a microfilm reader, onto plain white paper and the particle images were traced. The lengths were measured individually using either a ruler, for straight particles, or a map measuring device, for curved ones. It was found that a magnification factor of approximately 1 mm/5 nm was suitable for drawing and measuring particles from the size range observed (about 20 - 560 nm). The total magnification factor was determined by measuring the projected negative image of the diffraction grating.

Particle lengths were converted from mm into nm using the total magnification factor, and particle length distributions for each time point were constructed with the aid of a PDP10 computer and a Calcomp plotter. Particles were grouped into 14 length classes, each of which spanned 40 nm. Number (N) and weight (W) average particle lengths

were calculated according to the formulae

$$N = \frac{\sum n_i l_i}{\sum n_i} \quad \text{and} \quad W = \frac{\sum n_i l_i^2}{\sum n_i l_i}$$

where n_i represents the number of particles that fall into the i^{th} length class and l_i is the median length for the i^{th} length class. The total numbers of particles measured for each experiment are reported in the legends to the histogram figures.

CHAPTER 3

THE PMV COAT PROTEIN SUBUNIT AND ITS POLYMERIZATION INTO HELICAL RODS

3.1 Introduction

The coat protein from TMV can self-assemble to form virus-like helical rods (see Chapter 1). Under certain conditions, however, aberrant stacked-disc structures can also be formed (Franklin and Commoner, 1955; Durham et al., 1971). Helical and stacked-disc rods are also made by the coat protein of barley stripe mosaic virus (Atabekov et al., 1968). Tobacco rattle virus protein has been shown to form short helical aggregates of double discs as well as more complex rod-shaped structures, but long helices and stacked-discs have never been observed (Morris and Semancik, 1973; Fritsch et al., 1973b).

In contrast to the rigid rod viruses, the coat proteins from flexuous viruses have so far been assembled only into the stacked-disc form of a rod (see Chapter 1) and, in the case of narcissus mosaic virus protein, two-start helices (Robinson et al., 1975).

The results in this chapter show that the coat protein from PMV will self-assemble into virus-like helices in the absence of RNA. Some properties of these particles were examined and some environmental parameters were established. A preliminary report has been published

(Erickson et al., 1976).

3.2 The protein subunit

Estimates of the molecular weight of the PMV coat protein subunit were obtained by electrophoretic and hydrodynamic methods. PMV coat protein, either purified or freshly dissociated in SDS, migrated as a single species in 7.5% acrylamide gels containing 0.1% SDS. The average molecular weight of the protein was around 22,000 daltons. Coat protein degradation products with molecular weights of 13,000 - 14,000 and 15,000 - 16,000 daltons were observed with old or bacterially contaminated virus and protein preparations.

Independent molecular weight estimates for the protein subunit were also obtained by sedimentation equilibrium. The aggregation of PMV protein into a variety of polymers is concentration dependent, so that a monodisperse aqueous solution of monomers can only be obtained with dilute protein (0.1 mg/ml) at moderate ionic strength (0.1 M NaCl) or with moderate concentrations of protein (0.5 mg/ml) combined with extremes of pH (pH 3.0 or pH 10.0) and low ionic strength (0.01 M salt). At 0.4 mg/ml in 0.01 M glycine-HCl buffer, pH 3.0, a molecular weight of $21,600 \pm 3,000$ daltons was obtained for the PMV protein subunit. At 0.1 mg/ml in 0.01 M MES buffer, pH 6.0, containing 0.1 M NaCl a molecular weight of $20,300 \pm 3,000$ daltons was obtained.

The values for the molecular weight of the PMV coat protein subunit obtained by these different methods are in good agreement with each other, and also agree closely with the value of 22,500 daltons determined from the amino acid composition of the subunit (Bancroft and Rees, unpublished data).

At 0.3 mg/ml in 0.01 M glycine-HCl buffer, pH 3.0, the PMV protein subunit sediments at 1.9S in the analytical ultracentrifuge as determined by UV absorption.

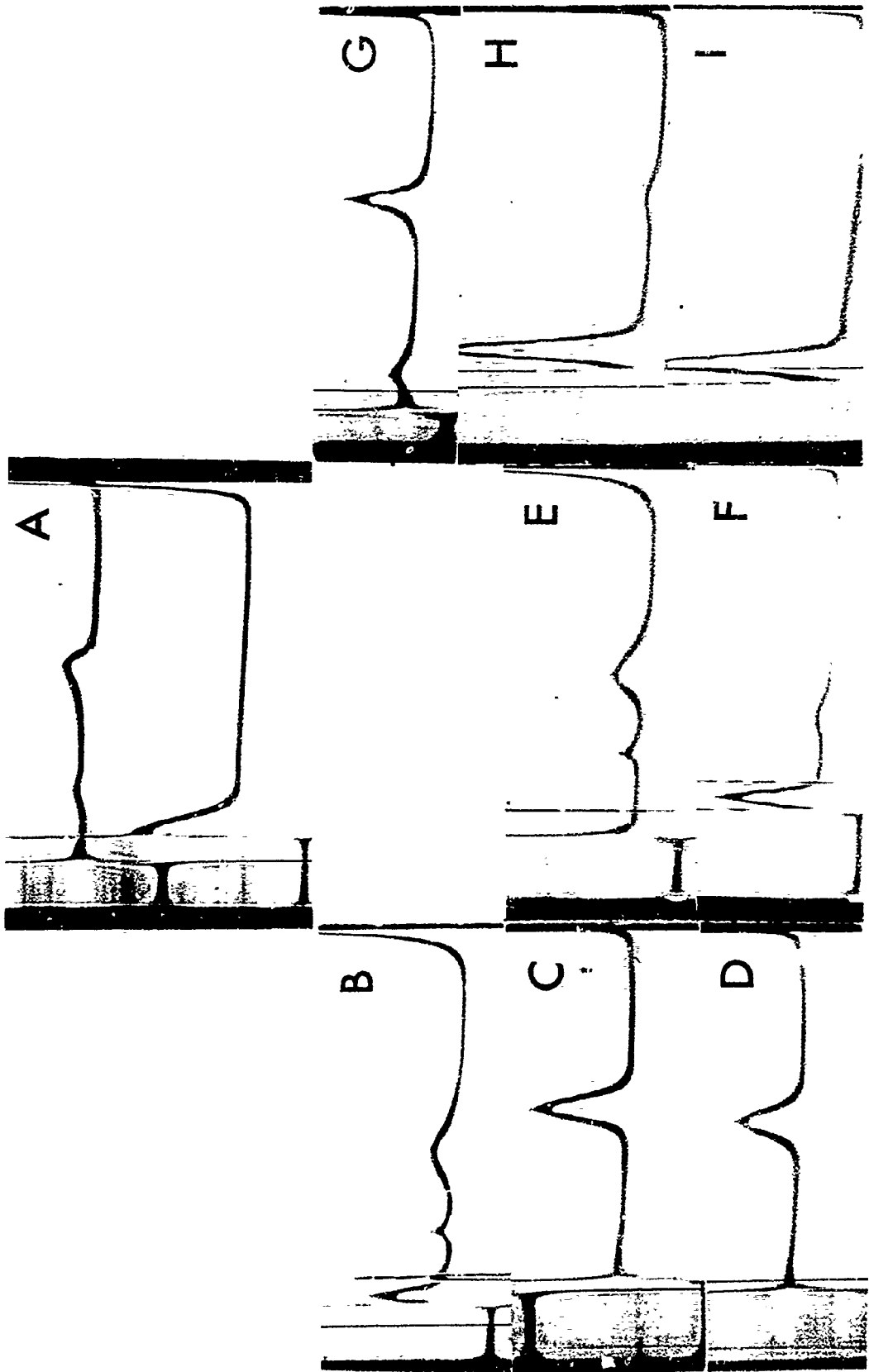
3.3 Environmental requirements for polymerization

3.3.1 pH

The effect of pH on the state of aggregation of PMV coat protein at 20°C was studied by analytical ultracentrifugation. Preliminary assembly experiments were performed by adjusting ionic conditions by 48 hour dialysis at 4°C prior to examination at 20°C. To allow for unforeseen hysteresis effects, the starting protein was either at pH 3.0 (0.01 M glycine-HCl buffer) or pH 8.0 (0.01 M tris buffer). A single species sedimenting at 2.7S probably corresponding to a dimer was found at pH 3.0 whereas the pH 8.0 material contained what appeared to be a series of small aggregates sedimenting between 14 and 33S (Fig. 1A). Closer inspection showed that the pH 8.0 pattern was consistent with the sedimentation pattern expected for two species, one sedimenting at around 14S and the other at about 25S

(see Chapter 4). Both types of starting preparation gave the same products upon further treatment. At pH 4.0 (0.01 M citrate buffer), polymers sedimenting at 14, 100 - 120 and 230 - 250S were formed (Fig. 1B). Such preparations were birefringent and contained very long particles (Fig. 2A). At pH 5.0 (0.01 M acetate buffer) and 6.0 (0.01 M 2-(N-morpholino) ethanesulfonate (MES)), the only product made was the 14S species (Fig. 1C, 1D). This may correspond to a double ring of subunits (see Discussion). A marked hysteresis effect was observed since protein initially assembled at pH 4.0 contained material which sedimented at 113 and 236S after dialysis to pH 5.0 (Fig. 1E). This material was dissociated upon further dialysis to pH 6.0 (Fig. 1F). If the assembly experiments were performed in 0.2 M NaCl, the same general pattern of results as found at the lower ionic strength were obtained in that large numbers of sinuous particles were found only at pH 4.0. However, these were not as long as observed in the absence of NaCl, the sedimentation coefficient being 73S (Fig. 1G) and the particles being clearly shorter as seen in the electron microscope. At pH 5.0 and 6.0, the principal species sedimented at 14S (Fig. 1H, I), a small amount of faster sedimenting material (101S) sometimes being found. The polymorphism of PMV coat protein at neutral and alkaline pH levels will be described in detail in the section on virus assembly (Chapter 4).

Fig. 1. Schlieren diagrams of papaya mosaic virus protein after various treatments. (A) Upper: 14 and 33S products in 0.01 M tris buffer, pH 8.0, after 13 min at 52,640 rpm; lower: 2.7S species in 0.01 M glycine-HCl buffer, pH 3.0. (B) 14, 117 and 248S products in 0.01 M citrate buffer, pH 4.0, after 5 min at 29,500 rpm. (C) 14S product in 0.01 M acetate buffer, pH 5.0, after 31 min at 52,640 rpm. (D) 14S product in 0.01 M MES, pH 6.0, after 31 min at 52,640 rpm. (E) 113 and 236S products after dialysis of (B) versus 0.01 M acetate buffer, pH 5.0, after 5 min at 29,500 rpm. Note the difference between (C) and (E). (F) 14 and 106S products after dialysis of (E) versus 0.01 M MES pH 6.0, after 6 min at 29,500. (G) 14 and 73S products in 0.01 M citrate buffer, pH 4.0, 0.2 M NaCl after 25 min at 29,500 rpm. Note the difference between (B) and (G). (H) 14 and 101S products in 0.01 M acetate buffer, pH 5.0, 0.2 M NaCl after 12 min at 29,500 rpm. The 101S product has not been observed under the same centrifugal conditions in the absence of NaCl. (I) 14S product in 0.01 M MES, pH 6.0, 0.2 M NaCl after 12 min at 29,500 rpm. Protein concentration was about 2 mg/ml at various bar angles. Sedimentation is to the right.



The structure of the particles made at pH 4.0 was resolved by optical diffraction. Electron micrographs for fine structure analysis were made of samples prepared by the method of Horne et al. (1974; 1975). Polymerized protein and native virus are shown in Fig. 2B and C and the corresponding optical diffraction patterns in Fig. 2D and E. Both types of particles have a helical configuration with a pitch of about 3.6 nm and a diameter of about 13.0 nm. Subsequent analyses have shown that the helix in both the virus and the protein rods repeats in four turns.

3.3.2 Temperature

In the polymerization experiments described above, the dialyses were done at 4°C whereas the sedimentation analyses were carried out at 20°C. To determine whether the temperature increase had an effect on the assembly of protein into 14S polymers as well as helices, low molecular weight (3S) protein was dialyzed in the cold to pH 4.0 and pH 6.0 in the presence of 0.2 M NaCl and analyzed in the ultracentrifuge at low temperature. At pH 6.0 a major species sedimenting at 14S was found along with lower molecular weight protein (Fig. 3A, upper). At pH 4.0, only the 14S polymer was observed at 6.4°C in contrast to the results at 20°C (Fig. 3A, lower). Thus the formation of protein helices and, to a lesser extent, 14S polymers

Fig. 2. Electron micrographs and diffraction patterns of papaya mosaic virus protein and virus. (A) Photograph of material from Fig. 1 (B) (X54,000). (B) High resolution photograph (X200,000) of the same material compared with (C) virus (X130,000). (D) and (E) diffraction patterns of (B) and (C), respectively. The near meridional reflections correspond to a helical pitch of 3.6 nm and the equatorial ones to a center-to-center spacing of 13.0 nm.

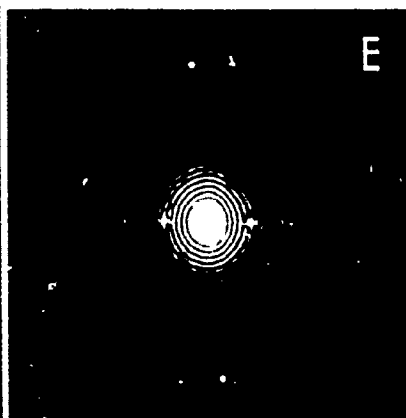
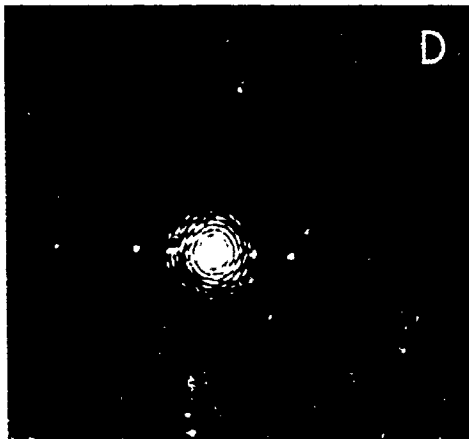
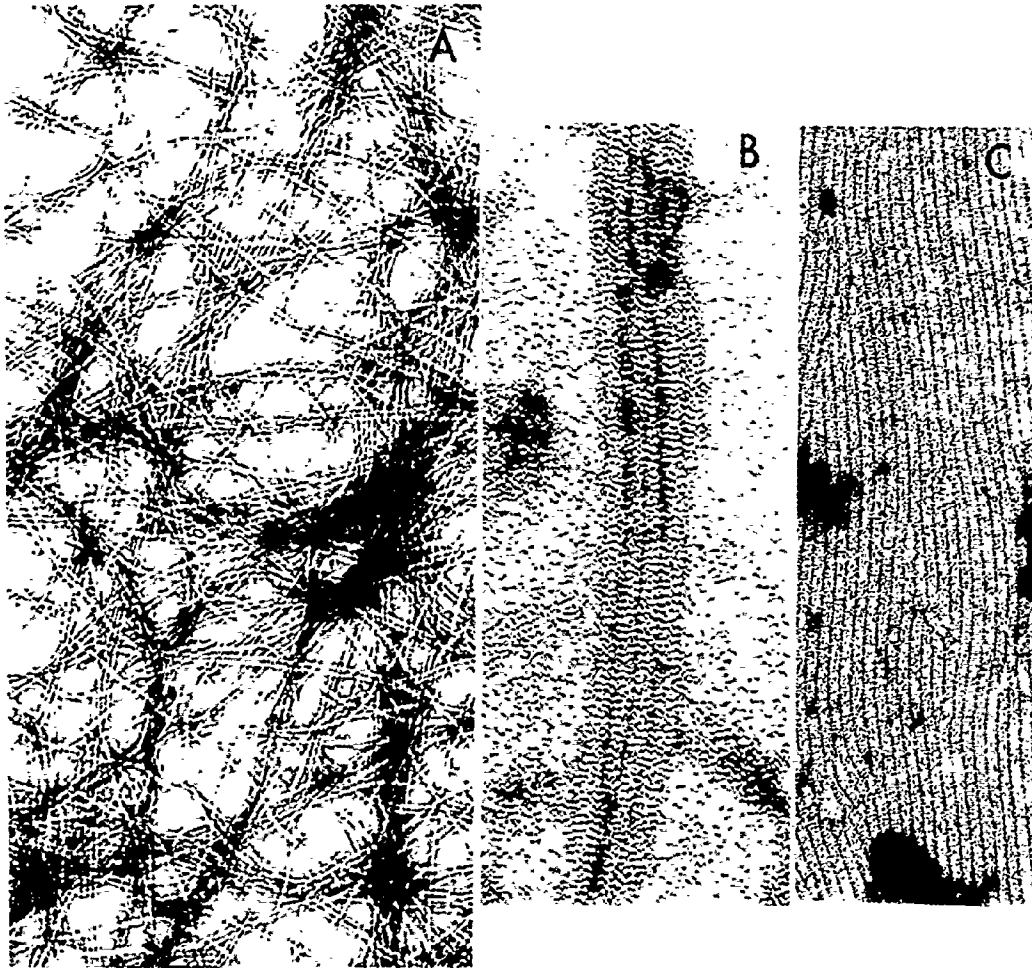
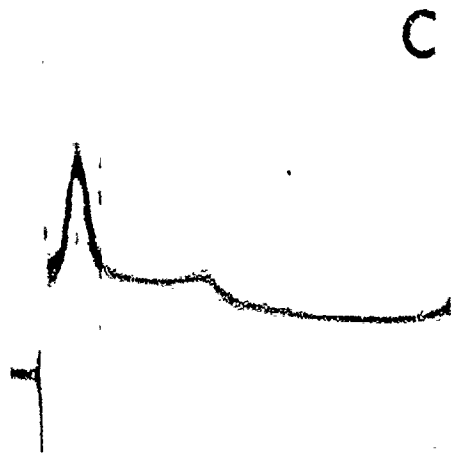
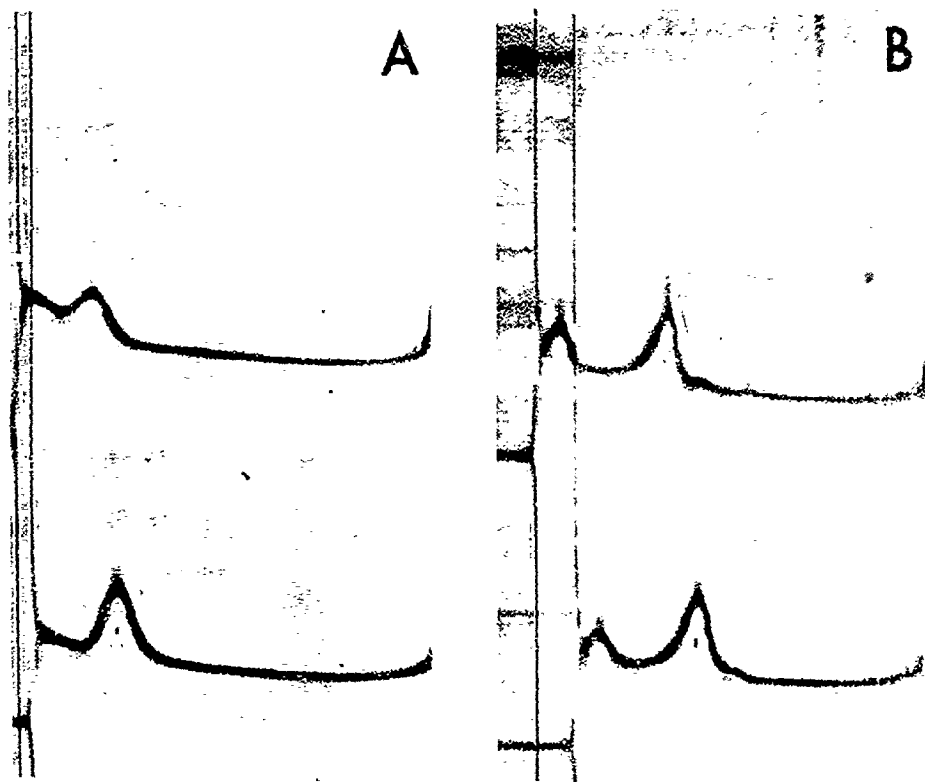


Fig. 3. Schlieren patterns of PMV protein polymerized under various conditions. (A) Protein at 2 mg/ml was dialyzed at 5°C for 24 hr in 0.2 M NaCl at pH 6.0 (0.01 M MES) (14S and slower sedimenting material, upper) or in 0.2 M NaCl at pH 4.0 (0.01 M citrate buffer (14S, lower). Run conditions: 6.4°C, 35,600 rpm, photograph taken at 19 min. (B) Protein at 1.5 mg/ml was dialyzed at 5°C for 24 hr: upper, 14 and 72S polymers in 0.2 M NaCl at pH 3.5 (0.01 M citrate buffer); lower, 14 and 68S polymers in 0.5 M NaCl at pH 4.0 (0.01 M citrate buffer). Run conditions: 5.5°C, 35,600 rpm, photograph taken at 12 min. (C) Protein at 2 mg/ml was dialyzed at 5°C for 24 hr in 0.2 M NaCl at pH 4.5 (0.01 M citrate buffer) (14 and 56S polymers). Run conditions: 20.5°C, 35,600 rpm, photograph taken at 12 min. Sedimentation is to the right.



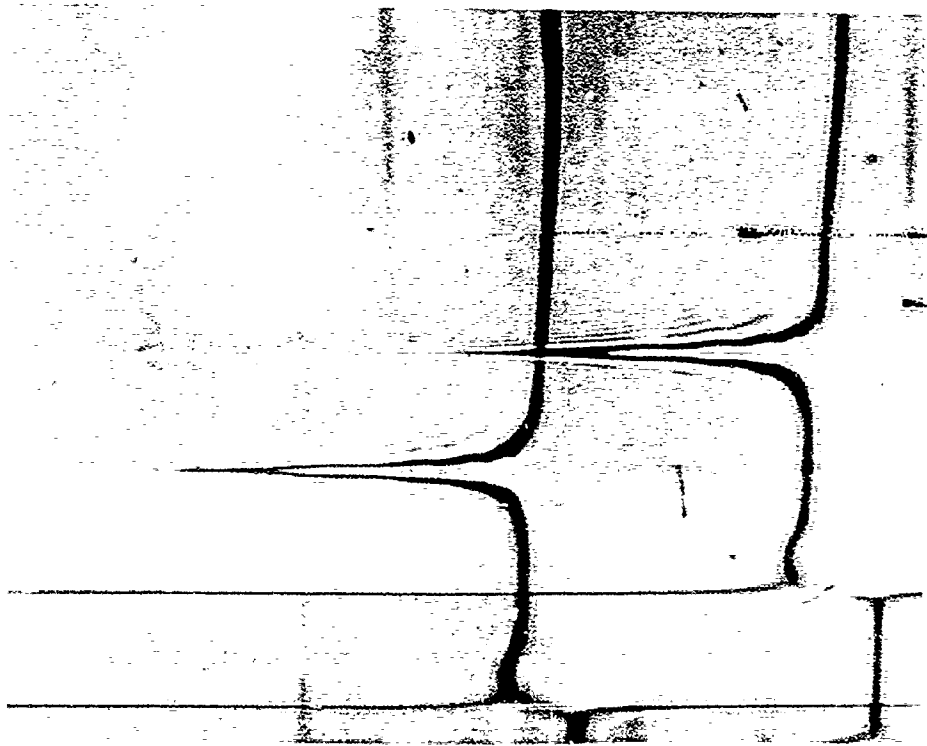
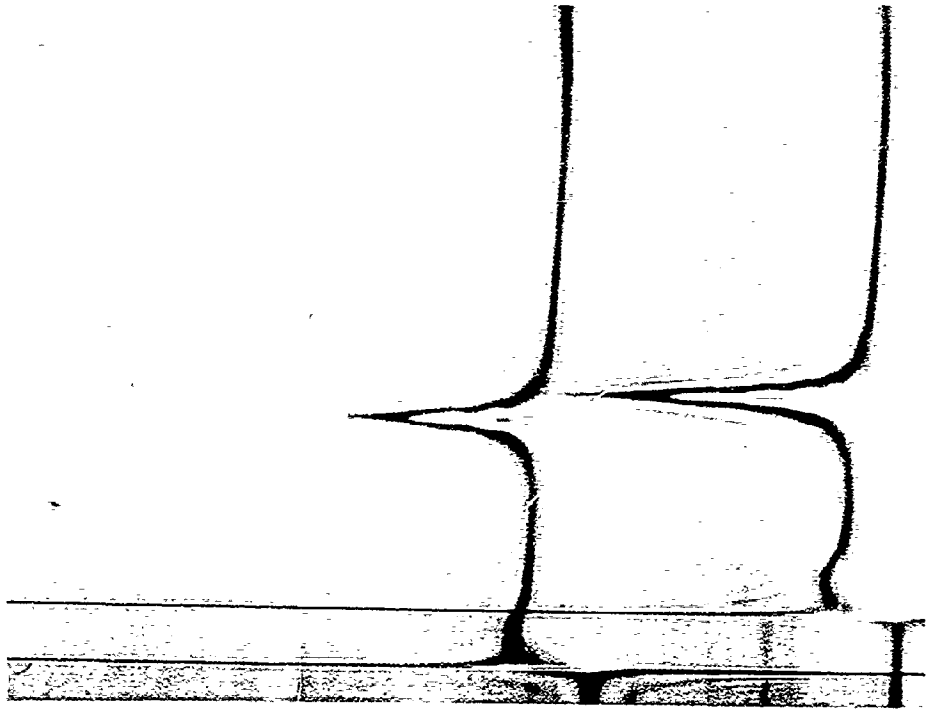
requires heat. Polymerization at lower temperatures did occur, however, when the pH was lowered or the NaCl concentration raised. Thus, in the presence of 0.2 M NaCl at pH 3.5 (Fig. 3B, upper) or in 0.5 M NaCl at pH 4.0 (Fig. 3B, lower) major species sedimenting at 72S and 68S, respectively, are found. On the other hand, rod formation is inhibited at pH 4.5 even at 20°C (Fig. 3C).

It is clear from the above results that the formation of protein rods in the earlier experiments must have occurred during the brief warming period that took place just prior to the centrifugations at 20°C and so it became desirable to determine if the assembly reaction was completed in that time. PMV protein was dialyzed to pH 4.0, 0.2 M NaCl at room temperature for 3, 6, and 12 hours prior to sedimentation analysis. The extent of polymerization was compared with an identical protein preparation which was dialyzed for 12 hours at 4°C and warmed just before centrifuging. The results were the same in all cases and demonstrated that protein rod formation was rapid and complete within minutes at 20°C (Fig. 4).

3.3.3 pH reversibility

The above experiments suggested that a rapid equilibrium is achieved between the 14S polymers and high molecular weight rods. This is supported by an ex-

Fig. 4. Schlieren patterns of PMV protein polymerized for various incubation periods at pH 4.0. Protein at 2 mg/ml in 0.01 M tris buffer, pH 8.0, was dialyzed versus 0.01 M citrate buffer, pH 4.0, containing 0.2 M NaCl, for 3 hr (81S polymer, upper left), 6 hr (79S polymer, lower left), and 12 hr (72S polymer, upper right) at 22^o C and for 12 hr at 5^o C (72S polymer, lower right). Run conditions: 21.5^o C, 29,500 rpm, photograph taken at 13 min. Sedimentation is to the right.



PMV protein is reversible with respect to pH. Starting protein at pH 8.0 (Fig. 5A), consisting mostly of the 25S aggregate with some 14S present, was dialyzed to pH 4.0 to form rods sedimenting at 79S (Fig. 5B). When the rods were back-dialyzed to pH 8.0, only the 14S and 25S polymers were found (Fig. 5C), the rods having dissociated. The protein concentration was reduced due to dilution from the back-dialysis and gave rise to the smaller schlieren peaks and also to the lower S value for the larger polymer in Fig. 5C (see Chapter 4 for protein concentration effects at pH 8.0).

3.3.4 Control of the extent of polymerization

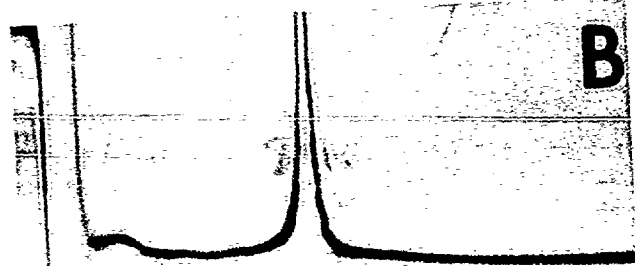
Rod formation in 0.2 M NaCl at pH 4.0 usually resulted in a surprisingly homogeneous population of polymers sedimenting at between 70 - 80S. To determine which factors control the extent of rod length during polymerization, two sets of experiments were performed in which either cold (Fig. 6A) or warm (Fig. 6B) 14S protein was added to freshly formed rods at pH 4.0 in an attempt to induce further growth. If the rate of growth onto existing rods greatly exceeds the rate of spontaneous nucleation of new rods then, in the extreme case, added 14S protein would polymerize onto pre-formed rods exclusively (Fig. 6, A1 and B1). If, on the other hand, nucleation is relatively rapid and the equilibrium condition at 20°C is reached quickly

Fig. 5. pH reversal of rod formation. PMV protein at 2 mg/ml, consisting of the 14S and 25S (31S as actually measured) polymers at pH 8.0 (0.01 M tris buffer) (A), was polymerized to 79S material by 24 hr dialysis at 5°C to pH 4.0 in 0.01 M citrate buffer containing 0.2 M NaCl (B). The polymers in (B) were then back-dialyzed for 24 hr to pH 8.0 (0.01 M tris buffer) and dissociated to the 14S and 25S (22S as actually measured) polymers (C). Run conditions: (A) and (C), 22.8°C, 52,640 rpm; (B), 29,500 rpm. Photographs taken at 13 min. Sedimentation is to the right.

A




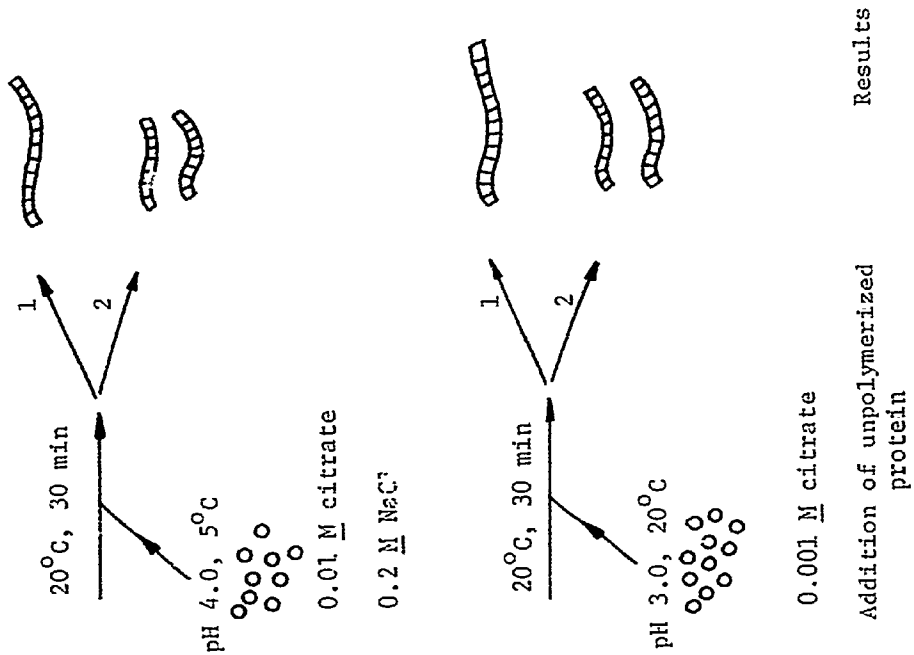
B



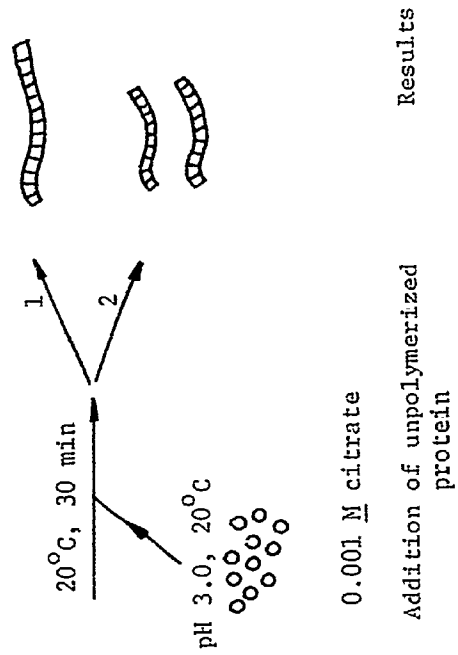
C



Fig. 6. Scheme used in the rod elongation experiments. (A) cold protein additions at pH 4.0; (B) warm protein addition at pH 3.0. o, 14S protein; , protein helices. The outcomes illustrated in each experiment represent the extreme cases which may result from the addition of an equal weight of protein to pre-formed rods: either doubling the length of the rods (A1 and B1) or doubling the number of rods with no change in length (A2 and B2).



A) pH 4.0, 5°C
0.01 M citrate
0.2 M NaCl



B) pH 4.0, 5°C
0.02 M citrate
0.4 M NaCl

Starting protein Polymerized protein Addition of unpolymerized protein Results

(see section 3.3.2) then, at constant protein concentration, the outcome should be independent of the starting ratio of polymerized protein/14S protein (Fig. 6, A2 and B2).

In the first experiment, cold 14S protein at pH 4.0 (Fig. 7C, lower) was added to freshly formed rods (Fig. 7A). The resulting preparation gave a sedimentation pattern (Fig. 7B) indistinguishable from that of the starting rods (Fig. 7A) (result A2 in Fig. 6). Also, if rods were cooled to 4°C prior to the addition of cold protein and sedimented at 5° the majority of the polymers were dissociated to the 14S species (Fig. 7C, upper), thus demonstrating that rod formation is reversible with respect to temperature.

In the event that the addition of the cold protein solution induced some depolymerization of the rods in the above experiments, a second set of experiments was performed in which warm 14S protein at pH 3.0 (Fig. 8A, upper) was added to polymerized protein at pH 4.0 (Fig. 8A, lower) at 20°C. The resulting preparation again yielded a sedimentation pattern (Fig. 8B, upper) similar to that of the starting rods (result B2 in Fig. 6A). A mixing control was performed by diluting twice-concentrated rods at pH 4.0 1:1 with pH 3.0 buffer. The result (Fig. 8B, lower) indicated that the rapid mixing probably did not affect the outcome of this experiment.

The results of the above two experiments are

Fig. 7. Effect of addition of cold 14S protein to protein rods. Protein at 2 mg/ml was dialyzed at 5°C for 24 hr versus 0.01 M citrate buffer, pH 4.0, containing 0.2 M NaCl and was treated in the following manner: (A) 1 ml warmed to 20°C for 30 min sedimented at 14S and 75S at 20°C; (B) 1/2 ml warmed to 20°C for 30 min followed by the addition of 1/2 ml cold (4°C) protein sedimented at 14S and 80S at 20°C; (C) upper, 1/2 ml warmed to 20°C for 30 min then cooled to 4°C for 30 min followed by the addition of 1/2 ml of cold (4°C) protein sedimented at 14S and 98S at 5°C; lower, 1 ml sedimented at 14S and 102S at 5°C. Run conditions: A-C, 29,500 rpm, photographs taken at 13 min. Sedimentation is to the right.

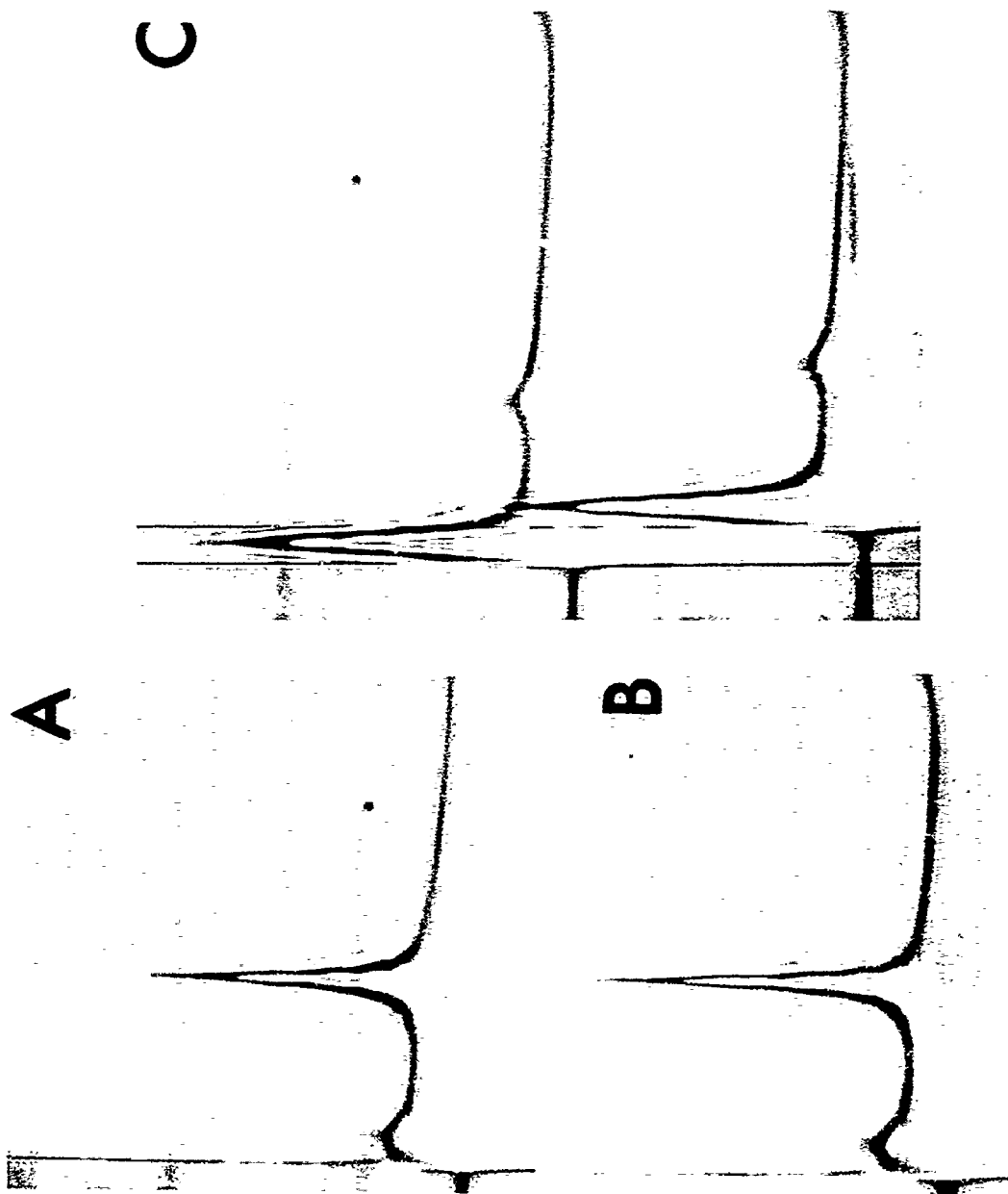
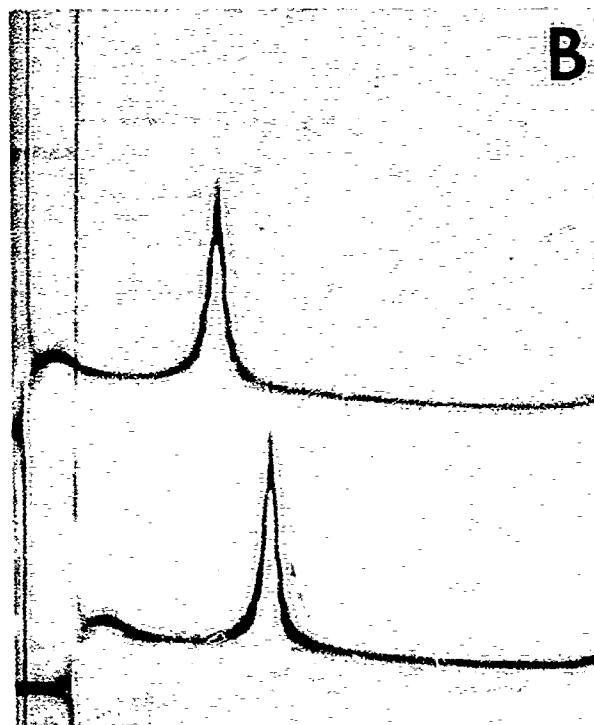


Fig. 8. Effect of addition of warm 14S protein to protein rods. Protein at 2 mg/ml was dialyzed at 5°C for 24 hr versus 0.02 M citrate buffer, pH 4.0, containing 0.4 M NaCl and was polymerized by warming to 20°C for 30 min. 14S protein was prepared by dialyzing protein at 2 mg/ml at 5°C for 24 hr versus 0.001 M citrate buffer, pH 3.0, and warming to 20°C for 30 min prior to use. (A) upper, pH 3.0 protein sedimenting at 14S at 20°C; lower, pH 4.0 protein sedimenting at 82S at 20°C. (B) upper, 1/2 ml of pH 4.0 protein to which was added 1/2 ml of pH 3.0 protein sedimented at 75S; lower, 1/2 ml of pH 4.0 protein (4 mg/ml) plus 1/2 ml of 0.001 M citrate buffer, pH 3.0, sedimented at 78S; the final pH of these samples was 4.0. Run conditions: 20°C, 29,500 rpm, photographs taken at 14 min. Sedimentation is to the right.

A



B



consistent with each other and suggest that the control of rod length, in the presence of NaCl, can be explained most simply as a consequence of a rapid spontaneous nucleation of growing helices followed by a fast approach to the equilibrium condition.

3.3.5 Ionic strength

Raising the NaCl concentration from 0.2 M to 0.5 M, while tending to salt-out the rods, otherwise had little noticeable effect on their formation at pH 4.0 (Fig. 9A). At 0.5 M NaCl the protein precipitated and gave rise to structures which had a rope-like appearance in the electron microscope and apparently consisted of two or more intertwined helices (Fig. 9B, C).

3.3.6 Cation effects

The effects of replacing Na^+ with other monovalent Group I and divalent Group II metal cations on rod formation were investigated. The nature of the Group I cation was apparently unimportant since 0.2 M LiCl and CsCl gave results indistinguishable from those obtained with NaCl (Fig. 10A, B). On the other hand, Group II divalent cations exerted an inhibitory effect on polymerization. The sedimentation coefficient of the rods was reduced to around 56S in the presence of 0.1 M MgCl_2 , CaCl_2 , SrCl_2 or BaCl_2 (Fig. 10C - F). Also the yield of rods was decreased,

Fig. 9. Effect of NaCl concentration on PMV protein polymerization. (A) Schlieren patterns of PMV protein polymerized in the presence of increasing NaCl levels. Protein at 2 mg/ml was dialyzed at 5°C for 24 hr versus 0.01 M citrate buffer, pH 4.0, containing 0.3 M NaCl (68S, lower) or 0.4 M NaCl (68S, upper). Run conditions: 20.6°C, 29,500 rpm, photographs taken at 12 min. Sedimentation is to the right. (B) and (C) High and low magnification electron micrographs of PMV protein ropes. Protein at 2 mg/ml was dialyzed at 5°C for 24 hr versus 0.01 M citrate buffer, pH 4.0, containing 0.5 M NaCl. Ropes were formed upon warming to room temperature, immediately upon which the protein formed a white precipitate. Bars represent 100 nm.

A

B

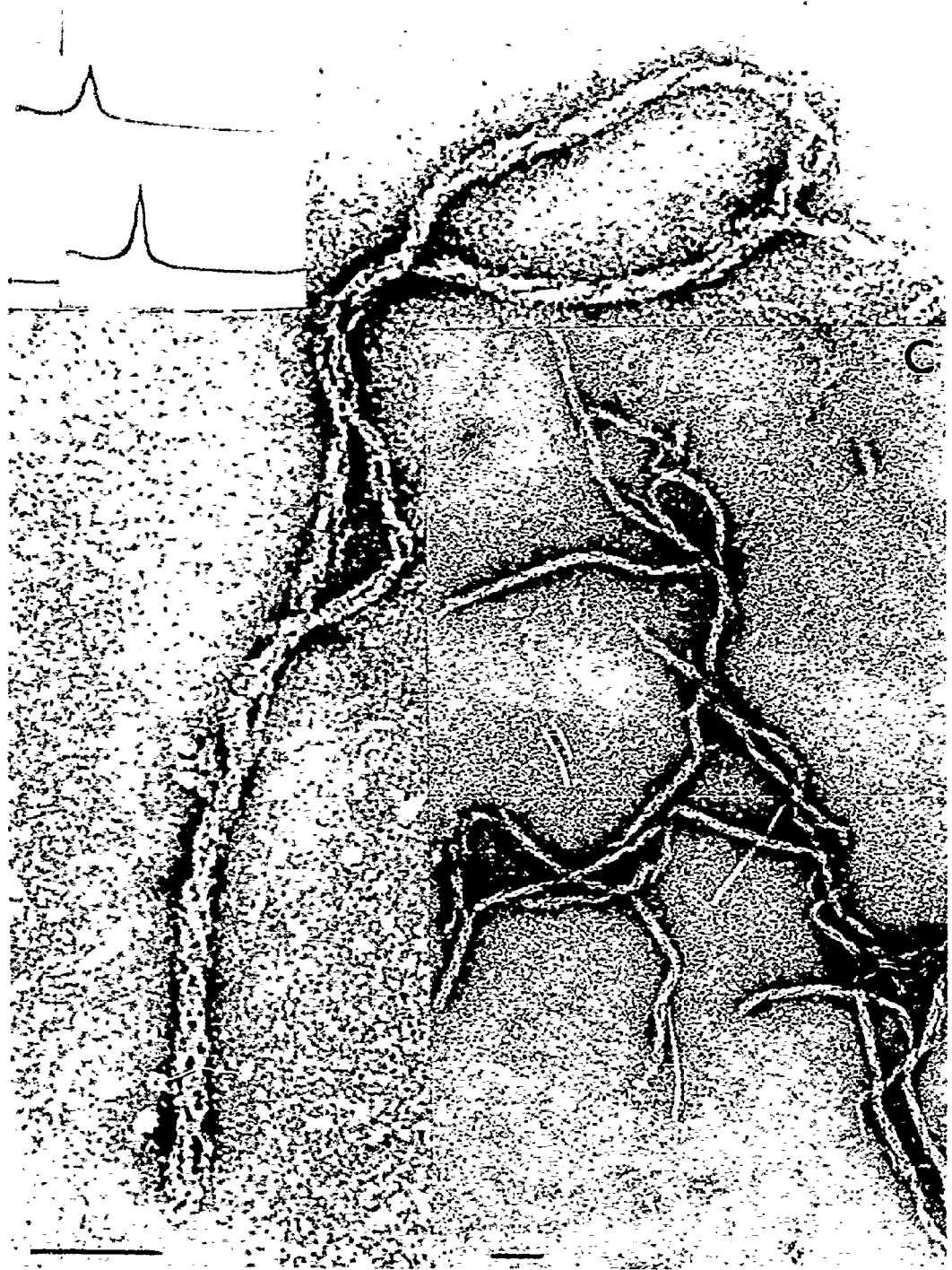
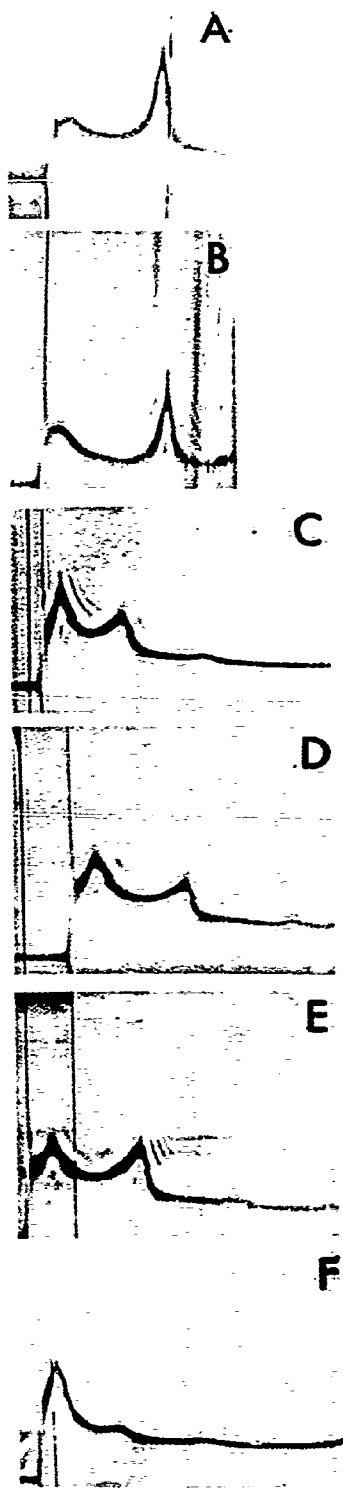


Fig. 10. Cation effects on protein rod formation. PMV protein at 2 mg/ml was dialyzed at 5°C for 24 hr versus 0.01 M citrate buffer, pH 4.0, containing: (A) 0.2 M LiCl (14S and 71S); (B) 0.2 M CsCl (14S and 68S); (C) 0.1 M MgCl₂ (14S and 57S); (D) 0.1 M CaCl₂ (14S and 57S); (E) 0.1 M SrCl₂ (14S and 56S); (F) 0.1 M BaCl₂ (14S and 53S). Patterns (C) - (F) also contained a trace of some high molecular weight material sedimenting around 100S. Run conditions: 29,500 rpm. (A) and (B), 21.2°C, photograph taken at 13 min; (C) and (F), 20.0°C, photograph taken at 13 min; (D) and (E), 20.8°C, photograph taken at 17 min. Sedimentation is to the right.



BaCl₂ effecting the most drastic reduction.

3.4 Discussion

The coat protein of PMV has a molecular weight of around 22,000 daltons and is similar in mass to the PVX protein subunit, MW ca. 23,000 daltons (Goodman, 1975). The most prevalent polymeric form of PMV protein in a variety of environmental conditions sediments at about 14S. By applying a rationale similar to that used by Caspar (1963) in calculating the number of subunits in the 20S disc of TMV protein, it is predicted that the 14S polymer of PMV protein exists as a double layer ring structure consisting of about 17 subunits. However, no obvious disc-type structures, such as those seen with TMV 20S protein (Durham *et al.*, 1971) and TRV 36S protein (Fritsch *et al.*, 1973b; Morris and Semancik, 1973), have been observed for PMV protein in the electron microscope.

Although there is some indication that the formation of the 14S polymer is temperature dependent (especially at alkaline pH, see Chapter 4) this aggregate generally prevails at low temperature over a wide range of pH in contrast to the TMV protein disc (Lauffer and Stevens, 1968; Durham and Klug, 1971). It is also stable at moderate (0.2 M) NaCl concentration in contrast to the TRV protein disc (Morris and Semancik, 1973). Thus, while disc-like structures may be a general subassembly aggregate for coat proteins

from simple rod-shaped viruses, their stabilities, which are reflected in the environmental requirements for their formation, may vary widely. Fourteen S polymers have also been observed with the coat protein of clover yellow mosaic virus (data not shown), another member of the PVX group, but they have not yet been reported for the PVX coat protein, although they probably occur.

PMV protein possesses the capacity to self-assemble into nucleic acid-free rods which have the same helical parameters as the native virus. This indicates that protein-protein interactions play a predominant role in the forces that stabilize the PMV particle. The basic requirements for rod formation, acidic pH and elevated temperature, are similar to those for TMV protein polymerization (Lauffer and Stevens, 1968; Durham *et al.*, 1971). Rod formation is reversible with respect to temperature as well as pH, although some hysteresis was observed over a narrow pH range. Thus, the self-assembly reaction for PMV protein is probably entropy-driven, as it is with TMV protein (see Lauffer, 1975), and this suggests that entropy-stabilized interactions are of major importance to the stability of the PMV particle.

PMV protein will also assemble into rods at 4°C if it is dialyzed for several days at pH 4.0 in 0.05 M KCl. Such rods are stable up to pH 7.5 (Durham and Bancroft, in preparation). Similar stability to low temperature and high pH is characteristic of rods which have been standing

at 20°C for several days after having first been polymerized by warming from 4°C to 20°C in the usual manner. The energetic relationship between these highly stable rods and those which are made reversibly after short times is unclear.

At low ionic strength at pH 4.0, a heterogeneously sedimenting population of rods, many of which are extremely long, was found. The polymerization of TMV protein is favored at high ionic strength (Lauffer and Stevens, 1968). At 0.2 M NaCl the polymerization of PMV protein yields a shorter and more homogeneous population of rods, sedimenting at 70 - 80S, than found in the absence of the salt. Because of the reproducibility and character of this reaction, further studies on the protein polymerization were conducted at moderate ionic strengths.

A stable length distribution of rods was reached within minutes after warming cold 14S protein, at pH 4.0, to 20°C, suggesting that some equilibrium condition had been satisfied. A rapid approach to equilibrium combined with a rapid helix-nucleation step could serve to explain the observations that the addition of 14S protein to preformed protein rods resulted in no change in the length distribution of the latter. These observations would also be expected if there were some physical constraints upon rod formation in these conditions such that rod growth is prevented beyond a length specified by the accumulation

of electrostatic free energy (Lauffer, 1975, pp. 92ff) or of interaction free energy due to the accumulation of assembly errors (Oosawa and Asakura, 1975, pp. 106ff). Kinetic studies of the polymerization process would be useful in discriminating between these alternative hypotheses.

Increasing the NaCl concentration from 0.2 M had no noticeable effect on the size distribution of polymers formed but it did promote aggregation of helices to form structures giving the appearance of ropes, especially at 0.5 M NaCl. Rope formation appeared to be the result of a salting-out effect since these structures tended to precipitate at room temperature. Ropes were not observed at low temperatures.

Changing the cation from Na^+ to Li^+ or Cs^+ had no noticeable effect on the protein polymerization; however, the Group II metal cations reduced both the average size and yield of rods. The cations tested may be ordered in decreasing effectiveness with regard to promoting depolymerization: $\text{Ba}^{2+} > \text{Sr}^{2+} \sim \text{Ca}^{2+} \sim \text{Mg}^{2+} > \text{Cs}^+ \sim \text{Na}^+ \sim \text{Li}^+$.

This order generally follows the Hofmeister or lyotropic series which approximates the order of effectiveness of these ions as water structure-breakers and thereby their potential as destabilizing or dissociating agents for structures which are stabilized by entropic unions (Hatefi and Hanstein, 1969; Dandliker and deSaussure, 1971). This

interpretation is consistent with the idea that the protein-protein interactions in the helix are entropy-stabilized. However, caution must be exercised in interpreting salt-specific effects on macromolecular interactions, as was pointed out with regard to the salt-induced disassembly of PVY (McDonald and Bancroft, 1977), since the thermodynamics of simple ionic solutions, and especially of biopolymer solutions, is poorly understood (see Jencks, 1969).

PVX protein has not yet been shown to assemble into nucleic acid-free helices. Attempts in our laboratory to polymerize CYMV protein into rods also have been unsuccessful. These observations may mean that protein-protein interactions are more important for virus stability with PMV than for other members of the PVX group. Alternatively, they may derive from the conditions used for preparing the proteins. PMV, unlike PVX, will not dissociate in 2 M LiCl (Francki and McLean, 1968) or 2 M CaCl₂ (Novikov et al., 1972) at pH 5.0 to 6.0. It will do so at pH 8.0 but the protein is insoluble when the CaCl₂ is removed and is soluble but incompetent for virus reconstitution when the LiCl is removed (data not shown).

Protein from PVY forms long particles composed of stacked rings or perhaps discs (McDonald et al., 1976) under conditions (pH 6.0 - 9.0) which are unfavorable to PMV protein rod formation. It seems that proteins from different flexuous virus groups have different assembly

requirements, as do proteins from rigid rod viruses such as TMV (Durham et al., 1971) and TRV (Morris and Semancik, 1973). One basic structural difference between a rigid rod and a flexuous rod must lie in the radial distribution of axial interactions between coat protein subunits. Such geometric constraints do not necessarily rule on the specific chemical groups involved, nor do they relegate such groups to a virus with a particular shape. Thus, carboxyl-carboxylate pairs are critical in the control of assembly of protein from both TMV (Caspar, 1963) and cowpea chlorotic mottle virus (Bancroft, 1970) which is spherical. The pH levels required by PMV protein to make helical structures suggest that a related mechanism involving acidic amino acid residues may also be operative in yet another group of viruses.

CHAPTER 4

THE SELF-ASSEMBLY OF PMV FROM ITS COAT PROTEIN AND RNA

4.1 Introduction

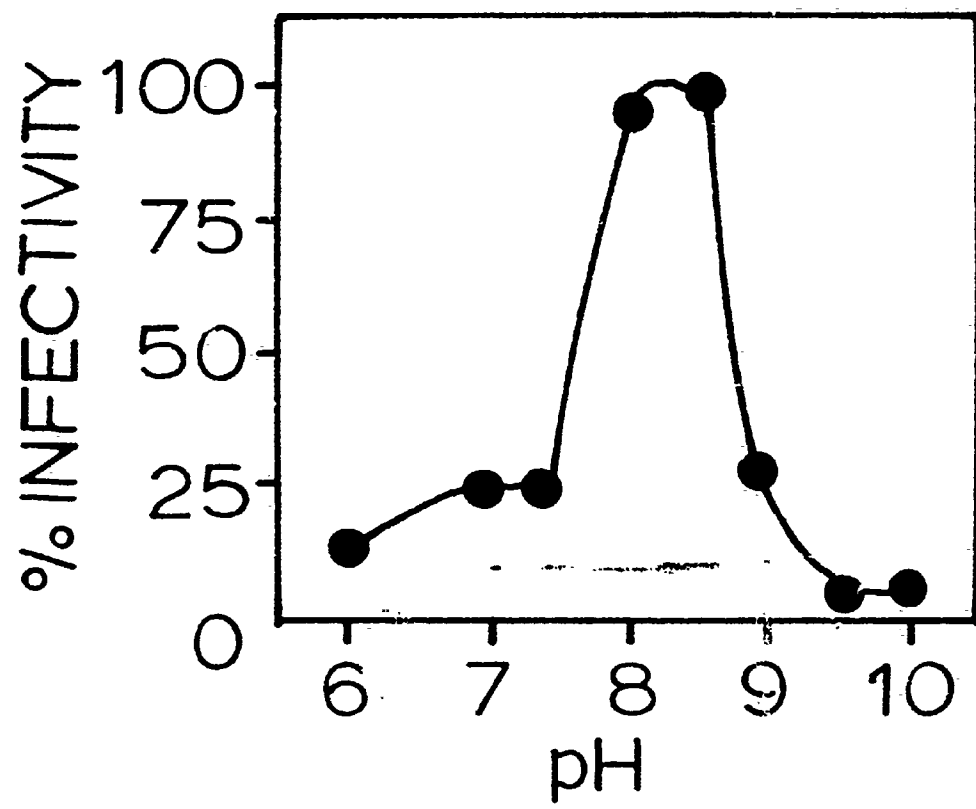
The polymerization of PMV coat protein to form helical rods demonstrated that the isolated coat protein was active in protein assembly. The next step was to reconstitute biologically active PMV from its isolated protein and nucleic acid. This chapter describes the properties of nucleoproteins assembled under various conditions, some of which did promote the assembly of infectious virus-like particles. The coat protein was found to exist in a complex equilibrium under conditions most suitable for virus reconstitution (pH 8.0), and studies on the protein polymorphism at pH 8.0 are described.

4.2 Experimental results

4.2.1 The effect of pH

The relative infectivities of ribonuclease T₁-treated virus reconstituted at 25°C from pH 6.0 to 10.0 in 0.01 M levels of suitable buffers show that the best pH for assembly lies between pH 8.0 and 8.5 (Fig. 11). The yield of virus at pH 8.0 to 8.25 was routinely high (>90%) as measured by rate density-gradient analyses whereas this

Fig. 11. The effect of pH level on the reconstitution of PMV. Relative infectivities of nucleoprotein assembled at pH 5.0 (0.01 M sodium acetate), pH 6.0 (0.01 M 2-(N-morpholino) ethanesulfonate-HCl (MES)), pH 7.5, 8.0 and 8.5 (0.01 M tris-HCl), pH 9.0, 9.5 and 10.0 (0.01 M glycine-NaOH) after incubation with 1 unit of RNase T₁ per 50 μ g RNA for 30 minutes at 37°C. Such treatment completely inactivated naked RNA. Assembly conditions: protein concentration, 1 mg/ml; RNA concentration, 0.05 mg/ml; temperature, 25°C; time, 30 min. Infectivities are expressed as percentages of that obtained at pH 8.5.



was not always true at pH 8.5, so the lower pH levels were used. The specific infectivity of virus made at these pH levels was about 2% that of natural virus.

Nucleoprotein assembly at pH 5.0, 6.0, 7.0 and 7.5 also gave high yields but the particles were segmented, resulting in a "kinked" appearance (Fig. 12A). The amount of segmentation was greater at pH 5.0 to 6.0 than at pH 7.0 and 7.5. Particles made at pH 8.0 to 8.5 were mainly sinuous (Fig. 12B). At pH 9.0 the particles had a sinuous appearance but were short. No rods were visible at or above pH 9.5.

Rate density-gradient analyses showed that nucleoprotein made at pH 6.0 sedimented marginally faster at pH 8.0 than natural virus, presumably because the discontinuities in the former reduced its frictional coefficient. Nucleoprotein assembled at pH 6.0 was partially degraded by RNase T₁, probably due to digestion of unprotected RNA in the "kinked" regions, whereas virus assembled at pH 8.0 was not (Fig. 13).

Attempts were made to correlate the assembly results with the behavior of the coat protein. In water (pH 5.0 to 6.0) and in solutions buffered at either pH 5.0 or 6.0 in 0.01 M acetate buffer or 0.01 M MES buffer, respectively, the protein sedimented as a single species at 14S (Fig. 14A, B, upper). At pH 7.0, the polymers were heterogeneous,

Fig. 12. Electron micrographs of nucleoprotein assembled at pH 6.0 (A) and pH 8.0 (B). See Fig. 11 for experimental conditions. The bar represents 100 nm.

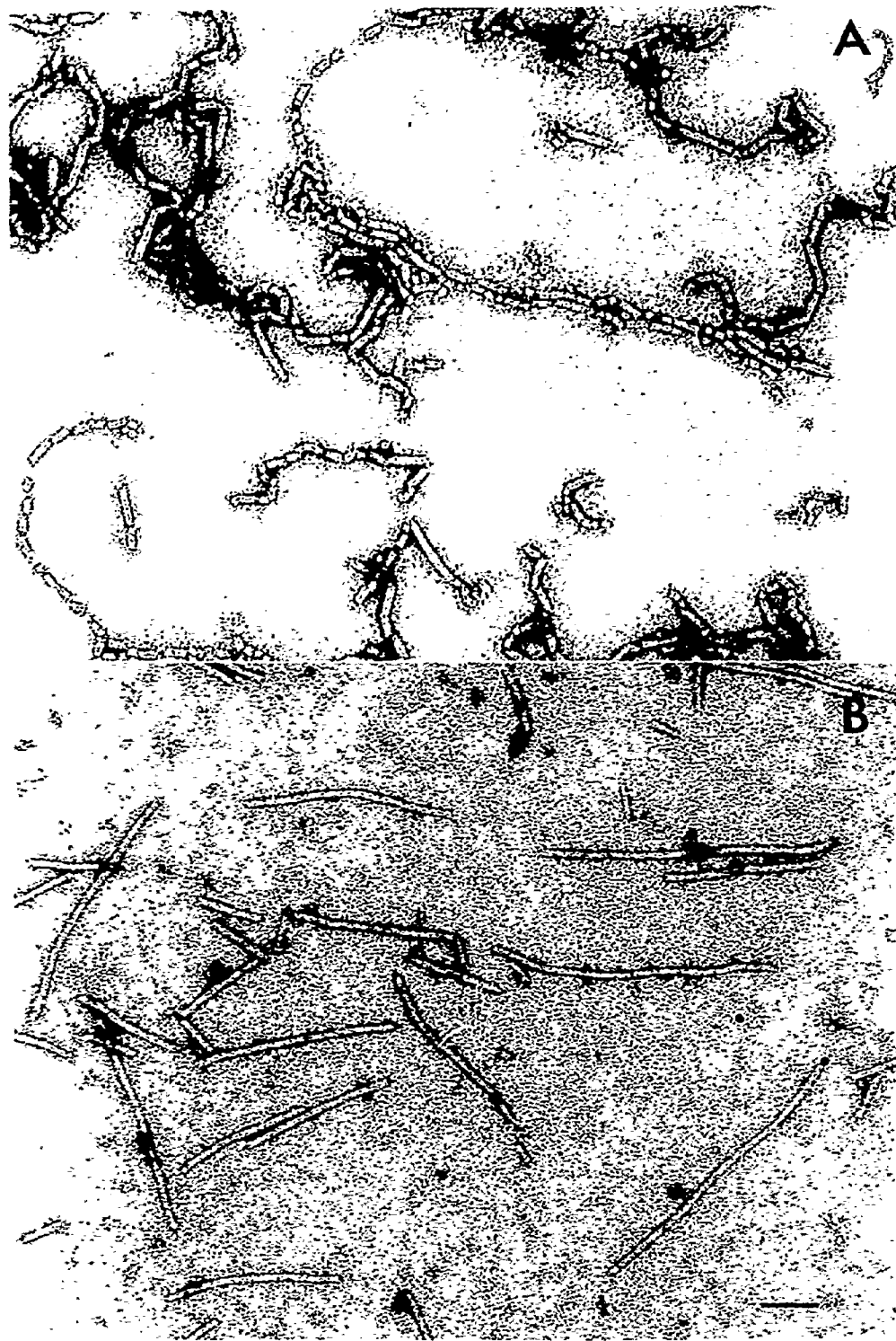


Fig. 13. Sedimentation of PMV assembled at pH 6.0 and pH 8.0. Sucrose density gradient profiles of nucleoprotein assembled at pH 6.0 before and after treatment with RNase T₁ (A and B) and at pH 8.0 before and after T₁ treatment (C and D). Gradients were composed of 10 - 40% sucrose containing 0.01 M sodium EDTA, pH 8.0. Preparations were centrifuged for 1 1/4 hours at 36,000 rpm in a Beckman SW 50.1 rotor at 5°C. Sedimentation is to the right. The arrow indicates the position of native PMV.

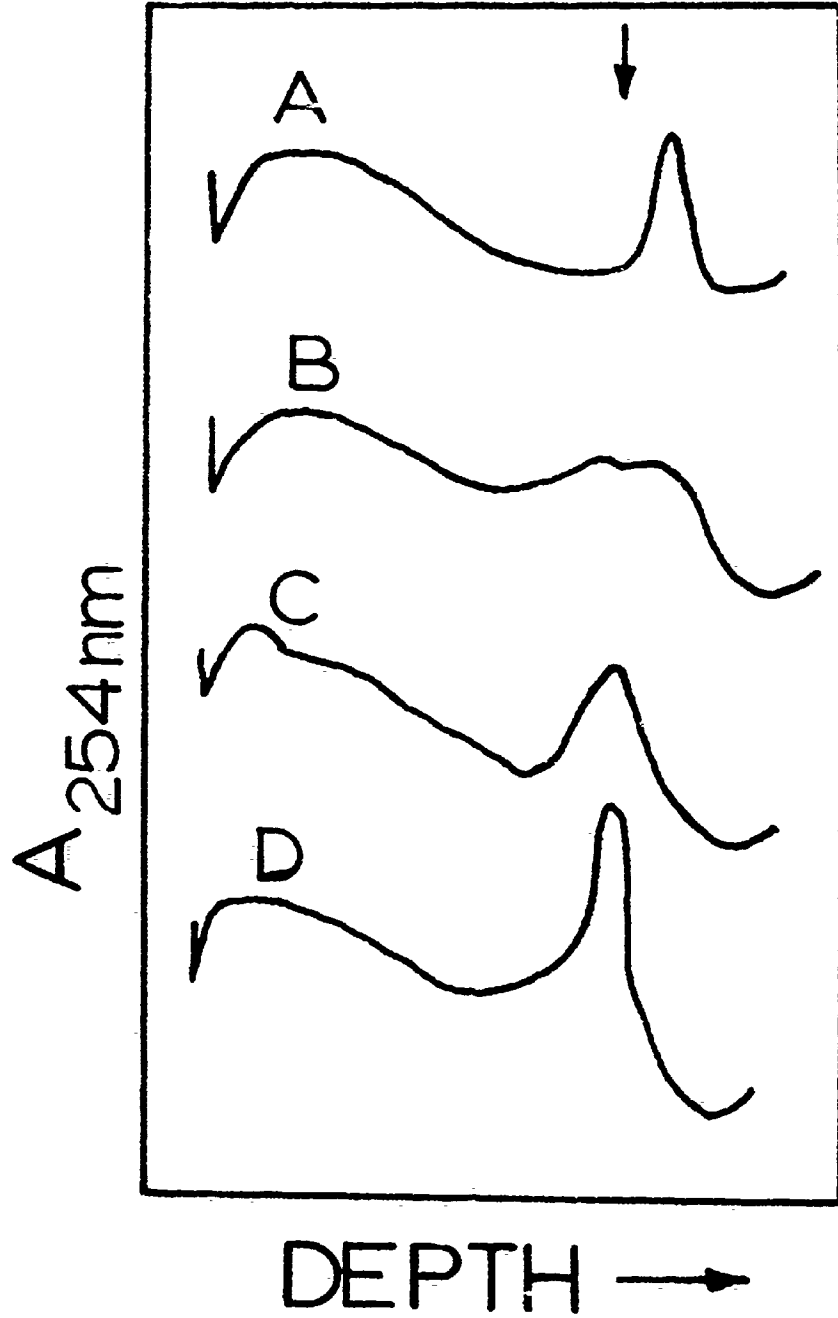
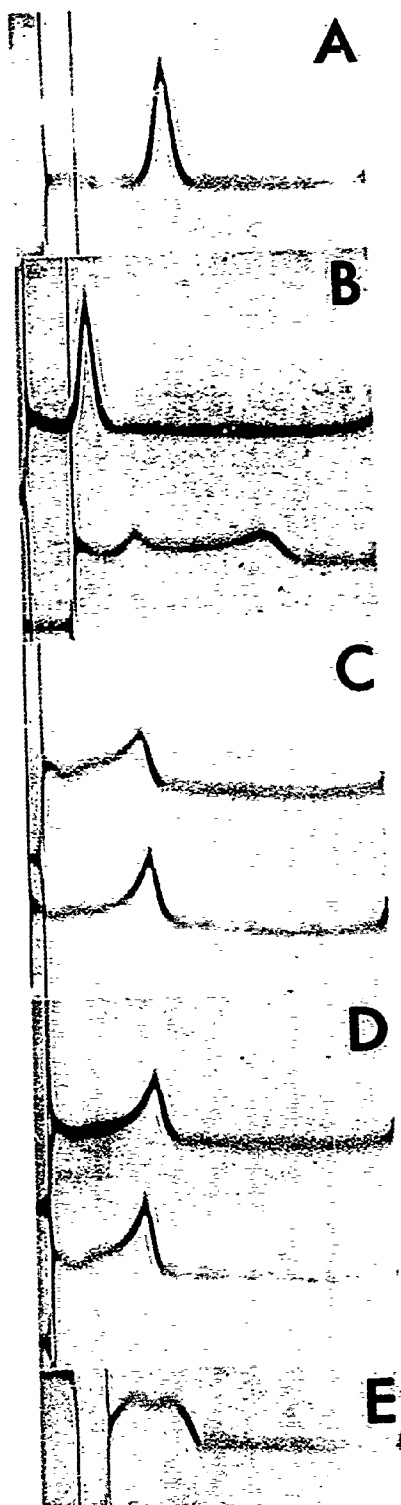


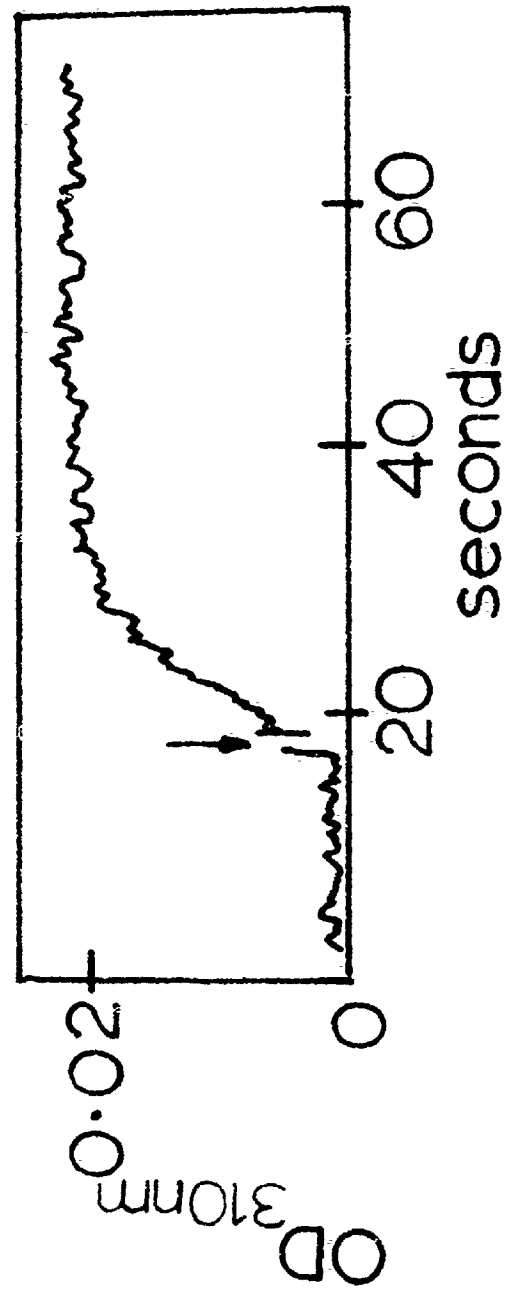
Fig. 14. Schlieren patterns of PMV protein at 3 mg/ml at various pH levels. (A) 14S species in 0.01 M acetate buffer, pH 5.0; (B) upper, 14S species in 0.01 M MES, pH 6.0; lower, 13S and 36S species in 0.01 M MES, pH 7.0; (C) upper, 12 and 24S species in 0.01 M tris, pH 7.5; lower, 12 and 27S species in 0.01 M tris, pH 8.0; (D) upper, 15 and 27S species in 0.01 M tris, pH 8.5; lower, 13 and 24S species in 0.01 M glycine, pH 9.0; (E) 3 and 8S species in 0.01 M glycine, pH 10.0. In all cases, buffers were added to the protein from the same large preparation 10 min before the cells were loaded. All runs were made at 22 and 23°C at a speed of 52,640 rpm. Sedimentation is to the right.



the principal components sedimenting at 13 and 36S (Fig. 14B, lower). From pH 7.5 to 9.0 (Fig. 14C and D) the main species had sedimentation coefficients of 24 and 27S and were in equilibrium, as will be shown later, with slower sedimenting polymers, some of which had $s_{20,w}$ values of 12 to 15S. The variations within the two groups of values may reflect experimental error although other explanations are possible; nevertheless, the sedimentation coefficients of the slower and faster species were taken to be about 14 and 25S, as averaged values from many runs. At pH 10.0, the 14S species which occurs in water is dissociated into two principal protein species sedimenting at 3 and 8S (Fig. 14E). On the basis of the sedimentation analyses alone, it might have been expected that the appearance and infectivity levels of particles made between pH 7.5 and 9.0 would be about the same, but this was not so.

The rate at which protein was converted from the 14S species in water at pH 5.5 to the 25S form upon addition of pH 8.0 tris buffer to 0.01 M was measured by turbidimetry. The reaction was complete within 30 sec, suggesting that equilibrium was reached within that period (Fig. 15). This means that prolonged preincubation of protein at pH 8.0 is not required for reconstitution.

Fig. 15. Kinetics of 14S - 25S interconversion in response to pH. 1 ml of protein at 1 mg/ml in water (pH 5.5) at 25°C was brought instantaneously to pH 8.0 by the addition of 10 μ l of 1.0 M tris, pH 8.0. Turbidity increase was monitored at 310 nm. The reference cell contained an equal weight of protein in 0.01 M tris, 0.1 M NaCl, pH 8.0. The presence of NaCl prevents formation of the 25S species (see text, below). The arrow denotes time of addition of the buffer.



4.2.2 The effect of temperature

Virus assembly, as measured by infectivity resistant to RNase T₁, was not efficient below about 25°C in 0.01 M tris buffer, pH 8.0 (Fig. 16A). However, partial rod growth did occur at lower temperatures as shown by turbidity and length measurements (Fig. 16B). Below about 10°C, a length of about 50 nm (number average) was attained by particles in assembly mixtures. Complete rod growth required an elevated temperature. These facts infer that PMV assembly is comprised of two distinct processes: an early, temperature-dependent event followed by a cold-sensitive phase as shown in the Arrhenius plot (Fig. 17). These two processes, which will be described more fully in the subsequent chapters, are defined as initiation and elongation, respectively.

Several other temperature-dependent aspects of elongation are of interest. Rod growth, once underway at a permissive temperature, can be stopped simply by cooling the assembly mixture to a non-permissive temperature. This led to the discovery of partially reconstituted rods, termed "extended particles". Such particles are characterized by a long narrow structure issuing from one end of a normal helix (Fig. 18A). Extended particles can also be detected after short incubation periods at 25°C (Fig. 18B). That extended particles are probably nucleoprotein structures was suggested by their sensitivity to RNase A. No such structures

Fig. 16. The effect of temperature on the reconstitution of PMV. (A) The effect of temperature on the assembly of PMV as measured by infectivity. PMV protein and RNA at 1.0 and 0.05 mg/ml, respectively, were reacted in 0.01 M tris, pH 8.0 for 30 min at various temperatures prior to treatment with RNase T₁ and assay. Infectivity is expressed relative to that obtained at 25°C. (B) The effect of temperature on the assembly of PMV as measured by rod length and turbidity. Assembly conditions were those described in (A). Rod growth was measured by turbidity at 310 nm, ●-●, and by weight average lengths of particles measured from electron micrographs, o-o. Turbidity and weight average lengths are expressed relative to those measured at 25°C (0.020 OD_{310 nm} and 280 nm, respectively).

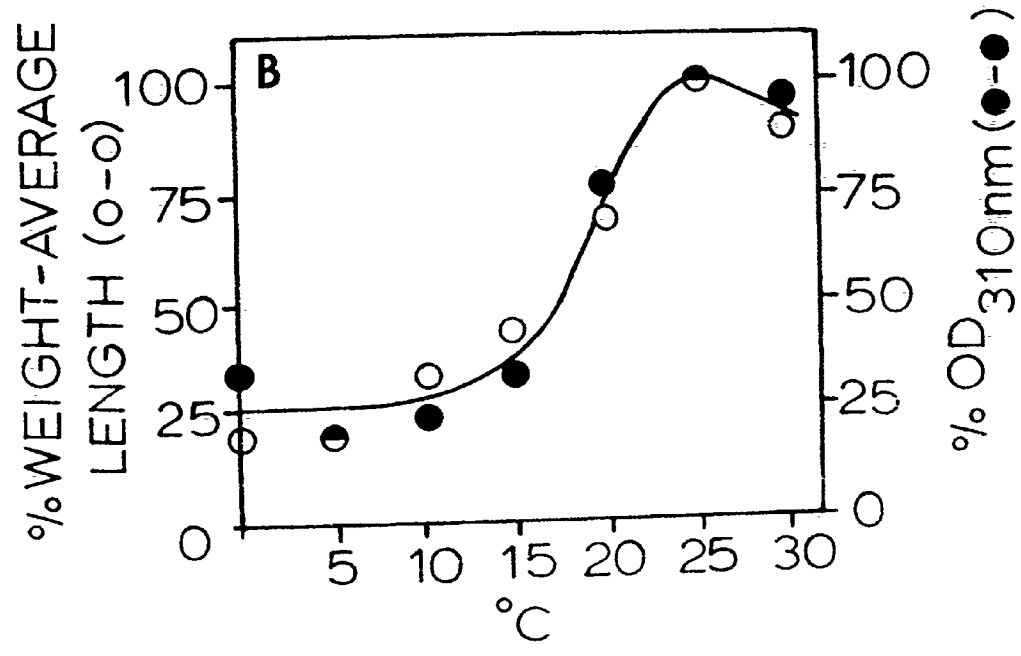
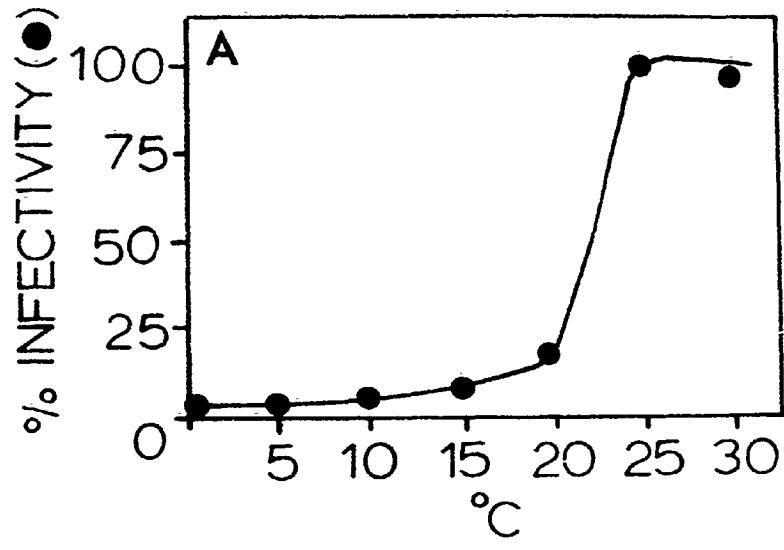


Fig. 17. Arrhenius plot of the effect of temperature on the relative rate, k , of elongation for PMV assembly at pH 8.0 in 0.01 M tris. Values for $\log k$ represent \log (percentage weight average rod length/30 minutes) relative to 25°C and were calculated from the experimental data presented in Fig. 16B. The calculated weight average rod lengths are accurate to ± 10 nm. The propagated standard error for the individual $\log k$ values is then given by

$$\frac{(12.7 + W_L \times 1.6 \times 10^{-4})^{1/2}}{2.303 \times k}$$

where W_L represents the weight average length after 30 min at the given temperature. This leads to a calculated standard error of 0.08 for the $\log k$ at 1°C and 5°C.

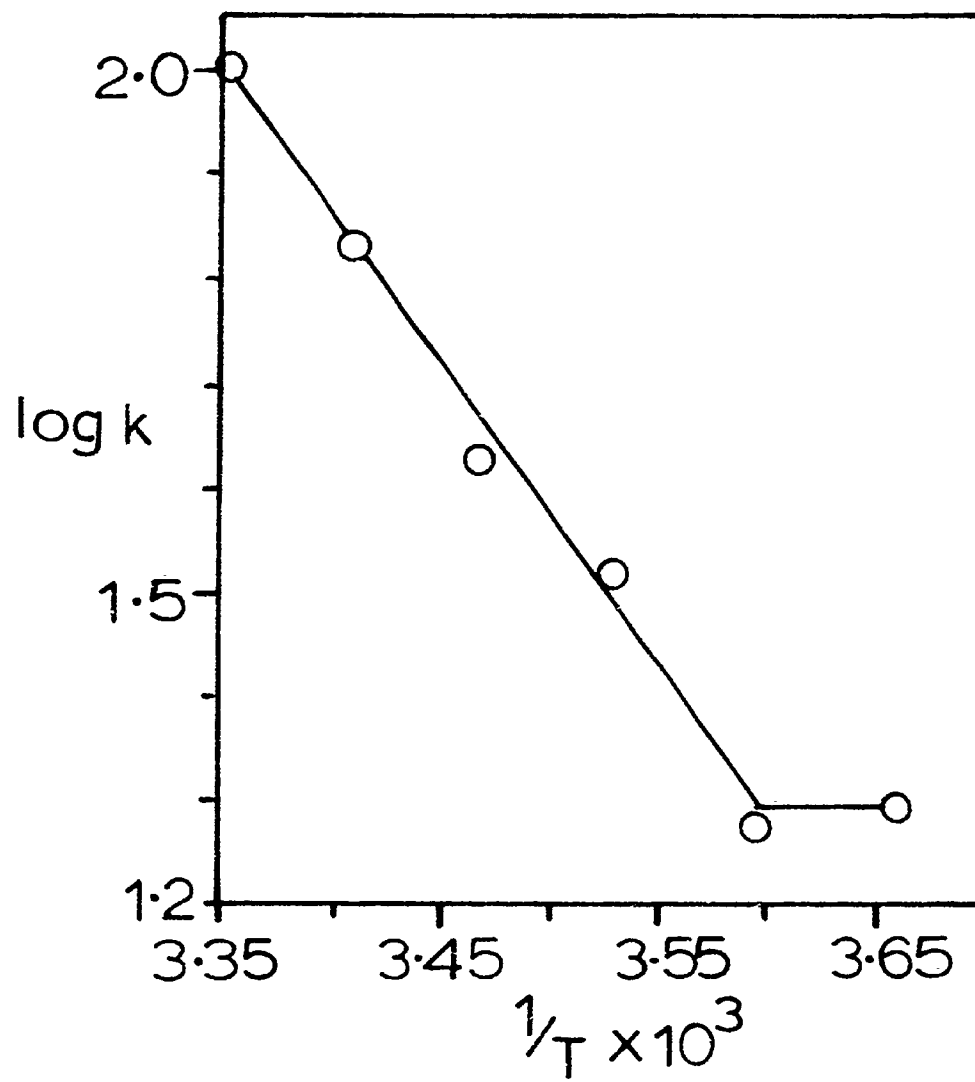
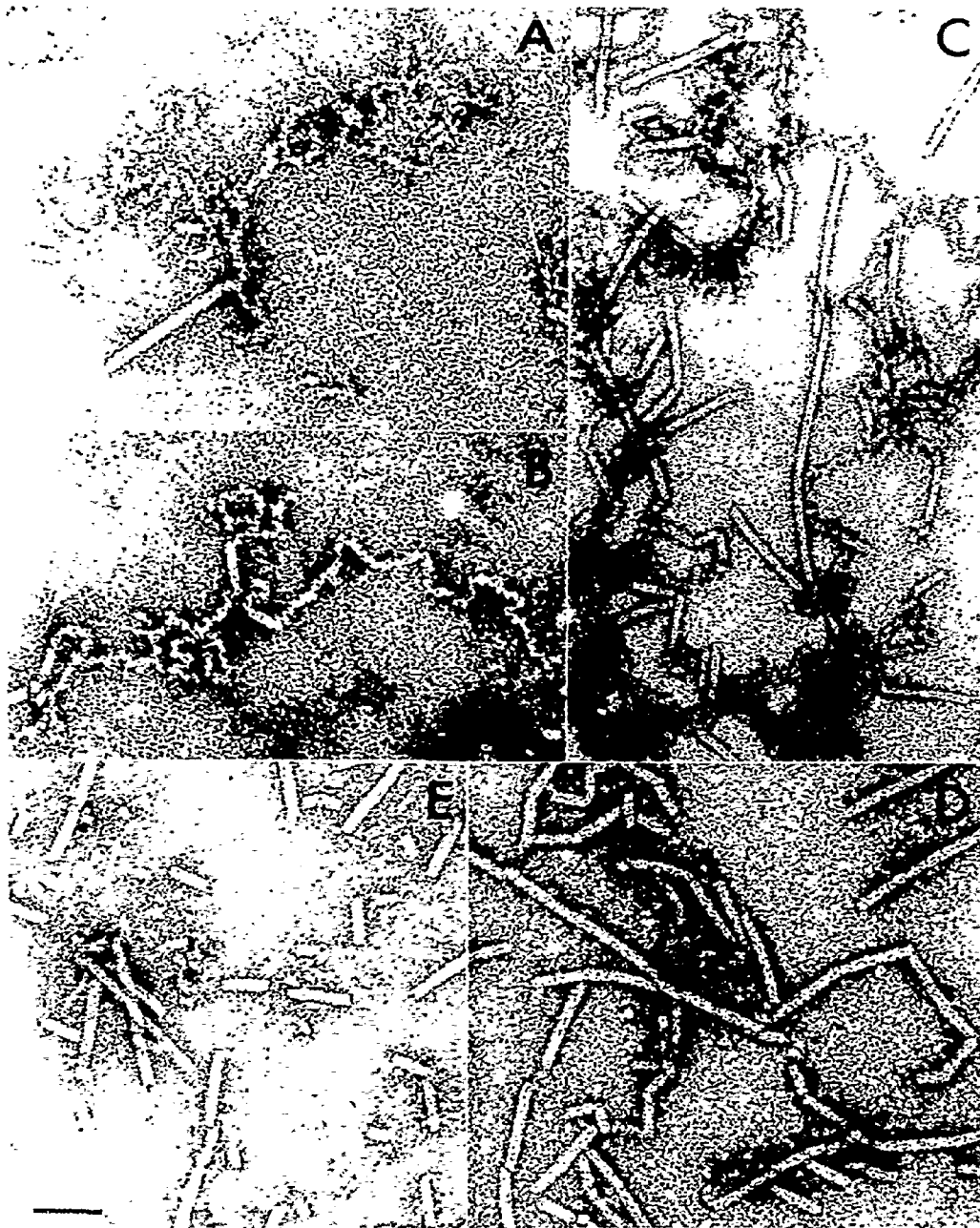


Fig. 18. Electron micrographs of PMV assembly products obtained from 1 mg/ml protein and 0.05 mg/ml RNA at pH 8.0 (0.01 M tris) after various temperature treatments. (A), 10°C, 30 min; (B), 25°C for 2 min; (C), 10°C for 30 min followed immediately by incubation at 25°C for 30 min; (D), 10°C for 30 min followed by storage for 17 days at about 5°C; (E), 10°C for 30 min followed immediately by RNase T₁ digestion, and then storage for 17 days at about 5°C. The bar represents 100 nm.



have ever been obtained, in similar or other conditions, with PMV coat protein alone. They were normally found only at pH levels optimal for virus assembly and were salt-labile (see below and Figs. 26 and 27).

Assembly could be initiated at low temperature and then brought to permissive temperature at which point elongation proceeded (Fig. 18C). This is not exactly equivalent to reconstituting PMV at 25^o, however, since the particles made in two stages were slightly kinked and were only about half as infective after RNase T₁-treatment as particles assembled entirely at 25^o (unpublished data). Rod completion occurred at low temperature over days (Fig. 18D) as judged by electron microscopy. That this was not simply due to polymerized protein was shown by the absence of long particles in the presence of RNase T₁ (Fig. 18E).

Finally, the effect of temperature on the polymerization of rods is pH dependent. In contrast to particle formation at pH 8.0, assembly at pH 6.0 occurred immediately at 0^oC as well as at 25^oC (unpublished data).

The effect of temperature on the behavior of PMV protein under normal reconstitution conditions (1 mg/ml, 0.01 M tris buffer, pH 8.0) was monitored by analytical ultracentrifugation. It can be seen from Table 1 and Fig. 19 that the 14S form predominates at 1 mg/ml over the range 5^o to 20^oC where reconstitution is inefficient. At

Fig. 19. The effects of temperature and concentration on the 14S - 25S equilibrium of PMV protein at pH 8.0. Schlieren patterns of PMV protein at 0.25, 0.50, 1.0 and 2.0 mg/ml (upper left, lower left, upper right, lower right, respectively) at 5°C (A), 10°C (B), 15°C (C), 20°C (D), and 25°C (E, where the inset corresponds to 0.10 mg/ml) in 0.01 M tris, pH 8.0. The sedimentation coefficients are listed in Table 1. The protein patterns marked r correspond to those used in the temperature reconstitution experiment (Fig. 16) and that in (E) to the protein concentration reconstitution experiment (Fig. 24). All runs were performed at 52,460 rpm. 30 mm cells were used for protein concentrations at 0.5 mg/ml or less. Sedimentation is to the right.

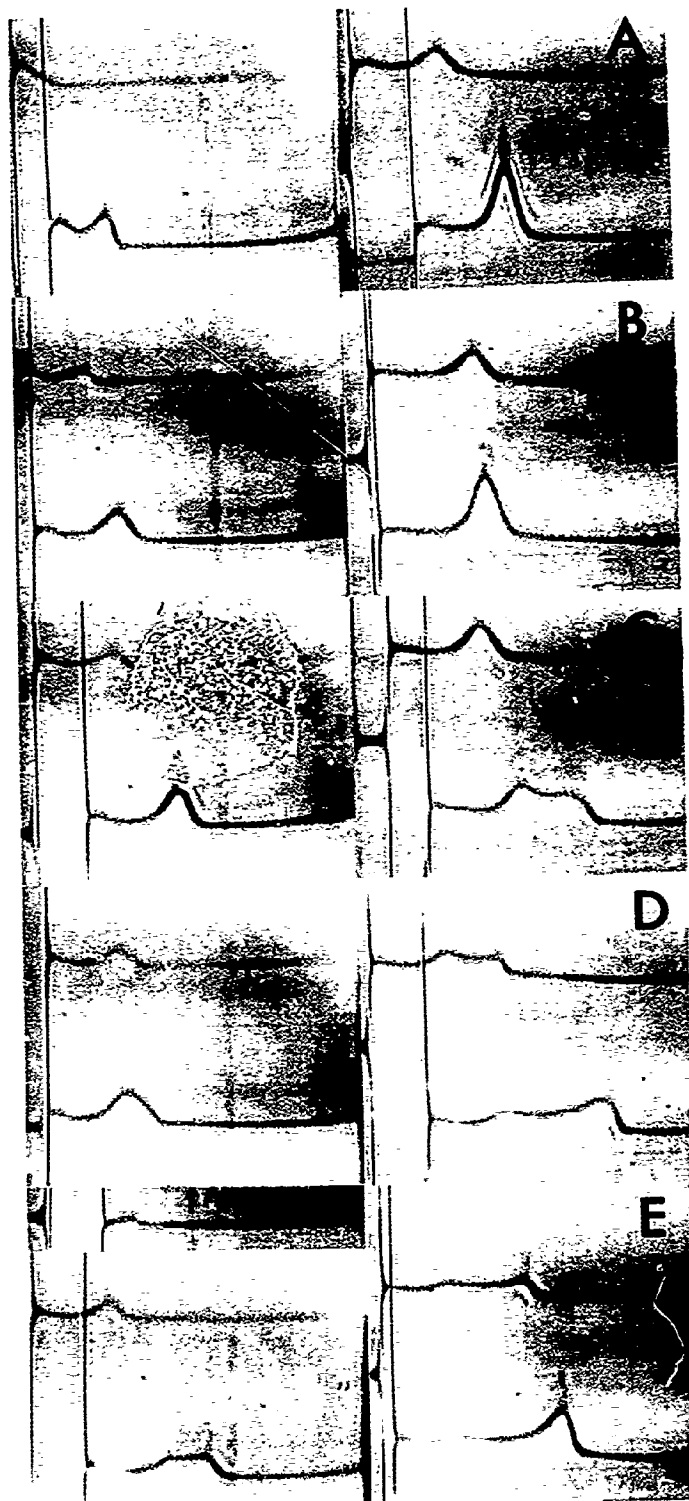


Table 1
Sedimentation coefficients of PMV protein
at different concentrations and temperatures

Protein conc. (mg/ml) ^a	Temperature (°C)			
	5	10	15	20
0.10	-	-	-	~1.8
0.25	1.8	1.8,11	1.8,11	1.8,13
0.50	1.8,12	1.8,12	1.8,13	13
1.0	3.5,12	12	13	14,21
2.0	3.3,12	13	13,18	14,26
8.0	-	-	-	-
				~3.2
				13
				12,18 ^b
				14,27
				14,31
				30

a) Protein in 0.01 M tris, pH 8.0

b) In some preparations, a 25S rather than an 18S species was observed.

25°C the 14S species is in equilibrium, as we will demonstrate, with the 25S aggregate, which predominates.

The formation of the 25S aggregate as a function of temperature was measured by turbidity (Fig. 20). Maximum light scattering occurred between 20° and 25°C (cf. Fig. 16A, B). Although the association-dissociation curves for the 14S - 25S equilibrium displayed hysteresis with temperature, the overall equilibrium was reversible. That the turbidity measured in these studies actually was related to the formation of the 25S polymer is shown in Fig. 21, in which the relative amount of 25S aggregate measured from Schlieren patterns is plotted along with the relative turbidity.

The rate of the temperature-dependent 14S to 25S interconversion was measured by temperature-jump light scattering kinetics (Fig. 22). The reaction was complete within about 1.5 minutes for both directions, association (heating) and dissociation (cooling). The heating time provides a measure of the period necessary to warm refrigerated protein for reconstitution; the cooling reaction for stopping it (see Chapter 5). The initial rate of the association reaction (about 2% of maximum $OD_{310 \text{ nm}}/\text{sec}$) was about twice that of dissociation (about 1% of maximum $OD_{310 \text{ nm}}/\text{sec}$) again signifying different kinetics for the association and dissociation reactions. The rate of the pH-driven conversion of 14S into 25S at 25°C was about

Fig. 20. Effect of temperature on the turbidity of PMV protein. PMV protein at 2 mg/ml in 0.01 M tris, pH 8.0, was equilibrated at 4°C and the change in turbidity at 310 nm with temperature was monitored up to 25°C. The reverse procedure was used to obtain the downward curve. The reference cell contained an equal weight of protein in 0.01 M tris, 0.2 M NaCl, pH 8.0. Temperature control was obtained from a thermostatically-controlled bath connected to the cuvette block. Rates of heating and cooling were maintained constant at about 1°C/1-1/2 min.

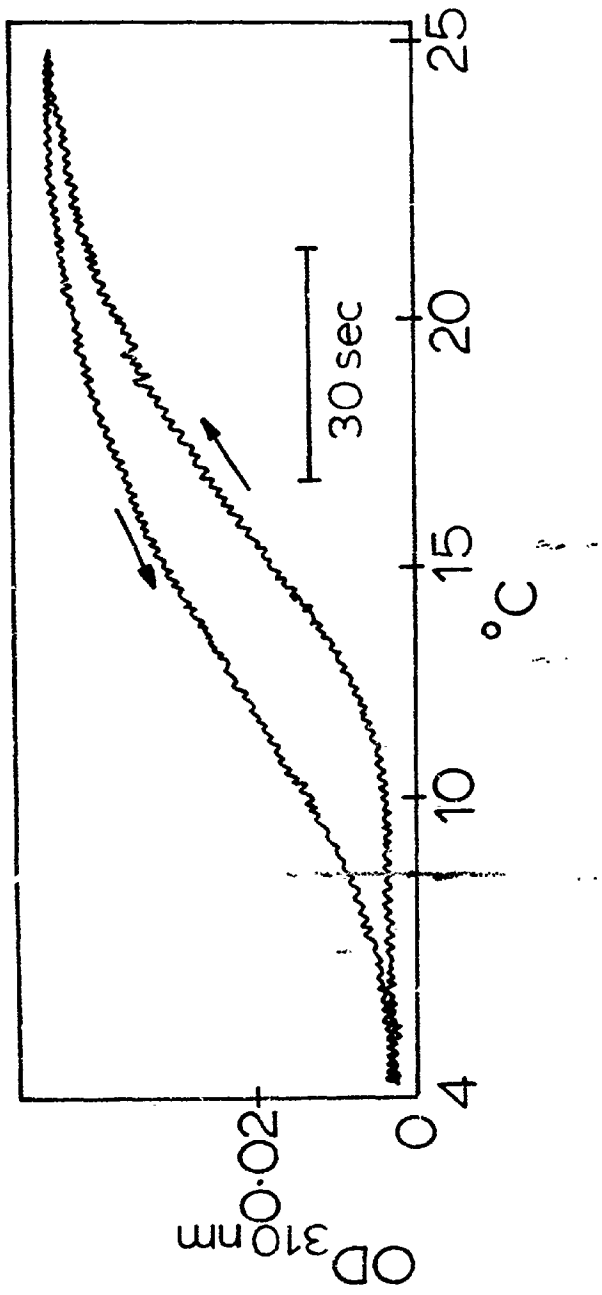


Fig. 21. Extent of formation of 25S aggregate of PMV protein as a function of temperature. ●-●, absolute proportion of 25S material measured from schlieren patterns (data from Fig. 19); o-o, proportion of total turbidity change at 310 nm between 5 and 25°C (data from Fig. 20), normalized to 93% (the value as measured from the corresponding schlieren pattern) at 25°C. The protein concentration was 2 mg/ml for both analyses. See Figs. 19 and 20 for further experimental details.

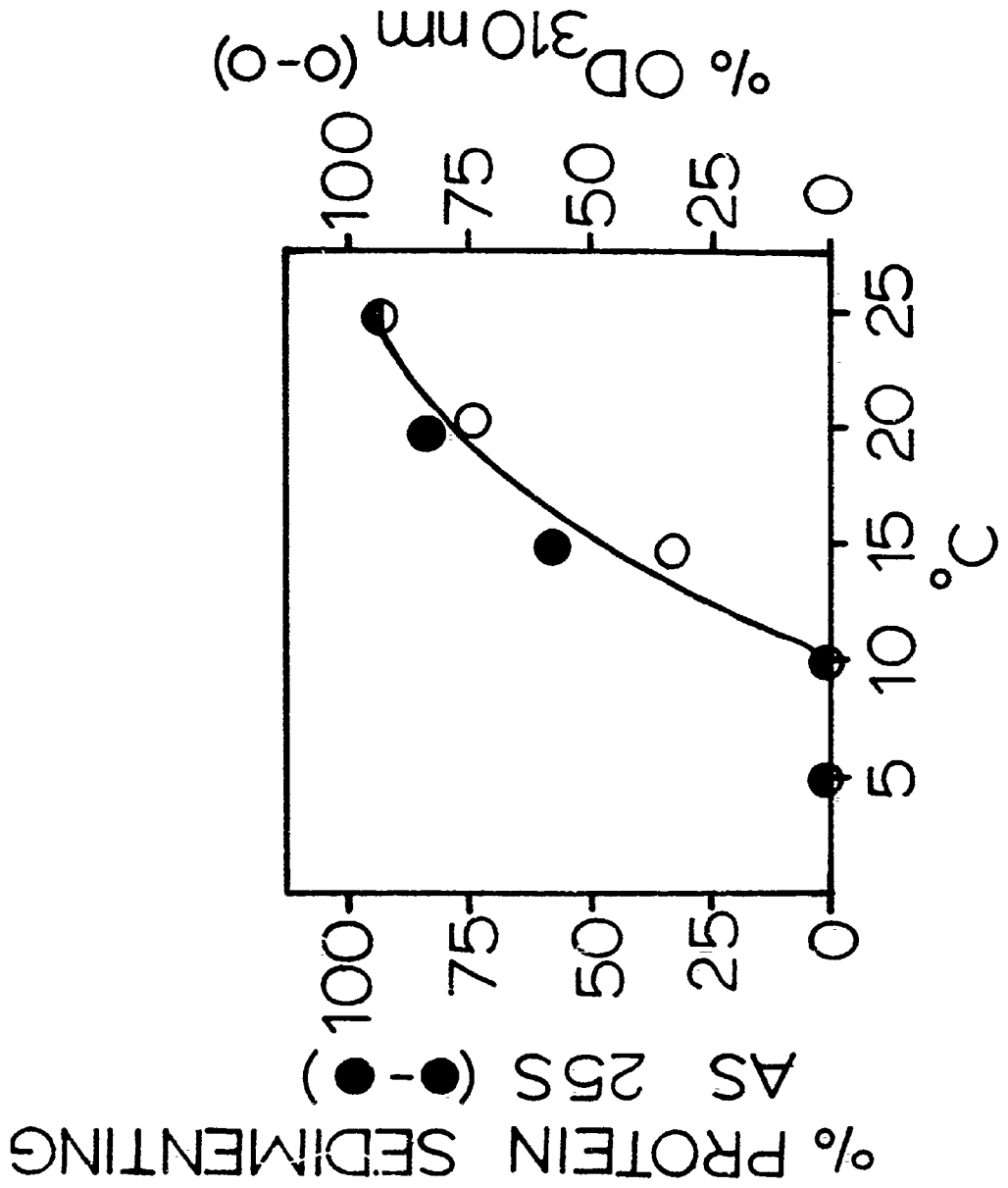
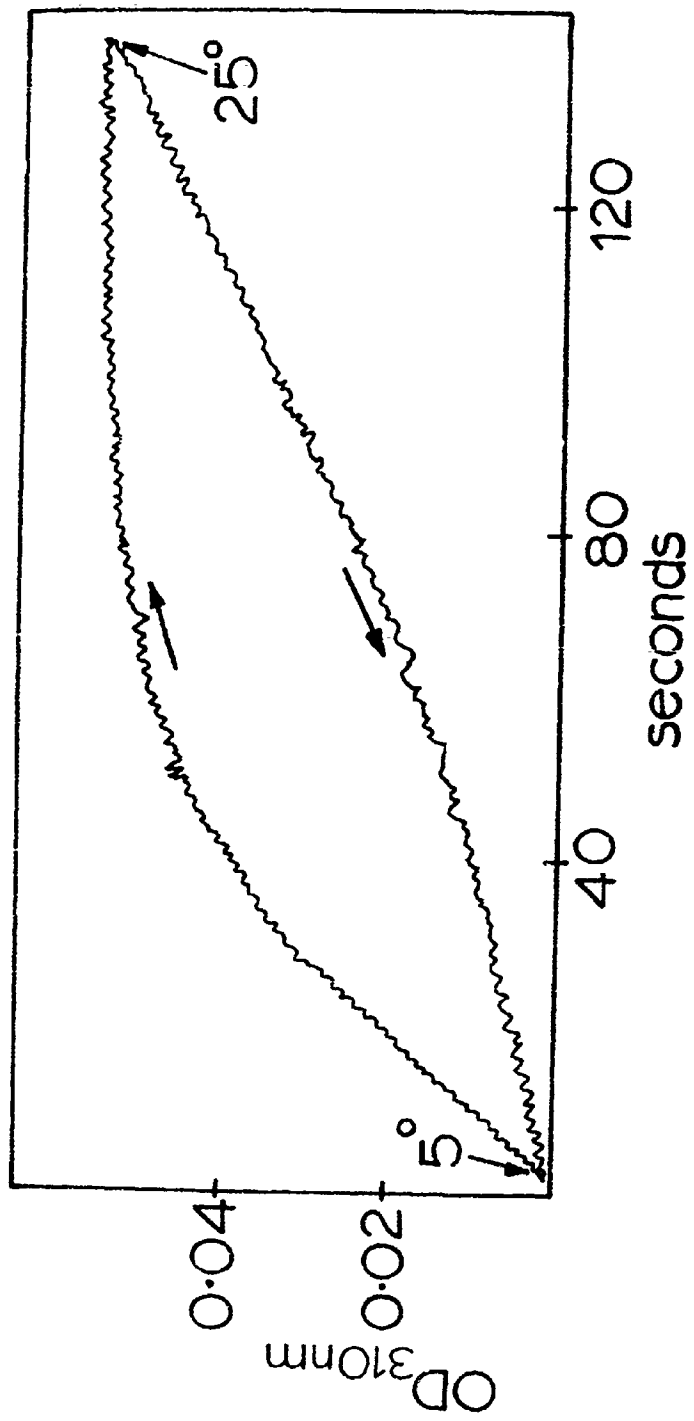


Fig. 22. Kinetics of 14 - 25S interconversion in response to temperature. Temperature shift-up (upward curve): PMV protein at 2 mg/ml in 0.01 M tris, pH 8.0, was equilibrated at 5°C and added to the sample cuvette in a temperature block pre-warmed to 25°C and the resulting change in turbidity was monitored at 310 nm. Temperature shift-down (downward curve): PMV protein (conditions as above) was equilibrated at 25°C and added to the sample cuvette in a temperature block pre-cooled to 5°C. In both instances the temperature in the sample cuvette went to within 5°C of the desired final temperature within 15 sec, and reached the final temperature by 2 min. The reference cell for both experiments contained an equal weight of protein in 0.01 M tris, 0.1 M NaCl, pH 8.0.



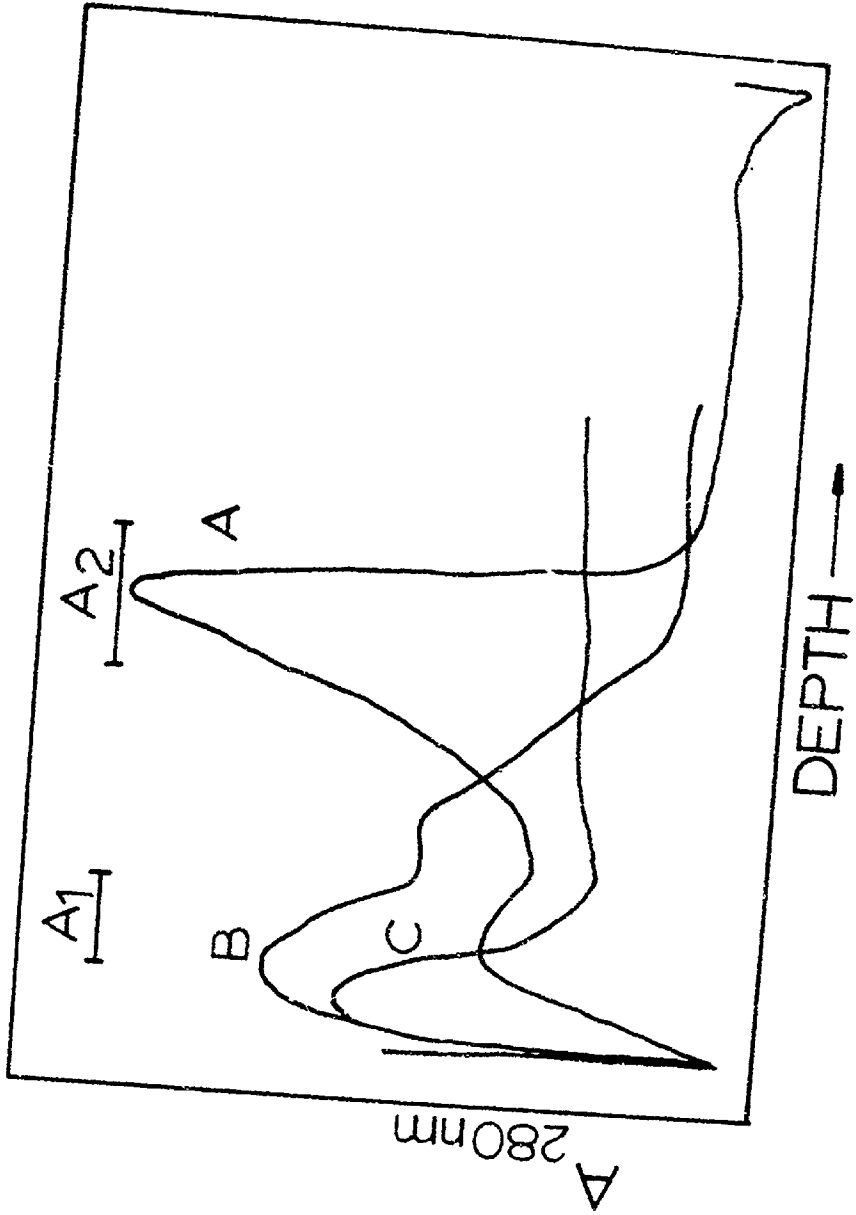
5 times faster than that of the temperature-driven association at pH 8.0.

4.2.3 The effect of protein concentration

Thus far, a consistent correlation was found between the presence and absence of the 25S species of PMV protein and the success and failure, respectively, of PMV assembly under the various experimental conditions employed. A tentative conclusion at this stage might be that the 25S aggregate is necessary for PMV assembly.

A proper test of this hypothesis would be to separate the various effects of temperature, pH and NaCl concentration (see next section) on the reconstitution and to focus mainly on the presence or absence of 25S protein under the best assembly conditions. Attempts to separate and isolate 14S and 25S aggregates on sucrose rate density-gradients proved unsuccessful because the forms equilibrate rapidly (Fig. 23). Therefore, the concentration dependence of the equilibrium was studied extensively by analytical ultracentrifugation (see Fig. 19 and Table 1). A series of protein polymers were obtained, whose size increased both with protein concentration and temperature. The slowest sedimenting species found, 1.8S, corresponds to the monomer. A 3S species (probably a dimer), which predominates at 0.1 mg/ml at 25°C, was found next followed by the 14S species and then the 25S aggregate. The 18 - 21S material

Fig. 23. Fractionation of PMV protein by sedimentation in sucrose. Sucrose density gradient profiles of unfractionated and fractionated PMV protein at various concentrations. (A) Sedimentation profile of PMV protein at a starting concentration of 2.0 mg/ml in 0.01 M tris, pH 8.0. (A1) corresponds to the 14S species and (A2) to the 25S species, both of which were collected. (B) Sedimentation patterns of (A2) at a starting concentration of 0.25 mg/ml. Note that most of the material sediments close to the 14S position. (C) Sedimentation pattern of (A1) at a starting concentration of 0.15 mg/ml. Note that the 14S species has been replaced by material sedimenting slower, probably corresponding to the slowly sedimenting protein seen in Fig. 19. Centrifugation was at 36,000 rpm for 5 hr at 25°C in 5 - 20% sucrose containing 0.01 M tris, pH 8.0, in a SW 41 rotor. Sedimentation is to the right.

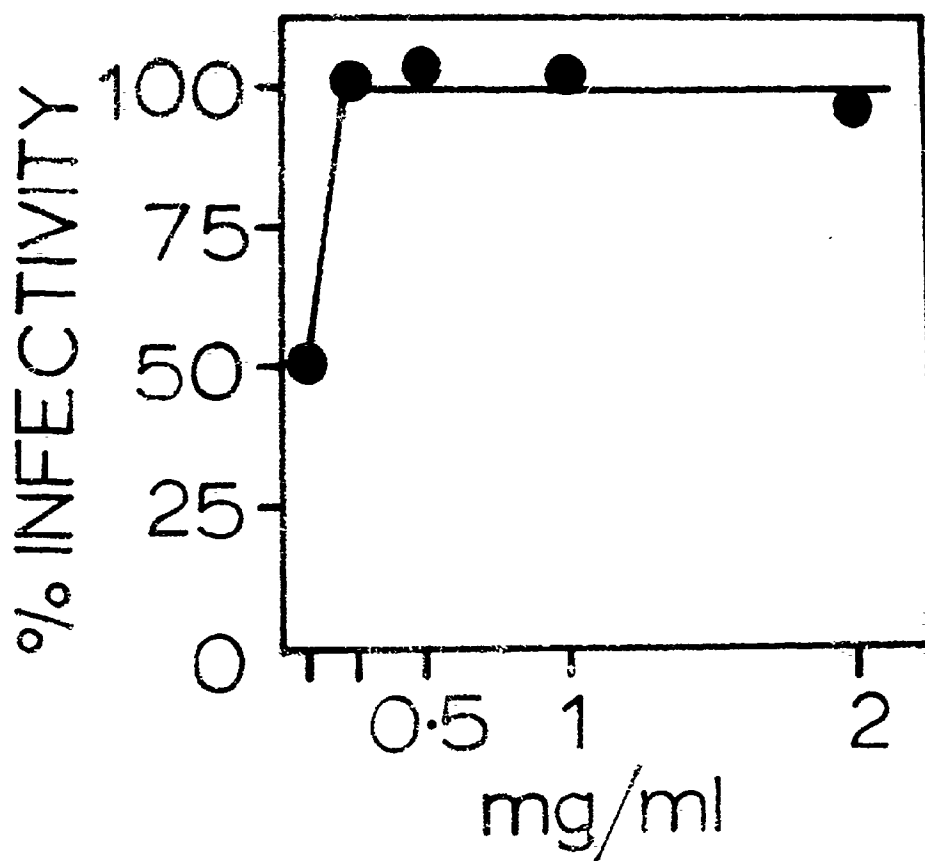


found under several conditions here and also at intermediate NaCl concentrations (see Fig. 28) is probably not a true equilibrium form for reasons discussed below (see Chapter 7).

The behavior of PMV protein at pH 6.0 differed from that at pH 8.0. The protein existed only in the 14S form from 0.1 - 8 mg/ml at 25°C and at 1 - 3 mg/ml (the only concentrations tested) at 5°C (unpublished data). No slower sedimenting species could be found at pH 6.0 in the absence of NaCl. Thus, the 14S species is more stable at the lower pH than it is near pH 8.0.

The concentration dependence of the coat protein equilibrium at pH 8.0 was exploited to test the efficacy of PMV assembly when various polymorphic forms of the protein were present in the starting material. The effect of protein concentration over the range 0.1 - 2 mg/ml on reconstitution at constant pH and temperature (pH 8.0, 25°C) is seen from Fig. 24. Virus assembly is equally efficient from 0.25 to 2 mg/ml starting protein concentration and is only halved at 0.1 mg/ml. This strongly suggests that the 25S aggregate is not required for virus assembly. Indeed, the observation that decreasing the protein concentration from 2 mg/ml down to 0.25 mg/ml had no effect on the yield of infective virus can best be explained by assuming that it is the 14S species of PMV protein which is required for assembly, since the equilibrium is shifted towards this

Fig. 24. The effect of protein concentration on the assembly of PMV at 25°C. PMV protein at various concentrations was reacted with RNA at a constant protein:RNA ratio of 20:1 in 0.01 M tris, pH 8.0, for 30 min before RNase T₁ digestion. The infectivity assays from 0.25 to 2.0 mg/ml protein were all made at a final concentration of 0.25 mg/ml (a 1/4 dilution of the 1 mg/ml mixture used as standard). That at 0.1 mg/ml was made against virus assembled at 1 mg/ml, diluted one-tenth.



species with decreasing protein concentration. The result at 0.1 mg/ml is difficult to interpret in this light since only 3S protein could be detected. The conclusion that no 14S protein is required is questionable as will be discussed.

4.2.4 The effect of NaCl

The presence of NaCl from 0.025 to 0.2 M inhibited the formation of PMV as assayed by infectivity (Fig. 25). The same effect was observed even if the assembly reaction was allowed to proceed for 2 minutes before the addition of NaCl, suggesting that both initiation and elongation were inhibited by this salt. These results were corroborated by morphological observations. No initiation complexes (short rods) were observed when 0.2 M NaCl was present at the start of assembly (Fig. 26A) and rod growth was stopped upon addition of the salt, resulting in structures with "brushes" localized at one end of the particles (Fig. 26B). These brushes may be a result of salt-induced collapse of the extended particles which were never found in the presence of NaCl.

A further feature of particle assembly came from these studies. Low temperature assembly, followed by salt treatment, resulted in a high yield of particles containing brushed ends (Fig. 27). At the end opposite the brushed end, presumed to be at or near the initiating region, a number

Fig. 25. Effect of NaCl concentration on the assembly of PMV as measured by infectivity. PMV protein (1 mg/ml) and RNA (0.05 mg/ml) were incubated at 25°C in 0.01 M tris, pH 8.0, in the presence of various concentrations of NaCl added at 0 time (●-○) and 2 min after the initiation of assembly (○-○). After 30 min the assembly mixtures were digested with RNase T₁ and assayed for infectivity. Infectivities are expressed as percentages of those obtained with the samples to which no NaCl was added.

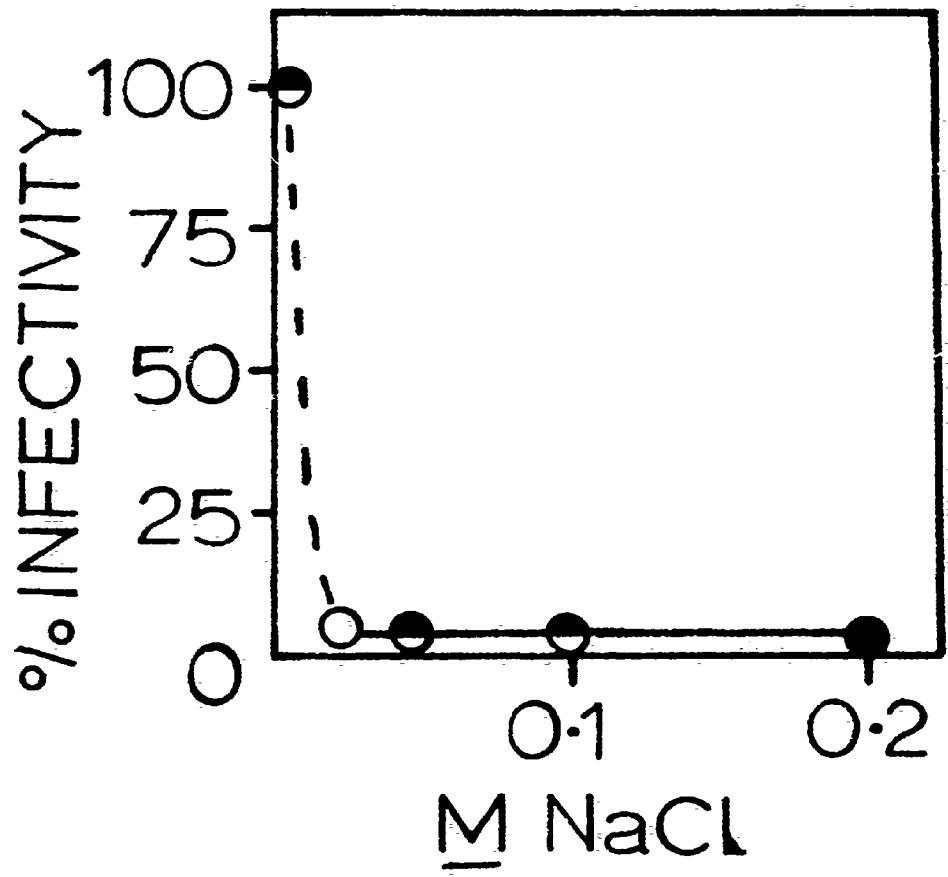


Fig. 26. Electron micrographs showing the effects of NaCl on PMV assembly. (A) NaCl added to 0.2 M at 0 time. (B) NaCl added to 0.2 M after 2 min. Assembly conditions are those described in Fig. 25. Bar represents 100 nm.

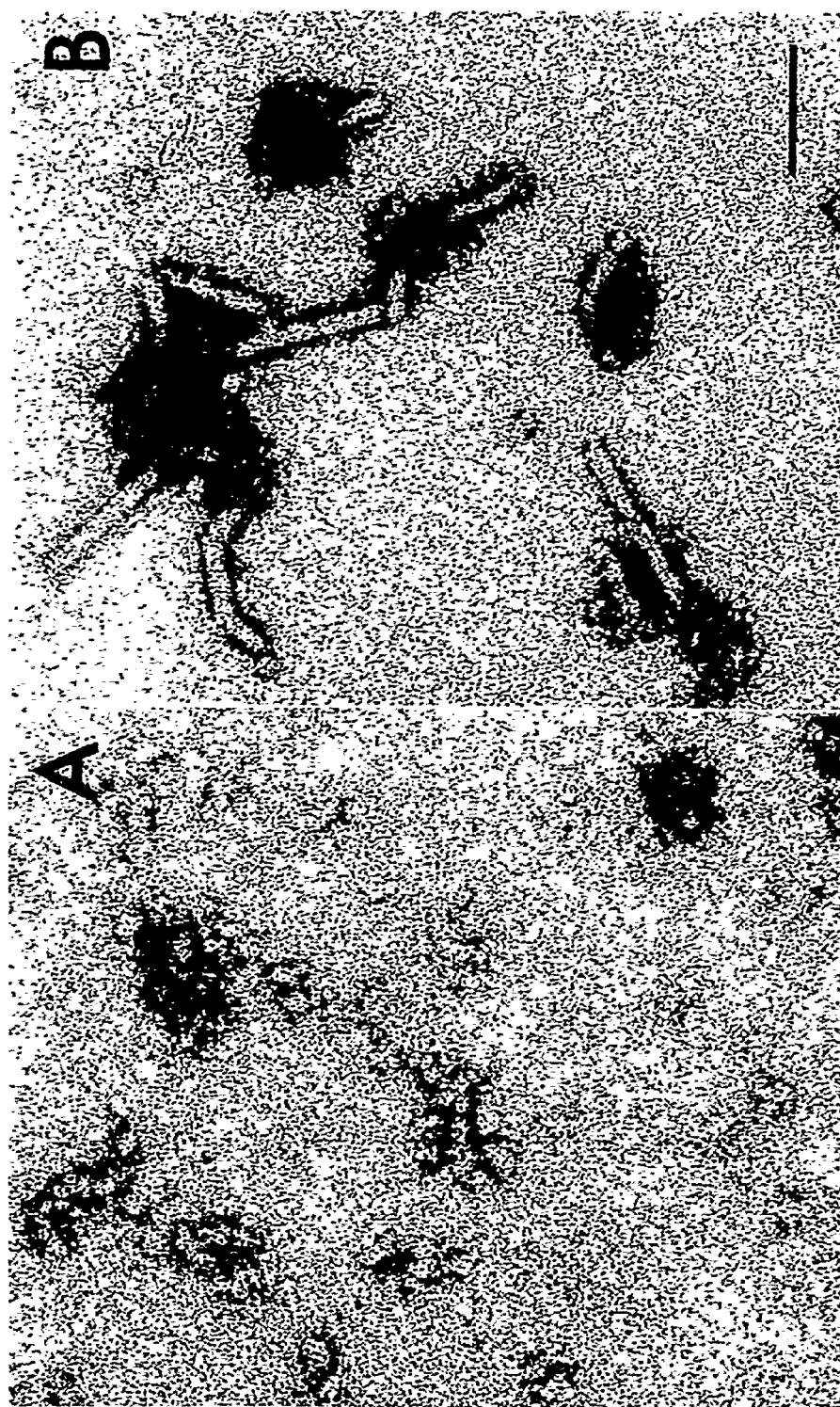
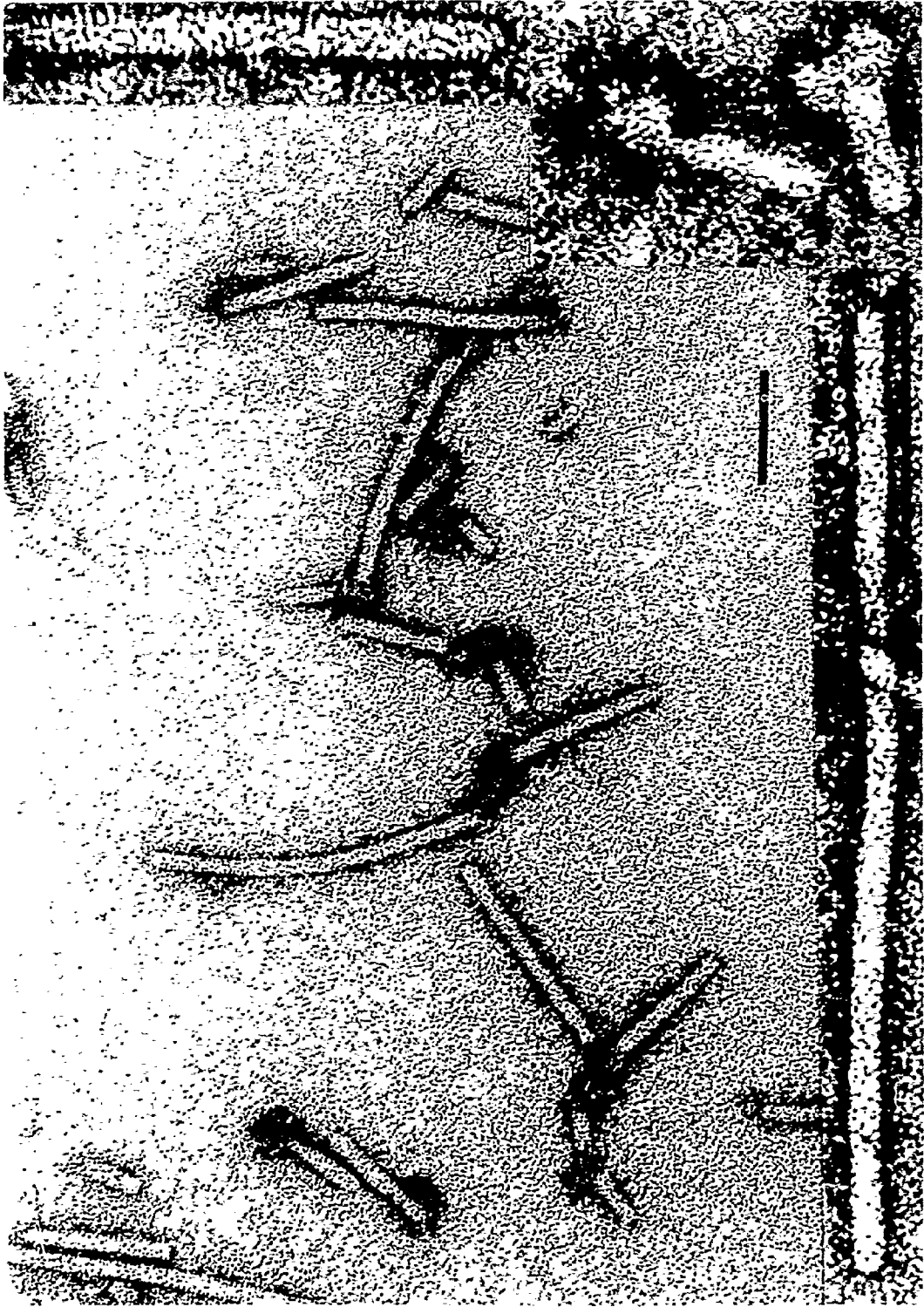


Fig. 27. The effect of NaCl on assembly. PMV assembled at 15°C for 20 min at pH 8.0 (0.01 M tris) and stopped by the addition of NaCl to 0.2 M. Bar represents 100 nm. Insets show high magnification micrographs of growing particles, stopped by NaCl, showing the rounded ends opposite the brushed ends. Bar represents 100 nm.



of convex-rounded ends, several of which are shown at high magnification for detail (Fig. 27 inset) are found. This suggests that the growing rod presents a concave surface at the elongating site.

NaCl greatly affected the 14S - 25S equilibrium of PMV protein. At pH 8.0 the sedimentation pattern was stable up to 0.025 M NaCl where, the 25S species predominated (Fig. 28A, B). At higher NaCl concentrations, however, the equilibrium was shifted increasingly towards the 14S species as is shown by the decrease in sedimentation coefficient and by the asymmetry of the Schlieren patterns (Fig. 28C - E). At 0.2 M NaCl only 14S and some slow sedimenting material (<3S, probably monomer) were found (Fig. 28F). These data, corroborated and extended by turbidity studies on the NaCl-induced disassembly of 25S protein which suggest a salting-in effect (Fig. 29), indicate that the presence of neither the 25S, the 14S, nor any minor protein species ensures that reconstitution will occur at 25°C if NaCl is present at a concentration of 0.025 M or greater at pH 8.0.

The rate of disassembly of the 25S aggregate in the presence of 0.2 M NaCl was rapid, the reaction being complete within 3 sec as judged by turbidity (Fig. 30). The rapidity of the reaction made it suitable for stopping assembly in kinetic studies (see Chapter 5).

Fig. 28. The effect of NaCl concentration on the 14S - 25S equilibrium of PMV protein at pH 8.0. Schlieren patterns of PMV protein at 1 mg/ml in 0.01 M tris, pH 8.0, containing: (A) no NaCl; (B) 0.025 M NaCl; (C) 0.05 M NaCl; (D) 0.10 M NaCl; (E) 0.2 M NaCl. The sedimentation coefficients of the fastest sedimenting species from (A) to (E) are 27S, 25S, 20S, 17S and 14S, respectively. (F) is a direct comparison of PMV protein at 3 mg/ml in 0.01 M tris, pH 8.0 in preparations containing no NaCl (upper) and 0.2 M NaCl (lower). All runs were performed at 52,460 rpm at 22 and 23°C. Sedimentation is to the right.

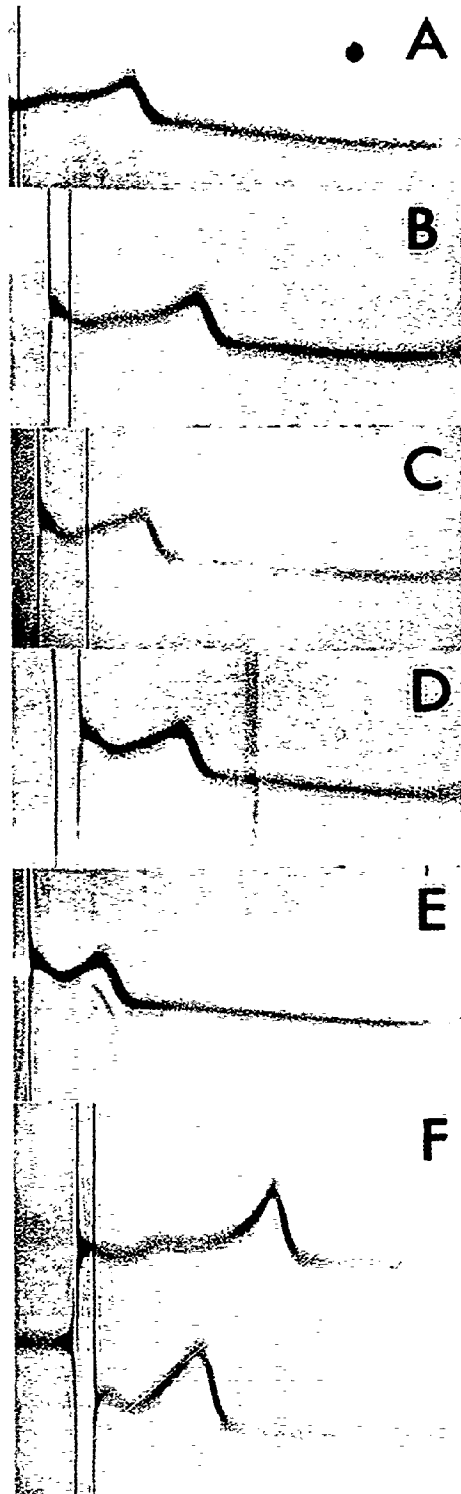


Fig. 29. Effect of NaCl concentration on the turbidity of PMV protein at pH 8.0. Protein at 2 mg/ml in water (pH 5.0) (A) was adjusted to pH 8.0 (0.01 M tris) by the addition of 10 μ l of 1.0 M tris, pH 8.0 (arrow). The change in turbidity at 310 nm was monitored in response to incremental additions of 2.0 M NaCl to final concentrations of: (B) 0.02 M; (C) 0.04 M; (D) 0.06 M; (E) 0.08 M; (F) 0.10 M; (G) 0.20 M. The reference cell was as for (G). The inset is a semilogarithmic plot of turbidity versus ionic strength (I) of NaCl. Temperature control was maintained throughout at 25°C.

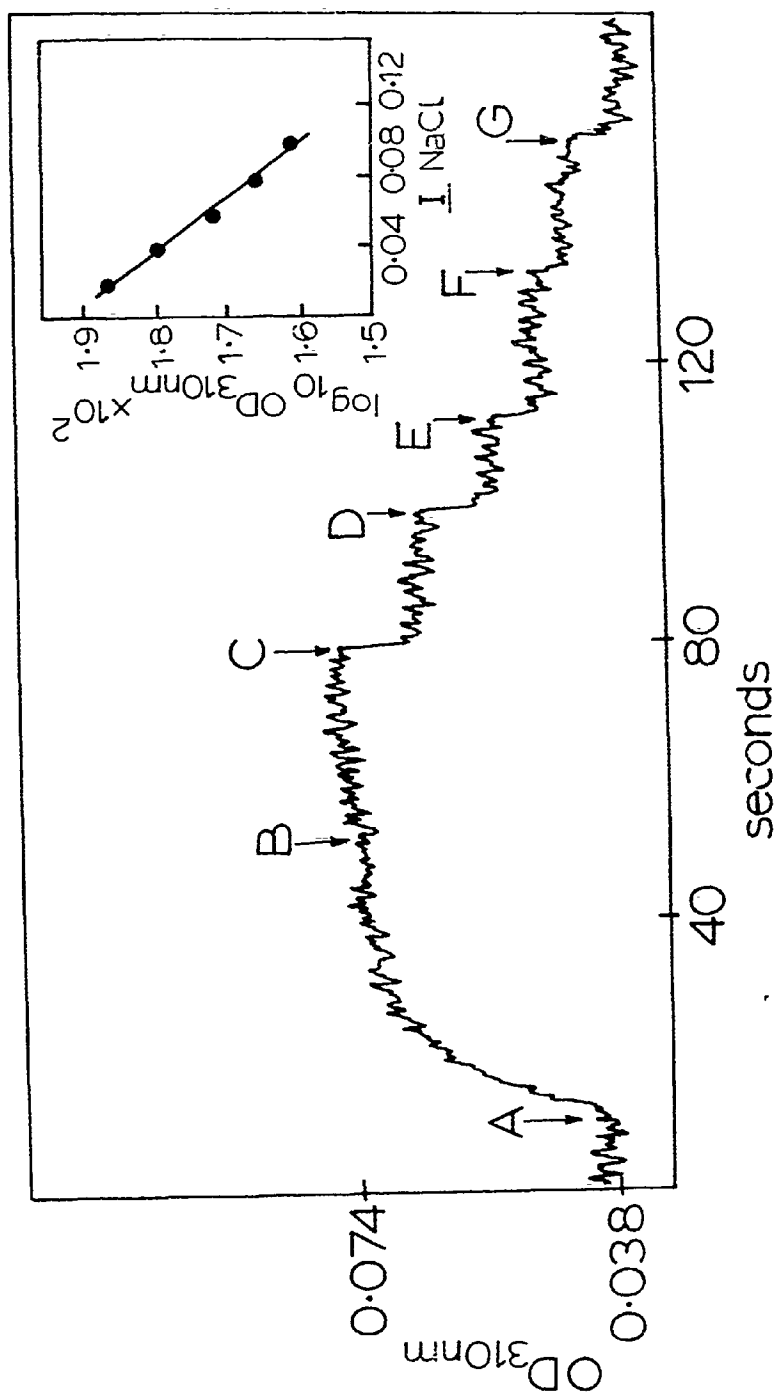
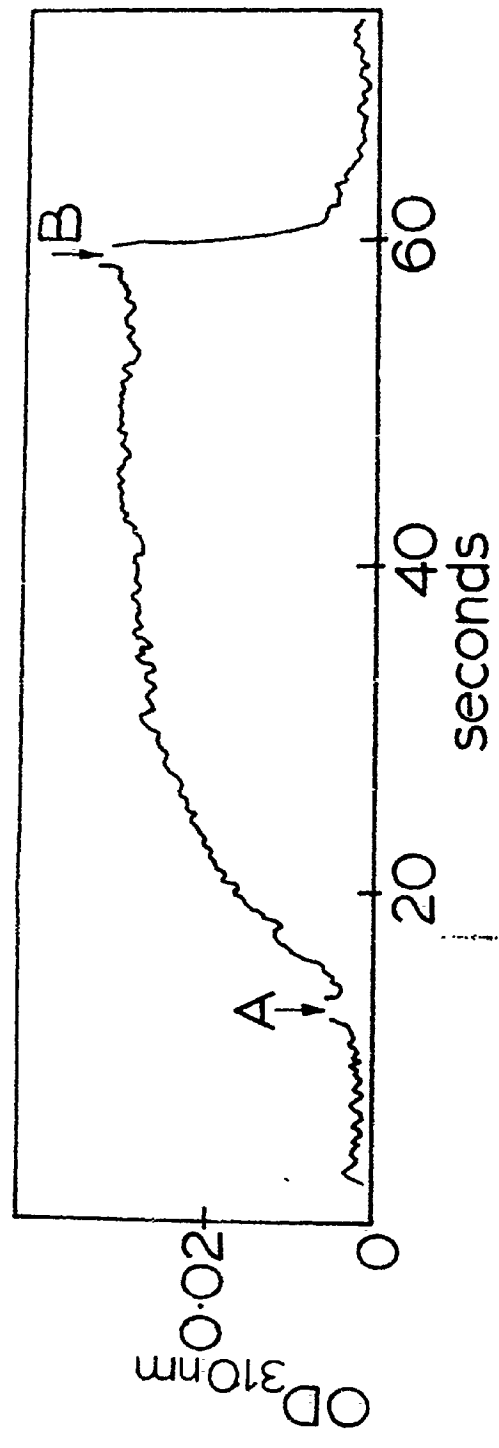


Fig. 30. Kinetics of NaCl-induced disassembly of 25S protein at pH 8.0. PMV protein at 1 mg/ml in water (pH 5.2) was adjusted to pH 8.0 (0.01 M tris) to form 25S protein (A). After equilibration in the cuvette, NaCl (0.1 ml) was added to 0.2 M (B) and the dissociation of 25S to 14S protein was monitored by the change in turbidity at 310 nm. The reference cell contained protein at 1 mg/ml in 0.01 M tris, 0.2 M NaCl at pH 8.0. Temperature was maintained at 25°C.



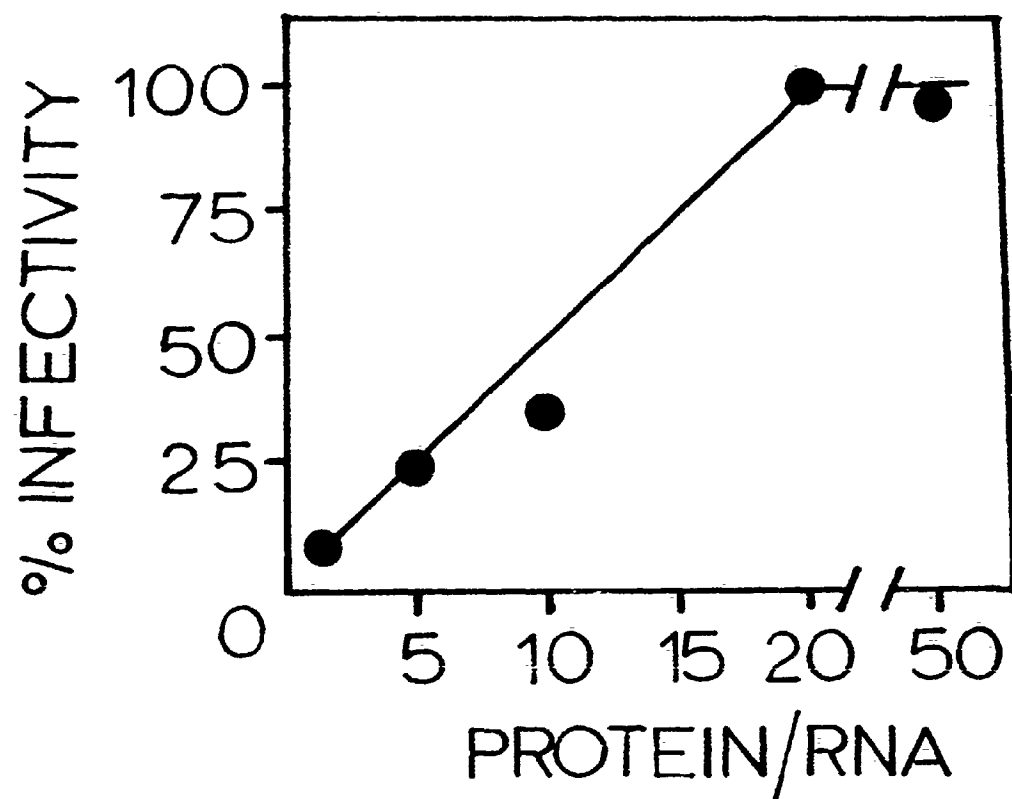
4.2.5 Stoichiometry

In typical reconstitution experiments a protein:RNA ratio of 20:1 was used since the RNA comprises about 5% of the weight of the native virus. That this is the optimal stoichiometry for virus assembly was tested by varying the incubation ratios of protein:RNA over the range 1:1 to 50:1 before measuring the yield of infective virus after treatment of the products with RNase T₁. When this was done under conditions of constant RNA concentration, the infectivity of assembled preparations increased linearly with increasing protein:RNA ratio up to 20:1 (Fig. 31). The fact that infective virus was found at the lower ratios (1:1 - 10:1) indicates that protein preferentially incorporated into growing particles. Alternatively, this may have been a reflection of partially degraded input RNA in which case only those RNA molecules that contained the coat protein binding site (AbouHaidar and Bancroft, 1978) produced proper products.

4.3 Discussion

The in vitro reconstitution of PMV has been described. Reconstitution proceeds best in stoichiometric mixtures at pH 8.0 - 8.5, requires moderate temperatures (25 - 30°C) and low ionic strength. PMV protein exists in a complex dynamic equilibrium among several polymeric forms under these conditions. The temperature, ionic

Fig. 31. Effect of protein:RNA ratio on PMV assembly at pH 8.0. PMV protein at various concentrations was reacted with RNA maintained at a constant concentration (0.04 mg/ml) in 0.01 M tris, pH 8.0, for 30 min before RNase T₁ digestion. Infectivities are expressed as percentages of that obtained at a protein:RNA ratio of 20:1. Temperature was 25°C.



strength and protein concentration dependencies of the equilibrium were studied in an effort to determine which protein aggregate is required for PMV assembly. The most prevalent form under a variety of environmental conditions sediments at 14S and contains about 16 subunits (see Chapter 3). A larger aggregate, the 25S protein, predominated under conditions usually employed in reconstitution and it is striking that the temperatures and ionic strengths required to form the 25S species were similar to those required for reconstitution at pH 8.0. These facts might suggest that the 25S species is a necessary subassembly form for virus assembly and indeed is a measure of the suitability of protein solutions for reconstitution if the 25S polymer is regarded simply as an indicator. But PMV could assemble efficiently at low protein concentrations where no 25S protein could be detected. This suggests, within the limits imposed by equilibrium mixtures, that it is not essential. Furthermore, protein from the related clover yellow mosaic virus (CYMV) forms only 4S and 14S polymers at 1 mg/ml at pH 8.0 at 25°C and yet it can reconstitute with its RNA (unpublished data). Also, potato virus X (PVX), which is related to PMV, reconstitutes in the apparent absence of large polymer (Goodman et al., 1976). On these comparative grounds and in terms of the present data, we believe that the pH 8.0 14S species may be necessary for at least part of the reconstitution process because we have not been able to demonstrate unequivocally that reconstitution occurs

in its absence. The reconstitution results at 0.1 mg/ml protein do not preclude the presence of a small quantity of the polymer. Initiation and elongation are two distinct phases in reconstitution. If, by analogy with TMV (Richards and Williams, 1972; Ohno et al., 1972a; Okada and Ohno, 1972; Butler and Finch, 1973; Ohno et al., 1977) or cucumber green mottle virus (Ohno et al., 1972b), the 14S polymer was necessary for initiation only, it would only have to represent about 1/75 by weight of the protein since the virus is 540 nm long and its pitch is 3.6 nm (Erickson, Bancroft & Horne, 1976). The 14S species may also be involved in elongation, but not in an obligatory sense, since reconstitution occurs in preparations at a protein concentration where only the 3S polymers can be detected as well as in preparations in which the 14S polymer is clearly present. However, it is conceivable that the presence of nucleic acid in the reconstitution medium may cause a rapid shift in the protein equilibrium.

The assembly of PMV can be divided into two distinct phases: initiation and elongation. Initiation is temperature independent over the range 0 - 25°C whereas elongation requires elevated temperatures. These conclusions are illustrated by the Arrhenius plot of the log percentage weight average rod length/30 min versus reciprocal absolute temperature (Fig. 17). The graph is linear from 25°C down to around 5°C, whereupon it tends to flatten out. This in-

dicates that there are at least two energetically and therefore mechanistically distinct components to assembly: a large, positive apparent activation energy-requiring component which occurs from 5 to 25°C; and a minimal activation energy-requiring component which occurs from 0 - 5°C. The latter component corresponds to the initiation phase, whereas the former described the elongation phase. Also, the activation energy is constant from 5 - 25°C and this suggests that elongation proceeds via the same mechanism over this temperature range.

The temperature requirement for elongation can best be considered to reflect the effect of temperature on the stability of protein-protein interactions in the virus. The rapid formation of helical capsids of PMV protein was found to require elevated temperature (see Chapter 3) as does the conversion of the 14S to 25S aggregate at pH 8.0. The latter polymerization is endothermic and entropy driven (see Chapter 7), and rapid helix formation probably is as well. The present results suggest that an entropy increase is required to overcome destabilizing electrostatic energies under certain conditions. Goodman (1977) concluded from studies on 8-anilino-1-naphthalene sulfonate binding that hydrophobic regions of PVX protein may be required for polymerization. The above considerations predict that the elongation phase of PMV assembly is endothermic but this can only be properly shown by thermodynamic studies of the assembly process.

Alternatively, the higher temperature may be required for an as yet undetected intermediate requisite conformational change of the protein and/or the nucleic acid. This intermediate step may be reflected by the positive apparent activation energy requirement for elongation (Fig. 17) in which case the temperature drive could be explained purely on kinetic grounds.

Initiation of PMV assembly takes place at low and high temperature. It is very rapid (see Chapter 5) and also specific at pH 8.0 (see Chapter 6). This event is probably mediated by a protein-nucleic acid recognition step characterized by having a very high affinity which overcomes the unfavorable protein-protein interactions at the lower temperatures. An interesting feature of initiation, as defined thus far, is that the average length of rods initiated in the cold is about 50 nm, or about 1/10 the length of native PMV. It is unlikely that the RNA recognition site for the coat protein amounts to 10% of the entire length of the RNA. This raises the question why rod growth proceeds, once initiated in the cold, to this particular length before stopping or becoming extremely slow. There are several possible explanations. One is that there are specialized nucleotide sequences for assembly within the PMV-RNA. For instance, there may be a highly favorable nucleotide sequence, composed of the first 600 nucleotides on the initiating end of the RNA, which is rapidly encap-

sidated even at low temperature. Zimmern (1977) proposed that the sequence of TMV RNA near the protein disc binding site contains at least three regularly repeated nucleotide sequences which promote dislocation and rearrangement of the 17 subunit disc form to the $16 \frac{1}{3}$ subunit "lock-washer" configuration and which is putatively required for proper helix elongation to occur. These sequences are probably distinct from those which promote disc binding. This hypothesis was employed to explain why, under protein-limiting conditions, the shortest initiation complex obtained with TMV RNA corresponds to a short rod containing three discs and about 150 nucleotides (Zimmern and Butler, 1977). An alternative way of looking at this is to postulate that there is a particularly unfavorable sequence at an appropriate distance in from the initiating end of the RNA for PMV. Unfavorable sequences have been postulated for TMV reconstitution (Stussi et al., 1969). A second possibility is that initiation and formation of the 50 nm rod on the one hand, and elongation on the other, are mediated by different protein subassembly aggregates. This idea follows from the observation that the protein at pH 8.0 exists in a particular equilibrium among a variety of polymorphic forms. A third explanation is based on Lauffer's hypothesis of electrostatic inhibition of rod polymerization (Lauffer, pp. 92ff, 1975). Assume that an initiation complex, presumably shorter than the 50 nm rod, forms in the cold and catalyzes elongation, even at the low temperatures. Rod growth, however, is a

function of the overall charge accumulation on the rod resulting from the successive addition of identically charged protein units. That is, at some critical charge level, the electrical work required to add the next protein unit becomes excessive and rod growth ceases unless the temperature is elevated. This explanation implies that the limited elongation found at 0 - 5°C is mechanistically equivalent to that which occurs at higher temperatures. This is unlikely since the Arrhenius plot is biphasic. On the other hand, a consequence of both the favored RNA sequence and the different subassembly requirement hypotheses is that initiation and elongation may proceed via energetically distinct mechanisms. This is in accord with the biphasic Arrhenius plot. Unfortunately, the present data as such cannot be utilized to distinguish between the two hypotheses.

An unusual feature of PMV assembly centers around the discovery of the extended particles. These particles, which probably result from a non-specific affinity of PMV protein for nucleic acid (see Chapters 5 and 6) are found at low and high temperatures at pH 8.0 (but not pH 6.0), are salt-labile and are sensitive to ribonuclease. Moreover, they are replaced by particles with virus-like morphology either by heating or by storage for several days at low temperature at pH 8.0. This is not due simply to further assembly of unreacted protein and RNA since virus-like particles can be formed from extended particles

which had been separated from unreacted assembly components by ultracentrifugation (unpublished data). Extended particles are also found at pH 8.0 when PMV protein is reacted with heterologous viral RNAs and DNA (see Chapter 6). Under these conditions initiation does not normally take place. The extended particles need not necessarily be assembly intermediates even if initiation has occurred as will be discussed in Chapter 5.

One other feature of PMV assembly worth mentioning is that growth seemingly occurs on a concave surface since the ends of the initiated particles appear to be convex. PMV assembly is initiated at or near the 5' terminus of the RNA (AbouHaidar and Bancroft, 1978). On the other hand, TMV is initiated nearer the 3' end (Zimmern, 1976). Nevertheless, rapid elongation, which proceeds toward the 5' end, also occurs presumably on a concave surface (Wilson *et al.*, 1976). Such a mechanism may provide a geometric advantage over growth on a convex surface. Indeed, most enzyme-substrate and antibody-antigen reactions occur in clefts, wherein the pre-formed combining site is protected from the external environment.

The assembly of PMV is inhibited by low levels of NaCl. This effect may be related to the behavior of the protein in NaCl. Protein helices formed at pH 4.0 in the absence of NaCl are very long whereas they are relatively short at the same pH but in 0.2 M NaCl (see

Chapter 3). Similarly the formation of the 25S aggregate at pH 8.0 is salt-sensitive. The linear dependence of the logarithm of the extent of 25S association upon NaCl concentration (Fig. 29) suggests that this is a result of a salting-in phenomenon. Typically, such phenomena are characterized by a salting-in equation of the form $\log_{10} f = -KI$ where f , K and I represent the activity coefficient of the salted-in species, the salting-in constant of the salt, and the ionic strength, respectively (Edsall and Wyman, pg. 304, 1958). The effect of NaCl can be viewed as a solubility enhancement of the 14S protein which, in turn, leads to dissociation of the 25S aggregate, the equilibrium having been shifted towards the 14S species. These considerations suggest that NaCl, at the concentrations employed, destabilizes protein interactions and probably therefore similar interactions in the virus. Extended particles cannot form in the presence of NaCl, and are collapsed upon addition of salt, showing that helical condensation of the nucleoprotein cannot occur in these conditions. The salt effect can be rationalized on thermodynamic grounds as resulting from its effect on water loss by the protein when it polymerizes (see Chapter 7), although there is no direct evidence on this point. Alternative explanations for the inhibition of PMV assembly by NaCl might involve the effect of salt on the stability of electrostatic interactions required for virus formation or on the secondary structure of PMV-RNA. It is unlikely that the salt-induced

inhibition of PMV assembly is the result of a chaotropic effect exerted by NaCl on the protein, as suggested for the inhibition of PVX assembly by salt (Goodman, 1977), since at the low concentrations employed the effect of NaCl on water structure is minimal. PMV will not assemble at pH 8.0 in the presence of a variety of simple salts around the 0.1 M level but will do so in 0.2 M glycine (unpublished data). Similar results have been found for PVX with salts in contradistinction to 0.2 M sodium N, N-bis (2-hydroxyethyl) glycine and 0.1 M sodium 2-(N-morpholino) ethane sulfonate (Goodman, 1977). It is clear that the supposed effects of large ions, particularly zwitterions, cannot be equated with those of less complicated additives, such as NaCl.

The formation of PMV nucleoproteins at pH 6.0 is characteristically different from that occurring at pH 8.0. The former process occurs at low temperature and takes only seconds. This can be visualized at 25°C as an immediate precipitation reaction which occurs upon the addition of RNA to protein at pH 6.0. The segmented or kinked appearance of particles made at lower pH (up to pH 7.5) indicates that multiple initiations occur under these conditions. The gaps between the segments may result from an intercalation problem, the helices being unable to anneal properly because they are out of phase. This probably accounts also for the increased sensitivity of these particles to ribonuclease T₁. Kinked particles have also

been observed as products of "mixed reconstitution" employing TMV protein with a mixture of TMV-RNA and RNA from the MS2 bacteriophage (Sugiyama, 1966). Such particles also were formed at pH levels below the optimum for TMV assembly and were susceptible to fragmentation by ribonuclease. There are several possible explanations for the pH effect on PMV assembly. The net charge on the protein at pH 6.0 is lower than at pH 8.0 and this should give rise to a more favorable enthalpy of the reconstitution reaction. Probably more important are the overall relative affinity and forward rate constants for the binding of the protein to the nucleic acid. They must be considerably higher at the lower pH, save for the recognition site, as is evidenced by the very rapid formation of nucleoproteins at lower pH and also by the increased stability of the virus in the presence of high concentrations of salts (see Chapter 3). Thus, nucleoprotein formation at low pH levels is thermodynamically "too easy" and the stringency imposed at the higher pH levels is lost, the nucleation barrier being broken. Also, the specificity of the reconstitution process found at pH 8.0 is lost at pH 6.0 with heterologous RNAs from unrelated viruses (see Chapter 6). Nucleoproteins, once formed at lower pH, are stable at pH 8.0 whereas the protein helices are not. This is the same effect as found for cowpea chlorotic mottle virus (Bancroft, 1970), TMV (Lauffer, pg. 160, 1975) and PVY (McDonald and Bancroft, 1977). The nucleoprotein particles are more stable than the capsids because

of protein-nucleic acid interactions which decrease the enthalpy of reconstitution at least for TMV (Lauffer, 1975).

The reconstitution of PMV occurs specifically under reasonable conditions except for the low salt level required which is troubling in view of what might be expected for an intracellular environment. Indeed, it may currently be most prudent to regard the assembly of PMV as merely an interesting example of ligand-nucleic acid interactions, notwithstanding that we have so far been unable to produce infectious particles in the presence of moderate concentrations of a number of common salts. In this regard, we note that not only PMV but all the flexuous viruses so far examined (potato virus Y (McDonald and Bancroft, 1977), PVX (Goodman, 1977) and CYMV (unpublished)) share the property of low salt inhibition which is also found with certain rigid tube viruses (tobacco rattle virus (Morris and Semancik, 1973), and barley stripe mosaic virus (Atabekov et al., 1970)), TMV being the exception, which may also be the only example of "correct" reconstitution of a helical virus. Nevertheless, it is not insignificant that the stabilities of nucleoprotein complexes for many common protein-nucleic acid recognition systems are reduced by several orders of magnitude when the concentrations of common monovalent salts, such as NaCl, are elevated over the range 0.01 M to 0.2 M (Record et al., 1976).

CHAPTER 5
KINETICS OF PMV ASSEMBLY

5.1 Introduction

A nucleoprotein resembling papaya mosaic virus may be assembled in vitro (Chapter 4). This chapter contains a description of the kinetics of the reconstitution reaction which starts on a unique region of PMV-RNA at or near its 5' end (AbouHaidar and Bancroft, 1978), and it is shown that the assembly process is composed of a rapid initiation phase and a slower elongation phase. The kinetics of the elongation phase are analyzed in terms of a bimolecular reaction model which is formally described by second-order kinetics. Additionally, detailed electron microscopic analysis of the particle length distributions resulting from the assembly experiments suggests a dependence of the elongation rate on the local RNA structure.

5.2 Experimental results

5.2.1 Assembly kinetics in stoichiometric (20:1) conditions

The time course of PMV assembly was studied at pH 8.0 (0.01 M tris buffer) at 25°C using approximately stoichiometric proportions of coat protein and RNA (20:1, respectively). Assembly was stopped by the addition of NaCl to 0.2 M (see Chapter 4). This procedure halts assembly

more rapidly than does a drop in temperature. Assembly mixtures acquired maximal RNase T_1 -resistant infectivity after about 20 minutes; turbidity measurements showed similar kinetics after an initial rapid rise (Fig. 32).

The kinetics of virus formation was analyzed more precisely by electron microscopy. Both number and length-weighted distributions of nucleoprotein particle lengths were constructed (Fig. 33). Rods in the 20-60 nm length classes were formed within about 20 sec, and this correlates well with the turbidity measurements (see Fig. 32). There was little change in the shape of the histograms between 10 and 20 min, signifying the completion of rod growth. The large number of short rods present at all times probably reflects the physical state of the RNA (see below). The maximum weight average length ranged from 210 to 370 nm in three separate experiments and averaged about 290 nm, the length of PMV being 540 nm. Butler and Finch (1973) found that the weight average length of reconstituted TMV particles was about 50% that of native TMV.

The time course of PMV assembly is most easily visualized by plotting the number average and weight average lengths of assembled particles versus time (Fig. 34). These plots clearly show that the reconstitution process is biphasic, consisting of an initial rapid growth phase (initiation reaction), which is finished by 20 sec, and a slower growth phase (elongation reaction), whose rate decreased with

Fig. 32. Kinetics of PMV assembly as measured by infectivity and turbidity. PMV protein and RNA at 1.0 and 0.05 mg/ml, respectively, were reacted in 0.01 M tris buffer, pH 8.0, at 25°C for the times indicated. Both turbidity ($A_{310 \text{ nm}}$) and infectivity of RNase T_1 -treated samples are expressed relative to the values obtained at 20 min.

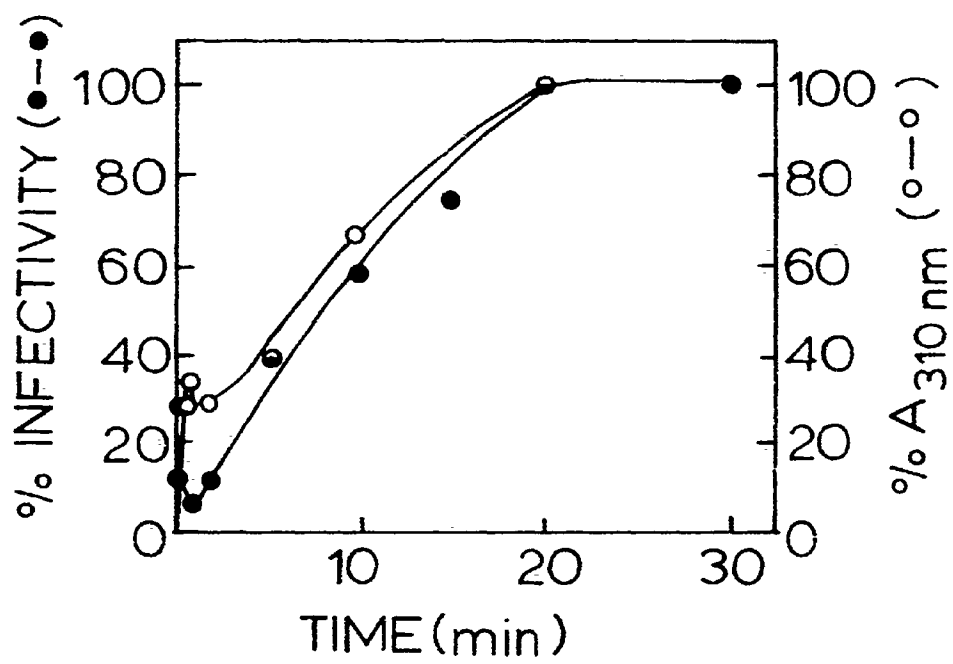


Fig. 33. Histograms of particle length distributions for PMV assembly products after various times. See Fig. 32 for reaction conditions. Protein:RNA ratio = 20:1. 4356 particles were measured in total for an average of 545 particles per time point.

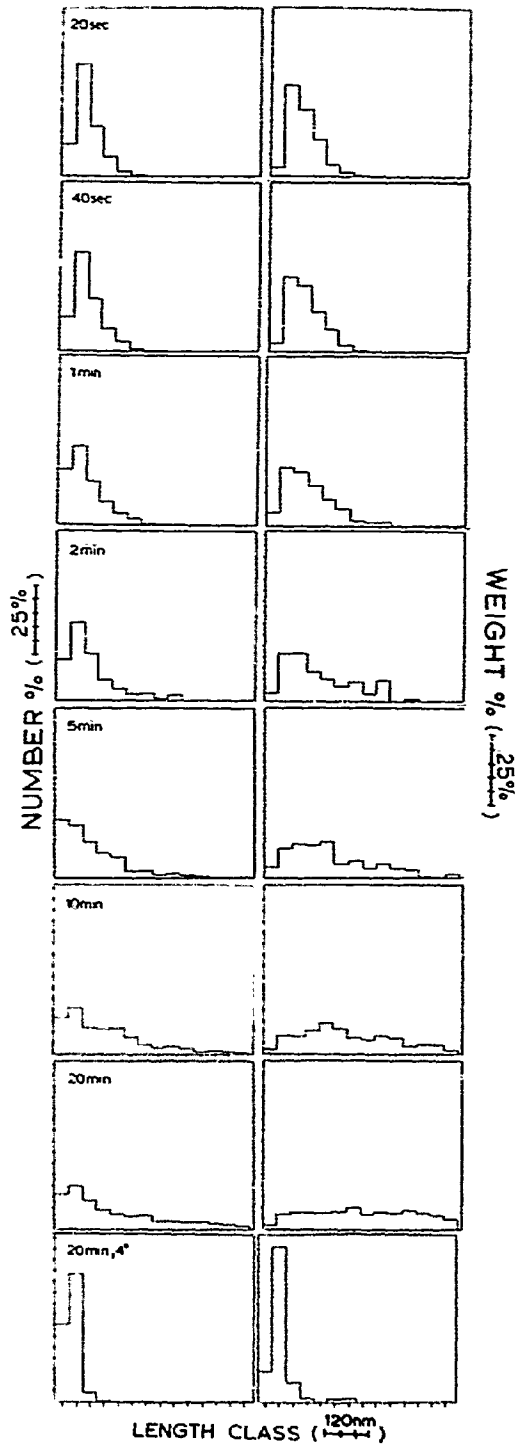
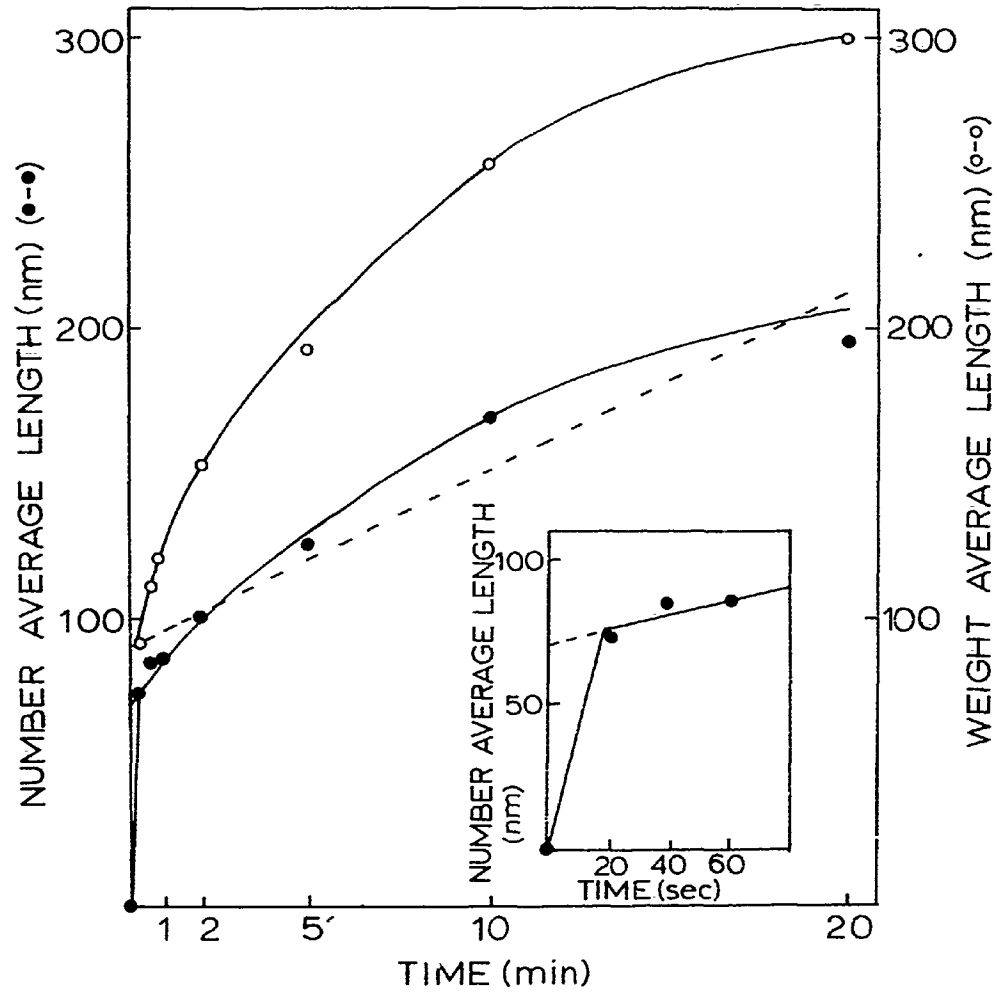


Fig. 34. Number and weight average rod lengths measured during the course of the PMV self-assembly reaction. See Fig. 32 for reaction conditions. ●-●, weight average length, empirical curve. ○-○, number average length, theoretical curve obtained after correcting for the time dependency of the number of growing ends. The dashed line represents the uncorrected theoretical curve for the number average length. See text for further details. The inset shows the relationship of the number average rod length with time on an expanded time scale in order to emphasize the biphasic assembly kinetics. The curves were empirically drawn and used for the graphical rate analysis which is described in the text.



time until completion of the reaction by about 20 min. The rate of the initial growth phase was difficult to measure precisely due to its rapidity, but certainly was greater than 10x that of the elongation phase, whose initial rate was estimated graphically (Fig. 34, inset) at around 15 nm/min.

Comparison of the weight average plot with the number average plot gives a relative measure of the heterogeneity of the length distributions. It can be inferred from the greater slope of the weight average plot that the heterogeneity of the length distribution of reconstituted PMV particles increased with time. This situation probably arose from a decrease, rather than an increase, in the number of growing centers with time since the initiation phase of assembly is very rapid and complete within 20 sec. A decrease in the number of growing centers is consistent with the idea that the RNA in the reaction mixture was broken into fragments of varying lengths. Alternatively, unfavorable sequences, which would represent stopping points for the elongation reaction, may exist at intervals throughout the RNA sequence.

5.2.2 Low temperature assembly

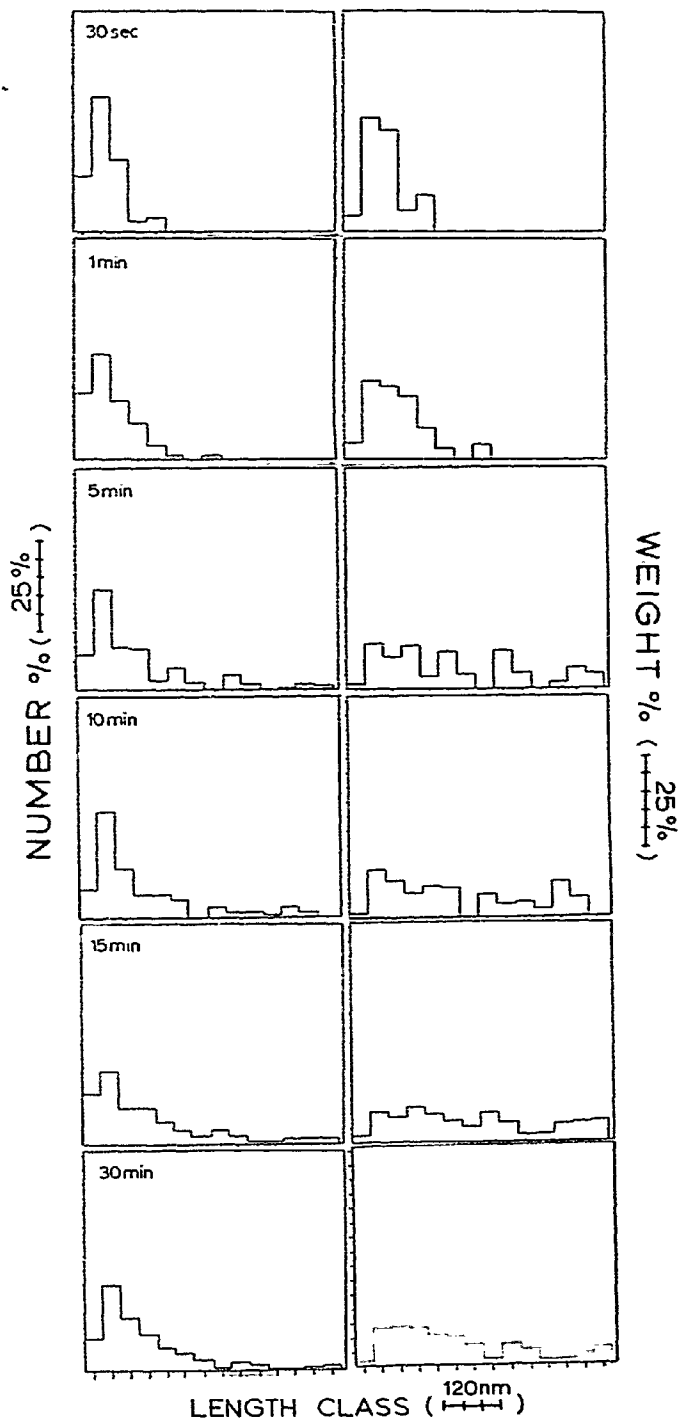
PMV reconstitution is also biphasic with respect to temperature (see Chapter 4). The assembly reaction consists of an early, temperature-independent initiation

phase and a temperature-dependent elongation phase. For purposes of comparison with the present series of experiments, a PMV assembly mixture was incubated for 20 min at 4°C. The length distributions are shown in Fig. 33. The resulting number average length was 55 nm, in good agreement with the previously reported value of about 50 nm (Chapter 4). The value is also close to the 73 nm number average length of the distribution which results from a 20 sec reconstitution at 25°C.

5.2.3 Assembly kinetics in protein excess (80:1)

The retardation of the elongation rate at later times in the assembly reaction with stoichiometric mixtures probably resulted from the free protein concentration becoming rate-limiting, suggesting an effective second-order reaction mechanism for the elongation phase of PMV assembly. This being so, an increase in the protein:RNA ratio at constant RNA concentration should result in a faster elongation rate. PMV was assembled with a protein:RNA ratio of 80:1 (w:w), under which conditions the free protein concentration is excessive throughout the entire course of the reaction. The RNA concentration was the same as for the 20:1 reaction. The particle length distributions (Fig. 35) from the 80:1 reconstitution were similar to those of the 20:1 reconstitution after short times (1 min or less). Thereafter, the distribution stabilized by about 5 min, as

Fig. 35. Histograms of particle length distributions for PMV assembly products after various times. PMV protein and RNA at 4.0 and 0.05 mg/ml, respectively, were reacted in 0.01 M tris buffer, pH 8.0, at 25°C for the times indicated. Protein:RNA ratio = 80:1. 883 total particles were measured for an average of 147 particles per time point.



compared to between 10 and 20 min for the 20:1 reaction.

An interesting feature of the particle length distributions which was particularly clear in the 80:1 experiment is that there is a tendency for assembly reactions not to produce observable particles in the 260-300 nm length classes. This is seen in both the 80:1 and 20:1 experiments as a minimum around the 260-300 nm classes in the particle length distributions (Figs. 33 and 35). Histograms from an independent 20:1 experiment, in which the minima are more pronounced, are shown in Fig. 36.

Graphical analysis of the number average and weight average particle lengths for the 80:1 reconstitution demonstrate again the biphasic character of the assembly kinetics (Fig. 37). The excessive concentration of free protein, however, resulted in a nearly linear growth rate for the elongation phase of assembly up until about 5 min, within which time the reaction was completed. The initial rate of elongation is about 66 nm/min, which is nearly 4x faster than that of the elongation rate in the 20:1 assembly experiment. This is the value predicted on the basis of a reaction mechanism which is first-order with respect to protein (see below), the ratio of the protein concentrations in the two experiments also being 4:1.

The weight average length increased at a faster rate than the number average length, again attesting to the

Fig. 36. Histograms of particle length distributions for PMV assembly products after various times. See Fig. 32 for reaction conditions. Protein:RNA ratio = 20:1. 1076 total particles were measured for an average of 359 particles per time point.

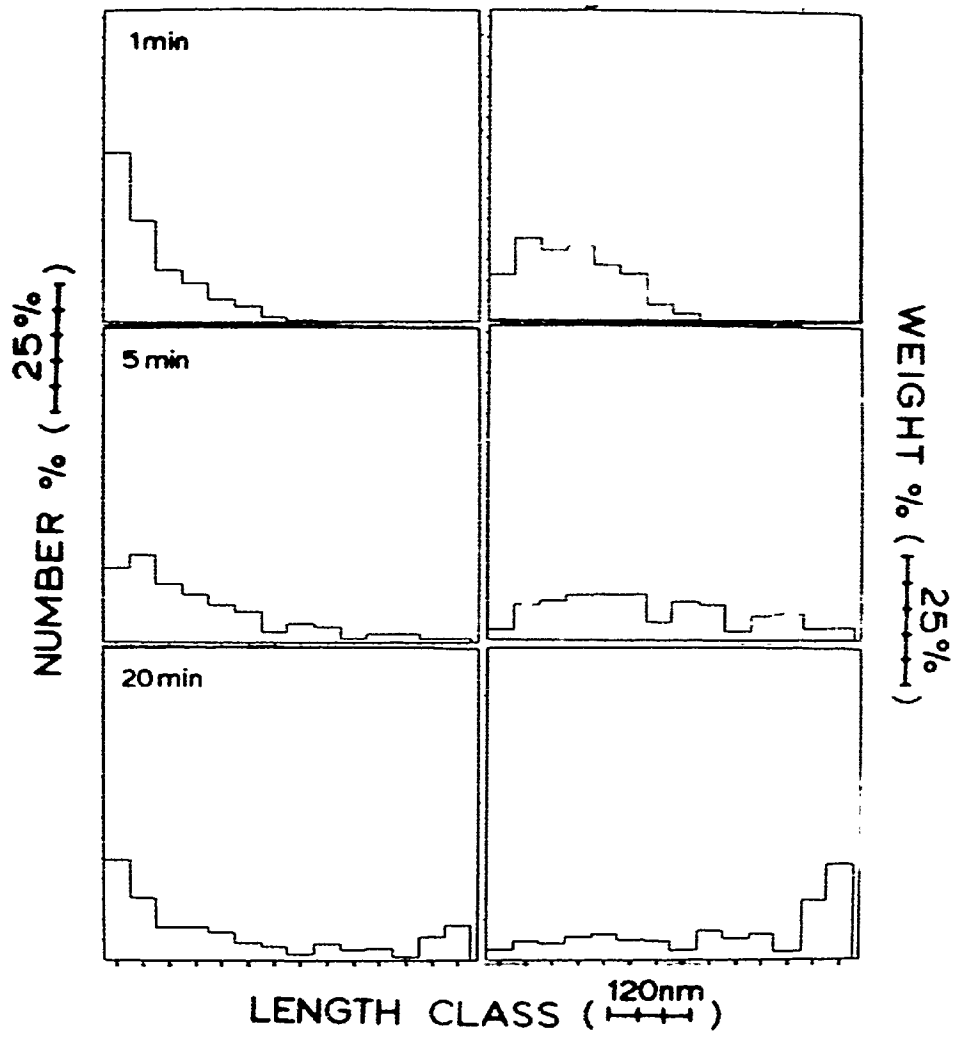
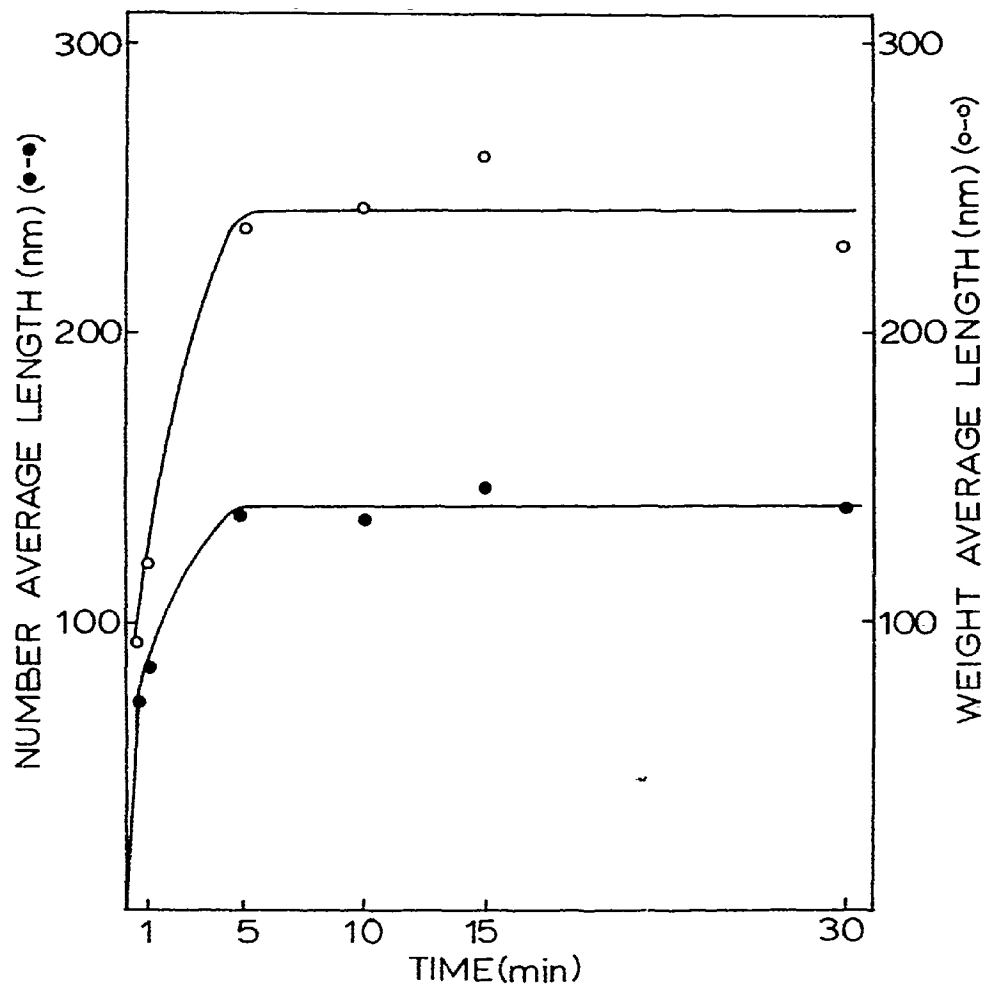


Fig. 37. Number and weight average rod lengths measured during the course of the 80:1 PMV assembly reaction. See Fig. 35 for reaction conditions: ●-●, weight average length, empirical curve; o-o, number average length, empirical curve.



increasing size heterogeneity of assembled products in the reaction mixture.

5.3 Kinetic model of assembly: theoretical analysis

The rate of elongation, or the average rate of rod growth, may be defined as dN/dt and must be proportional to the rate of consumption of protein subassembly units, $-dP_1/dt$, and inversely proportional to the number of ribonucleoprotein growing ends, RP , so that

$$\frac{dN}{dt} = \frac{C}{[RP]} \frac{d[P_1]}{dt} \quad (2);$$

where N is the number average particle length, and the brackets denote molar concentration. C is a proportionality constant, in units of nm, which represents the incremental length increase per subassembly unit per growing end. An expression for $d[P_1]/dt$, and thus dN/dt , can be derived from a consideration of a simple model for assembly in which the rate of consumption of protein is proportional to the instantaneous concentrations of growing ends and free protein subassembly units. Such a model may be represented by



where RP_n and RP_{n+1} represent growing ends containing n and $n+1$ protein subassembly units, respectively, and k_g and

k_d represent the rate constants for the forward and backward reactions, respectively. The actual identity of P_1 , whether monomer or 14S polymer, for example, is not a critical factor for the mathematical treatment of this model.

The rate of disappearance of P_1 for the reaction model described by equation (3) may be given by

$$-\frac{d[P_1]}{dt} = k_g [P_1] \Sigma [RP_n] - k_d \Sigma [RP_{n+1}] \quad (4).$$

Assuming that $k_g \gg k_d$, and since $\Sigma [RP_n] = [RP]$, equations (2) and (4) may be combined to yield

$$\frac{dN}{dt} = C k_g [P_1] \quad (5).$$

Let N_{\max} represent the maximum number average length attainable (assuming that the RNA is infinitely long) in a particular assembly reaction, so that

$$N_{\max} = C \frac{[P_1]_0}{[RP]_0} \quad (6),$$

where $[]_0$ designates initial molar concentration. Then, as elongation proceeds, the instantaneous concentration of P_1 is given by

$$[P_1] = \frac{(N_{\max} - N)}{C} [RP] \quad (7);$$

and, by substitution into equation (5),

$$\frac{dN}{dt} = k_g [RP] (N_{\max} - N) \quad (8).$$

Integration and rearrangement of equation (8) yields

$$\ln \left(\frac{N_{\max}}{N_{\max} - N} \right) = k_g [RP] t \quad (9),$$

which is the desired relationship between the readily measured quantities of number average length and time. Equation (9) is another form of the common exponential function $Y = Y_{\max} (1 - e^{-ax})$, where $a = k_g [RP]$ for this case. While this function is common to kinetic descriptions of first order-reaction mechanisms (see Moore, 1962, pg. 260), it also appears in solutions to second-order processes in the special case where the concentration of one of the reactants remains constant throughout the reaction.

If the number of growing ends remains constant (except for initiation and completion of assembly) throughout the reaction, then $[RP]$ equals the input RNA concentration $[RNA]_0$ and a plot of $\ln \left(\frac{N_{\max}}{N_{\max} - N} \right)$ versus t should give a straight line whose slope is $k_g [RNA]_0$. Fig. 34 (dashed line) shows the theoretical curve obtained by fitting the experimental data to equation (9), where $[RP]$ equals $[RNA]_0$. This curve approximates the observed points poorly; moreover, the predicted initial rate of elongation, given in equation (8), is about 7 nm/min, only about half the observed rate.

5.3.1 Correcting for the time-dependent distribution of growing ends

Comparison of the weight and number average plots in Fig. 34 indicated that the number of growing ends decreased with time (see above), so that the assumption of constant [RP] might easily be responsible for the observed deviation between theory and observation. In order to approximate the time-dependence of [RP], the particle length distributions were corrected in a manner somewhat similar to the method used for correcting TMV particle length distributions for degraded RNA (Butler and Finch, 1973).

The ultimate length-proportion distribution attainable for a particular experiment was determined from the histograms at later times. In the 20:1 experiment, the 20 min histogram was assumed to represent the ultimate proportion distribution of particle lengths; in the 80:1 experiment, the final proportion distribution was determined by averaging the 5, 10, 15 and 30 min histograms. Next, the time at which the proportion of particles in a given length class exceeded the final proportion was determined, and from that distribution and all subsequent ones (excepting the last) the final proportion was subtracted from the appropriate length class, and the remainder was taken to represent the corrected proportion of growing ends of that class. For each distribution, the corrected proportions

for each length class were summed to give the fractions of growing centers for each time. For example, if the final distribution of particles resulted in 200 out of 1000 in the 60 nm length class, and if there were 400 out of 1000 particles in that same class by one minute, then of those 400 particles only 200 may represent growing ends. Thus, the concentration of growing centers at one minute would be reduced by 200 out of a 1000, or 20%. In this manner, the fractions f of growing centers at the various times were calculated relative to zero time. The zero time concentration of growing centers $[RP]_0$ was assumed to equal $[RNA]_0$. Equation (9) can then be written as

$$\ln \frac{N_{\max}}{N_{\max} - N} = k_g f [RNA]_0 t \quad (10).$$

Fig. 34 shows the theoretical curve obtained by fitting the data of the 20:1 experiment to equation (10). The correlation for the fit is >0.99 . This demonstrates that when time-dependence for the concentration of growing ends is taken into account, the elongation process can be satisfactorily described by a second-order reaction mechanism.

5.3.2 Kinetic parameters for elongation

In the model described above, the rate constant, k_g , for the elongation reaction should be independent of

protein concentration. This can be tested by plotting $\ln \left(\frac{N_{\max}}{N_{\max} - N} \right)$ versus $f[\text{RNA}]_0 t$ for the data from the 20:1 and 80:1 experiments. These plots are presented in Fig. 38 and, while the plot for the 80:1 experiment contains only two experimental points, the slopes are very similar. Values for k_g of 1.7×10^6 and 1.9×10^6 $\text{l mole}^{-1} \text{min}^{-1}$ for the 20:1 and 80:1 experiments, respectively, were calculated. The linear least-squares method was employed to obtain best-fitting equations of

$$\ln \frac{844 \text{ nm}}{844 \text{ nm} - N} = 1.7 \times 10^6 \text{ l mole}^{-1} \text{ min}^{-1} f[\text{RNA}]_0 t + 0.087 \quad (11)$$

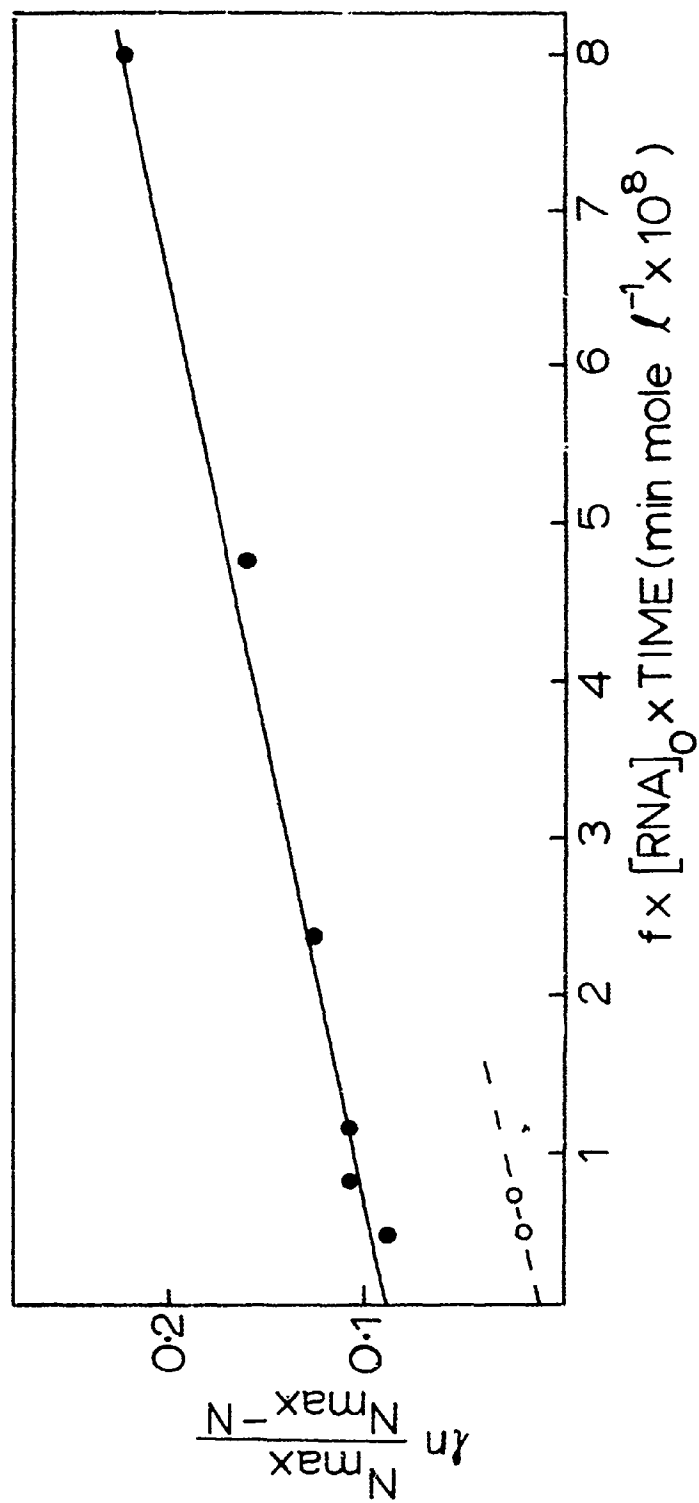
for the 20:1 experiment, and

$$\ln \frac{3375 \text{ nm}}{3375 \text{ nm} - N} = 1.9 \times 10^6 \text{ l mole}^{-1} \text{ min}^{-1} f[\text{RNA}]_0 t + 0.012 \quad (12)$$

for the 80:1 experiment. The values for N_{\max} were calculated based on the starting concentrations of protein and RNA. The non-zero intercepts resulted from the initiation phase of assembly.

The initial rates of elongation were calculated from equation (8) as 33 nm/min and 158 nm/min for the 20:1 and 80:1 experiments, respectively. These rates, while exhibiting approximately the correct ratio, are higher than the observed rates by factors of 2 and 2.4, respectively; however, these differences can be reconciled by assuming that the concentrations of growing ends at zero time equalled

Fig. 38. Interpretation of the data for the 20:1 and 80:1 experiments according to equation (9). It was assumed that the values of N_{\max} are 844 and 3325 nm for the 20:1 and 80:1 experiments, respectively. Lines were drawn according to a linear least-squares fitting routine.



0.5x and 0.4x $[RNA]_0$, respectively. This is reasonable because the corrected [RP] for the 20 sec (20:1 experiment) and 30 sec (80:1 experiment) length distributions were .56x and .41 x $[RNA]_0$, respectively.

5.4 Discussion

The kinetics of PMV reconstitution reflects the mechanics of the assembly process. Two distinct phases, initiation and elongation, can be distinguished. The biphasic kinetics correlates with the biphasic temperature dependence of PMV assembly (see Chapter 4). Initiation at 25°C or at 1°C is the same process; the particle lengths in both cases are similar and encapsidation starts at or near the 5' end of PMV-RNA at either temperature (AbouHaidar and Bancroft, 1978). At 25°C at 1 mg/ml of protein and with a protein:RNA ratio of 20:1, elongation initially proceeded at an observed rate of about 16 nm/min, which is less than 1/10 that of the observed rate of initiation. TMV assembly also displays biphasic kinetics, having a rapid initiation phase and a slower elongation phase (Butler and Klug, 1971), but, unlike the case with PMV, both phases have the same temperature requirement.

The initiation phase of PMV assembly occurred too rapidly for a detailed kinetic analysis. The kinetics of the slower elongation phase is more readily measured and can be described by a bimolecular, second-order

reaction mechanism in which the rate-limiting step is the productive collision of a protein sub-assembly unit with a growing end. It is easy to show experimentally that the diffusion rate, per se, of the reactants is not rate-limiting since, at pH 6.0, rods are made instantaneously upon mixing the RNA and protein (see Chapter 4). A minimum estimate for the diffusion-controlled rate constant for a bimolecular reaction between PMV protein (14S polymer) and RNA can be calculated for the 20:1 reaction by applying von Smoluchowski's treatment of collision theory (see Hague, 1971, pg. 12); it approximates to 10^{12} l mole⁻¹ min⁻¹. This value is roughly 6 orders of magnitude higher than that (1.8×10^6 l mole⁻¹ min⁻¹) calculated for the forward rate constant for the elongation reaction and emphasizes the relatively low productive collision probability which governs the elongation rate.

Although when the time-dependence of the concentration of the growing ends is approximated a theoretical growth curve exhibiting an exponential time-dependence and closely fitting the experimental points can be generated (Figs. 34 and 38), another theoretical curve can be drawn. The latter, which also closely fits the experimental points, exhibits a linear time-dependence and is suggestive of a rearrangement rate-limited reaction. Such a mechanism should be characterized by a rearrangement rate constant which is independent of protein concentration.

However, when the 20:1 and 80:1 experiments were analyzed according to this scheme, their rate constants differed by more than 5-fold. Therefore, it seems unlikely that a rearrangement model is correct. This does not mean that there is no conformational rearrangement step required in elongation, but it does mean that, if it occurs, it is not rate-limiting.

The distinction between a rearrangement and a productive collision rate-limiting step is important for a consideration of a possible role for the extended particles observed in PMV assembly experiments (see Chapter 4). It was shown that, in the apparent absence of free protein, extended particles, which are formed very rapidly, could give rise to tubular ones. We considered the possibility of a rearrangement mechanism in which the rearrangement, at the growing end, of the extended particle into the virus helix would be the rate-limiting step. Elongation by such a mechanism has been rejected on kinetic grounds. This rejection can be reconciled with experimental observation only if protein subunits in the extended particles are in rapid equilibrium with a free protein pool. Experiments with ³⁵S-labelled PMV protein have shown that radioactive protein subunits bound to the extended particles are indeed exchanged relatively rapidly with added unlabelled subunits indicating a dynamic equilibrium between free and extended particle-bound protein (unpublished data). On the other

hand, protein incorporated into virus-like rods does not exchange detectably. Thus, assuming the equilibrium is rapid enough, there is no compelling need to consider extended particles as a necessary intermediate in virus elongation since the protein subassembly units can be considered to exist in a pool of free protein. It is conceivable that extended particles serve to concentrate, in the vicinity of the growing centers, free protein thus acting, in a sense, as catalysts for the elongation reaction. Using the lac repressor-operator system as a model, Berg and Blomberg (1976) have hypothesized that non-specific site binding facilitates the specific site binding exhibited by regulatory proteins for nucleic acids via a one-dimensional diffusion process. However, it is probably more realistic to envisage the formation of extended particles simply as the result of a non-specific, non-functional affinity of PMV protein for nucleic acid under low ionic strengths.

TMV elongation has been analyzed according to Michaelis-Menten enzyme kinetics as a two-step process: a bimolecular productive collision event, which is first-order with respect to protein concentration, followed by a conformational rearrangement step which is independent of protein concentration and which, at high protein concentration, becomes rate-limiting (Butler, 1972; 1974). Evidence for a rearrangement step in PMV elongation has not been found, perhaps because the protein concentrations used

in these studies were not high enough. Nevertheless, under similar assembly conditions, 25°C, protein:RNA ratio 80:1, .05 mg/ml RNA, the rates of TMV and PMV elongation are comparable in magnitude. Thus, under the above conditions, the maximum rearrangement-limited elongation rate for TMV was calculated to be between 330 and 460 protein subunits/min, while the productive collision-limited elongation rate for PMV was calculated from theoretical considerations to be about 158 nm/min or about 420 subunits/min.

There are at least two inhomogeneities in the particle length distributions for PMV assembly. One is the 50 nm long particle formed as a result of the rapid initiation phase. The second results in a minimum in particle length distributions around 260 - 300 nm. Conceivably, there is a nucleotide sequence about 1/2 way along the RNA which allows elongation to proceed at such a rapid rate that very few particles are actually detected elongating in that region. Evidence for local RNA structure influencing elongation has been presented for TMV assembly as well (Stussi et al., 1969; Zimmer, 1977). Thus, kinetic models of virus assembly, while certainly being useful for elucidating general mechanisms, tend to be oversimplifications of a basic process, the rate of which can apparently be influenced locally by the fine structure of a complex molecule.

CHAPTER 6
SPECIFICITY OF PMV ASSEMBLY

6.1 Introduction

This chapter presents evidence to show that the virus assembly reaction with PMV protein is specific to PMV-RNA or that from at least one related virus and this behavior is compared with that obtained with synthetic homopolymers. It is also demonstrated that at least two types of non-specific reactions can occur with a variety of nucleic acids under certain conditions.

6.2 Experimental results

6.2.1 Assembly with plant virus RNAs

The specificity of the PMV assembly process was investigated by mixing PMV protein with PMV-RNA, CYMV-RNA, TMV-RNA and BMV-RNA at different pH levels. At pH 6.0 the products formed sedimented at rates not greatly different from that of PMV (Fig. 39, A1 - A4). Electron micrographs of the preparations showed "kinked" particles (see Chapter 4) in all cases (Fig. 40 A - C, left) indicating that the assembly reaction at pH 6.0 was non-specific and that the products were faulty.

Fig. 39. Specificity of the assembly reaction of PMV protein with various plant virus RNAs as a function of pH: sedimentation analysis. Density-gradient profiles of results from assembly experiments with PMV protein incubated at:

(A) pH 6.0, with PMV-RNA (A1), CYMV-RNA (A2), TMV-RNA (A3) and BMV-RNA (A4), the arrow denotes the position of PMV;

(B) pH 8.0, with PMV-RNA (B1), CYMV-RNA (B2), TMV-RNA (B3) and BMV-RNA (B4), the arrow denotes the position of PMV;

pH 7.0 (C1) and 7.5 (C2) with TMV-RNA, the upper arrow marks the position of PMV and the lower one marks the position of TMV-RNA reacted with PMV protein at pH 8.0; pH 7.0 (C3) and 7.5 (C4) with BMV-RNA, the two arrows marking the position of BMV-RNA reacted with PMV protein at pH 8.0. Sedimentation is to the right.

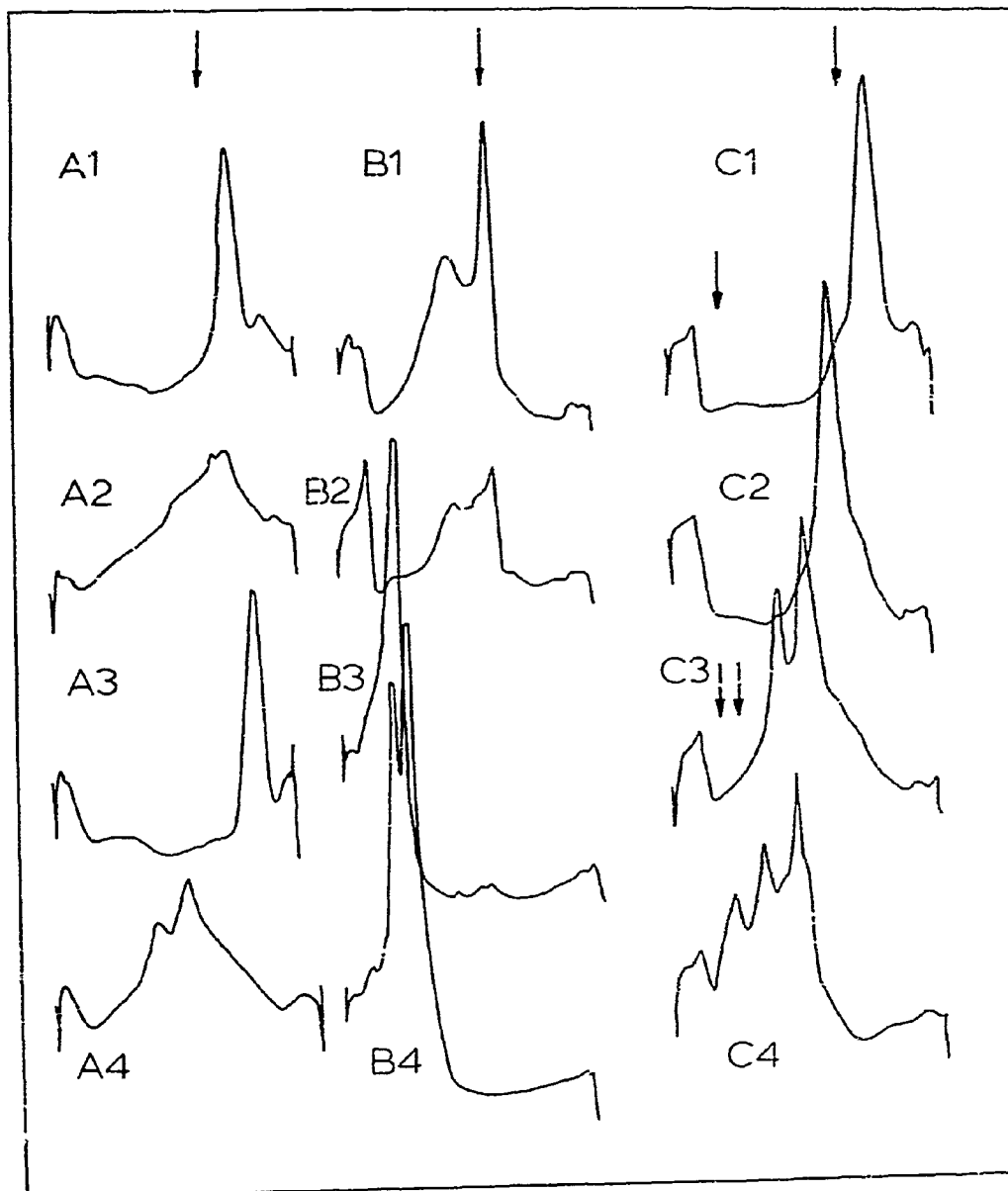
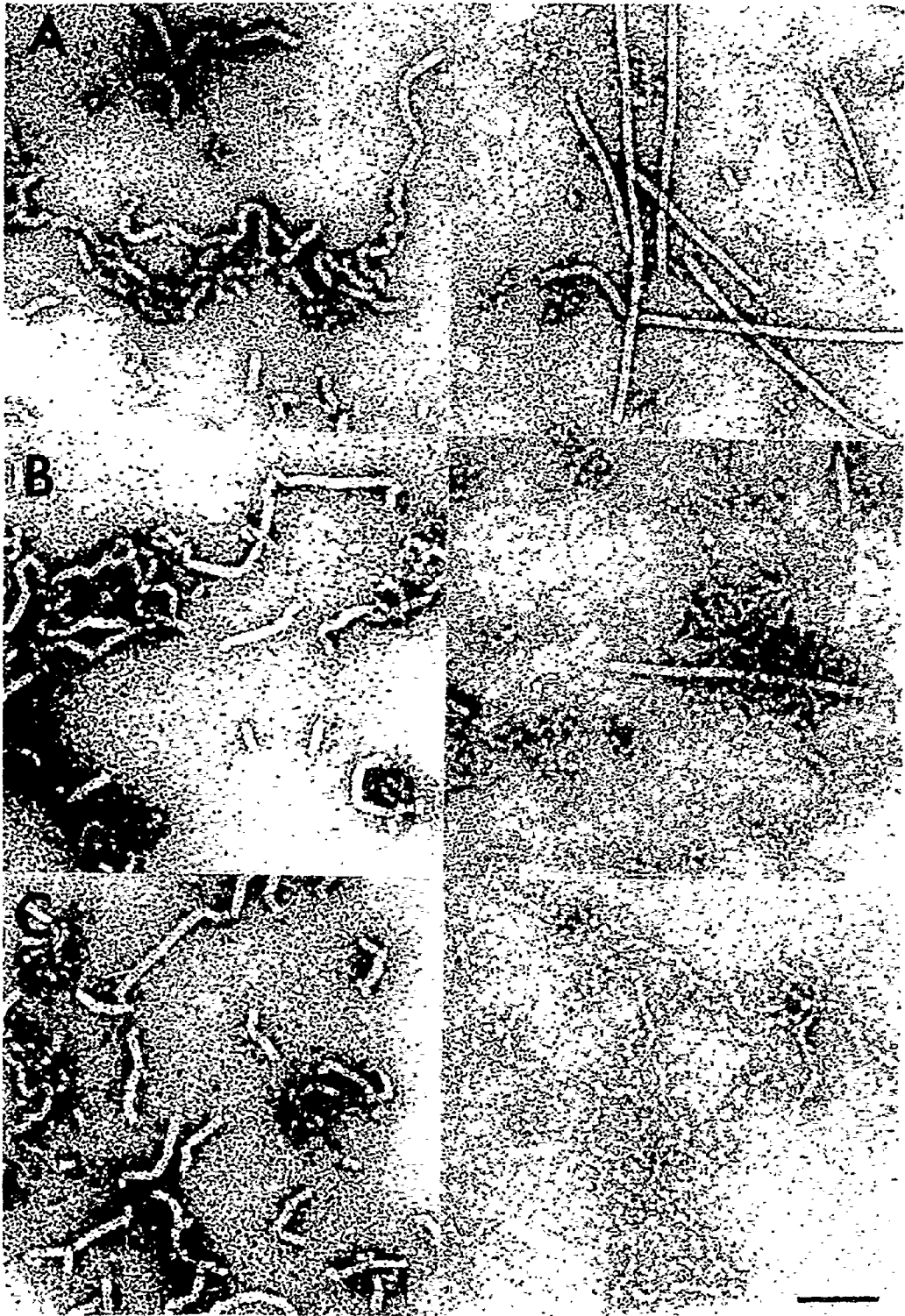


Fig. 40. Specificity of the assembly reaction of PMV protein with various plant virus RNAs as a function of pH: particle morphology. Electron micrographs of: (A) CYMV-RNA; (B) TMV-RNA; and (C) BMV-RNA reacted with PMV protein at pH 6.0 (left) and at pH 8.0 (right). The bar represents 100 nm.



At pH 8.0 the PMV and CYMV-RNAs, but not those from TMV and BMV, combined with PMV protein to produce particles sedimenting at about the rate of PMV (Fig. 39, B1 to B4). Electron micrographs of PMV and CYMV-RNAs, reacted with PMV protein, showed long flexuous particles (Fig. 40A, right) (see Chapter 4). When TMV-RNA was used most of the population was composed of narrow extended particles, a few rods also being present (Fig. 40B, right). BMV-RNA reacted with PMV protein produced only the narrow particles (Fig. 40C, right). The data thus show that tube formation at pH 8.0 with PMV protein is largely specific to PMV-RNA or that from a related virus.

The observations on the pH-dependent differences in the specificity of assembly were refined by mixing PMV protein with TMV and BMV-RNA at pH 7.0 and 7.5. At pH 7.0 both heterologous products sedimented at about the same rate as at pH 6.0 (Fig. 39, C1 and C3). At pH 7.5 the sedimentation rates were slower (Fig. 39, C2 and C4) than observed at pH 7.0 but were still much more rapid than after the pH 8.0 reaction. The multiplicity of peaks found with BMV in this and the preceding experiments probably arose from the various size classes of BMV-RNA. Electron micrographs (not presented) showed "kinked" particles similar to those found at pH 6.0.

These experiments show that specificity resulting in normal particle formation is confined to a pH between 7.5 and 8.0.

6.2.2 Assembly with DNA

Salmon-sperm DNA was reacted with PMV protein at pH 6.0 and 8.0 to determine if the results obtained with RNA could be transposed to DNA. Fig. 41 shows the product made at pH 6.0. Encapsidation clearly occurred, although it is quite likely that detailed analysis will show considerable structural disorder. Thin extended particles, which were the only product observable after incubation at pH 8.0, were also formed but in relatively small numbers at pH 6.0 (Fig. 41). In general, the pH response of PMV protein to DNA is not dissimilar to that with heterologous RNA.

6.2.3 Assembly with synthetic polyribonucleotides

In order to assess specificity more precisely than is possible with naturally-occurring RNAs, PMV protein was mixed separately with poly A, poly C, poly U and poly I at pH 6.0 and 8.0.

PMV protein encapsidated all the homopolymers at pH 6.0 as determined by electron microscopy (Fig. 42, A - D). Particles made with poly A have a less rigid appear-

Fig. 41. Electron micrograph of salmon-sperm DNA reacted with PMV protein at pH 6.0. The bar represents 100 nm.

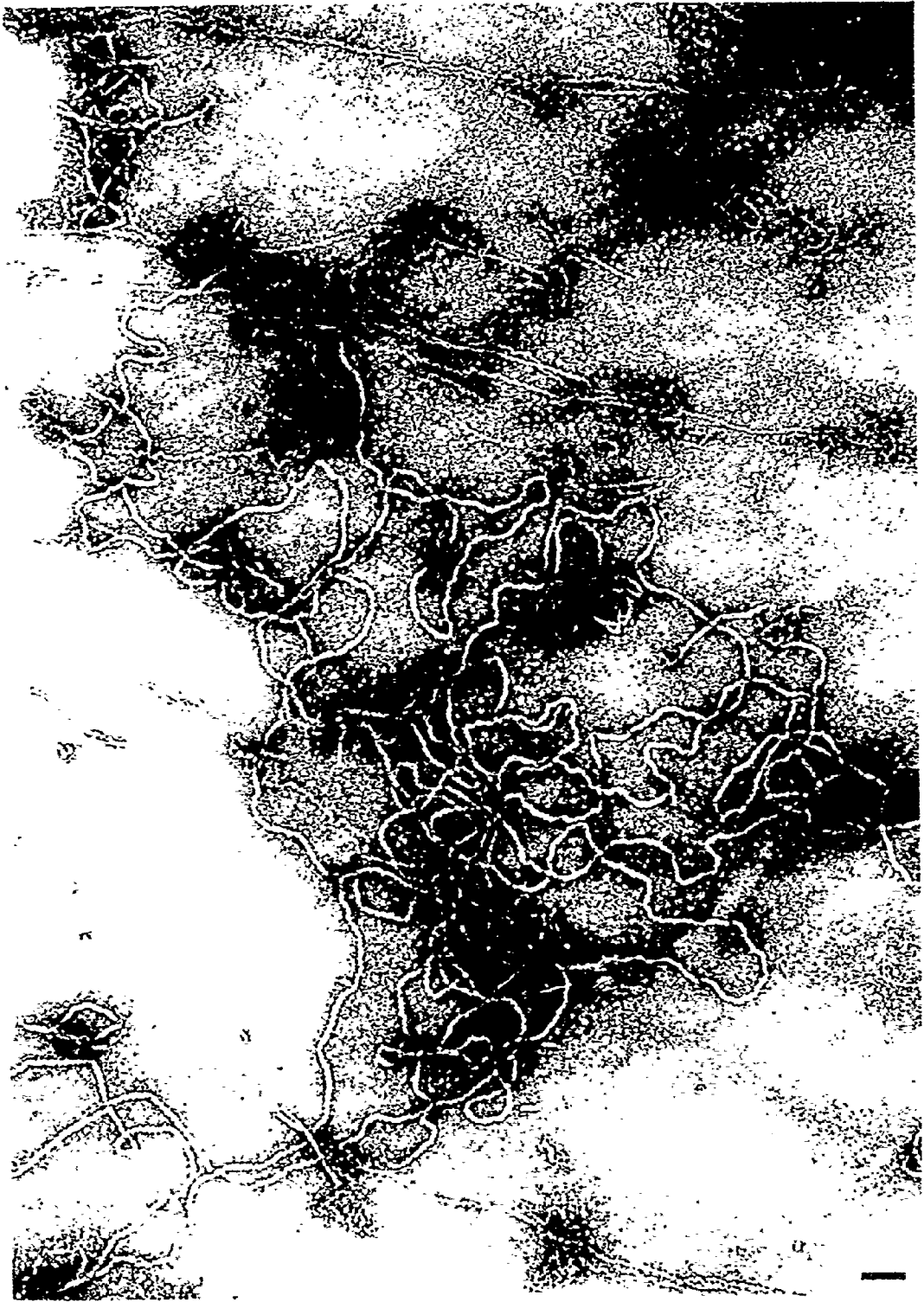
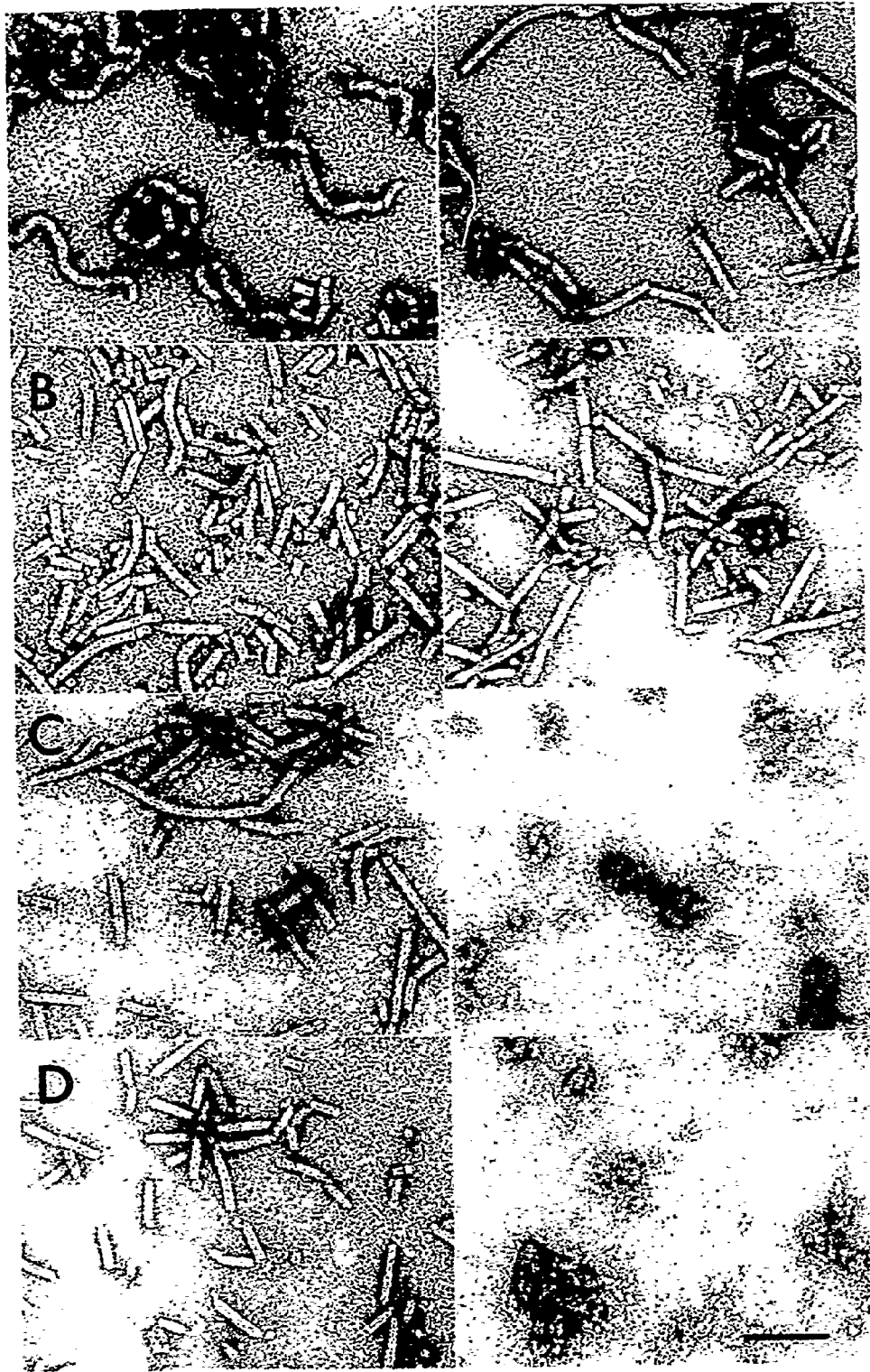


Fig. 42. Electron micrographs of polynucleotides reacted with PMV protein at pH 6.0 (left) and pH 8.0 (right): poly A (A), poly C (B), poly U (C) and poly I (D). The bar represents 100 nm.



ance than those containing the other polynucleotides signifying some structural difference.

Only poly A and poly C were encapsidated at pH 8.0 to give tubular particles (Fig. 42, A and B). Poly U and poly I gave rise to disorganized structures and some narrow particles, but not tubes (Fig. 42, C and D).

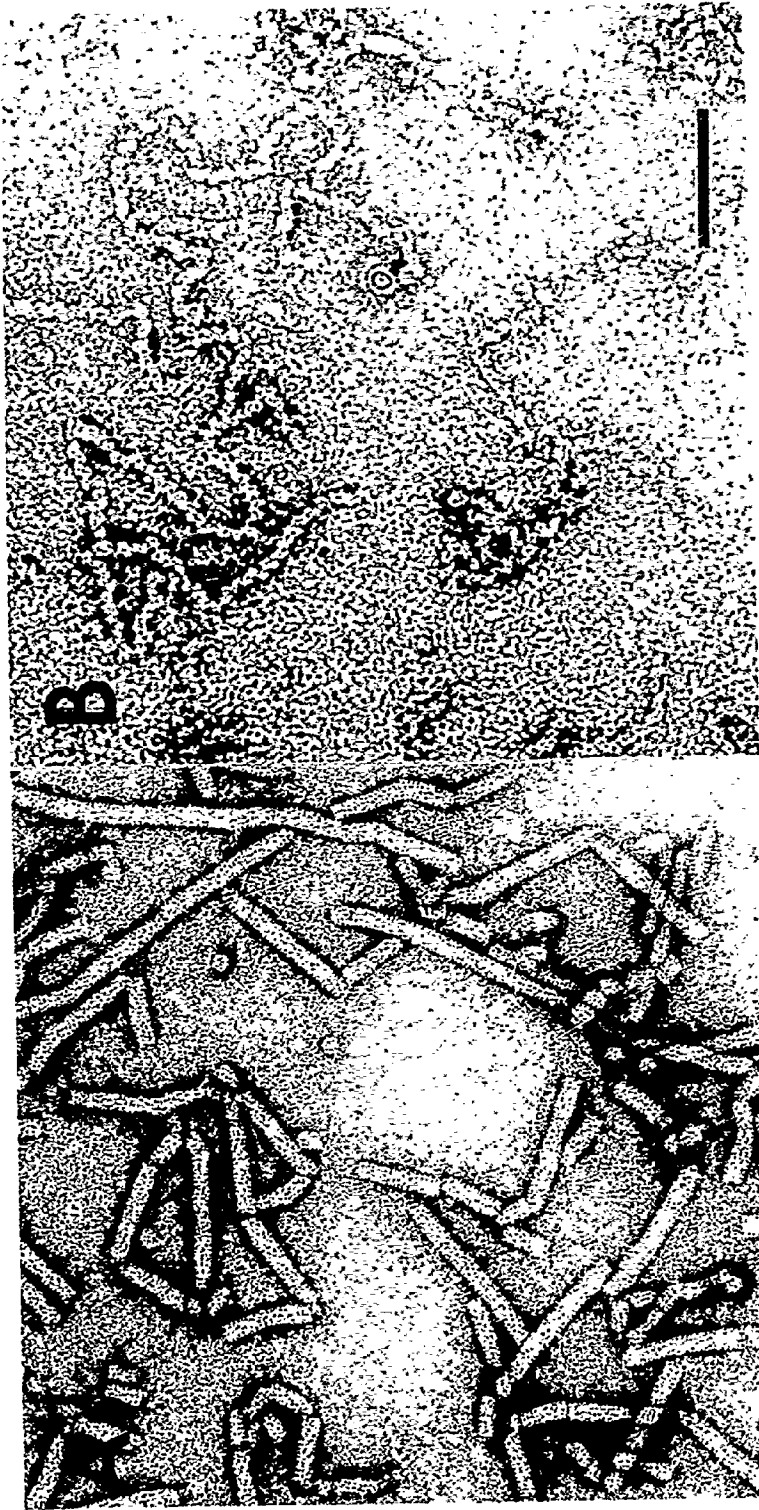
6.2.4 Assembly with chemically modified PMV-RNA

Since poly C, but not poly U, was encapsidated at pH 8.0, the effect of a C \rightarrow U transformation in PMV-RNA on assembly specificity was determined. Fig. 43 shows that transformed RNA is encapsidated at pH 6.0 and that at pH 8.0 only thin extended particles, similar in appearance to those obtained with unrelated RNAs, were formed.

6.3 Discussion

Reconstitution of PMV at pH 8.0 results in smooth tubular particles whereas that at pH 6.0 produces particles with numerous discontinuities, presumably resulting from multiple initiations along the RNA (see Chapter 4). The multiple initiations were regarded as resulting from a breakdown in the specificity of the recognition event which, at pH 8.0, is near the 5' end of the RNA (see Chapter 4; AbouHaidar and Bancroft, 1978). The contention that specificity is lost at pH 6.0 is correct otherwise TMV and BMV-

Fig. 43. Electron micrographs of C → U transformed PMV-RNA reacted with PMV protein at pH 6.0 (A) and pH 8.0 (B). The bar represents 100 nm.



RNAs would not have been encapsidated. Results similar to those at pH 6.0 were also obtained at pH 7.5 but not at pH 8.0, where extended particles were formed with TMV and BMV-RNAs. It is clear that the formation of these extended particles, in contrast to initiation, is non-specific at pH 8.0.

The non-specific encapsidation into segmented rods from pH 6.0 to pH 7.5 is not simply an entrapment of RNA by protein that would form a helix by itself. Helices are not normally formed with PMV protein alone above pH 6.0; those that are made at pH 6.0 occur in very low yields, are very short and take days to assemble, unlike the situation at pH 4.0 - 5.0 (see Chapter 3). The selectivity of TMV protein for its own RNA is also decreased at relatively low pH levels (Fraenkel-Conrat and Singer, 1964; Matthews, 1966, Sugiyama, 1966; Atabekov et al., 1970; Fritsch et al., 1973a).

The formation of homologous and heterologous particles may be conveniently categorized (Table 2). The reaction of PMV protein at pH 6.0 with either homologous or heterologous RNAs is rapid and temperature independent - there is no maturation step in stoichiometric mixtures and the entire process may be currently regarded as one of unregulated initiation. At pH 8.0 the initial reaction to form extended particles with homologous or heterologous

Table 2
 Some properties of non-specific and specific
 assembly reactions with PMV protein

	<u>Non-specific</u>		<u>Specific</u>	
			<u>Initiation</u>	<u>Elongation</u>
pH	6.0-7.5	8.0	8.0	8.0
Morphology	"kinked"	thin extended	normal	normal
Relative speed	fast	fast	fast	slow
Temperature requirement	1° - 25°C	1° - 25°C	1° - 25°C	25°C

RNAs is also extremely rapid compared with normal particle completion (about 10^3 x faster) and, as argued elsewhere (see Chapters 4 and 5), is not an unexpected consequence of reaction conditions. If, however, there is initiation which is also rapid at pH 8.0, then an elongation process may result which follows second-order kinetics. A fast interaction between RNA and protein is the rule; a fast specific interaction is not, being restricted to homologous RNA. Elongation can only follow the latter; there are no variants of elongation as defined and described (Chapters 4 and 5) as far as we are aware.

The specificity of the protein-nucleic acid recognition step in PMV assembly is regulated by a pH switch; specificity is turned off/on between pH 7.5 and 8.0. This is precisely the range where homologous RNA is encapsidated to form either "kinked" or normal particles, respectively (see Chapter 4). The mechanism by which this switch operates is not yet understood but may be related to anomalously titrating groups on the protein (Durham and Bancroft, unpublished) which bear some resemblance to those found in TMV. Further studies have shown that the precise pH where the specificity cut-off lies may vary slightly (by a few tenths of a pH unit) from one protein batch to another.

The encapsidation of the various homopolymers at pH 6.0 was not unexpected. Considering the appearance of

the particles, it seems that poly A was recognized along its length, giving rise to the characteristic kinked particles which arise from multiple initiation events, whereas the other polynucleotides were initiated only at their ends. The results at pH 8.0 clearly show that poly A and poly C, but not poly U or poly I, can be recognized in specific reaction conditions. This recognition conceivably centers around the amino group of cytosine which is lacking in uracil and that of adenine in position 6 which is lacking in inosine. TMV protein also recognizes poly A (Fraenkel-Conrat and Singer, 1964), although less rapidly than TMV-RNA (Butler and Klug, 1971). It also recognizes poly I, thus seeming to prefer purines unsubstituted in the 2-position (Fraenkel-Conrat and Singer, 1964). The natural recognition sites of PMV and TMV-RNAs are rich in adenylic acid (AbouHaidar and Bancroft, 1978; Zimmern, 1976). That of TMV is deficient in cytidylic acid (Zimmern, 1976) and TMV protein does not encapsidate poly C (Fraenkel-Conrat and Singer, 1964). On the other hand, the results with PMV protein and poly C, particularly in conjunction with those obtained with the transformed RNA, indicate that cytidylic acid, which also appears to play a role in determining the specificity of the protein-RNA interaction in turnip yellow mosaic virus (Jonard *et al.*, 1976) is important. Thus, poly C as well as poly A may somehow mimic at least a portion of the nucleotide sequence or resulting structure found in the recognition site of PMV-RNA.

The specificity displayed by PMV protein for its RNA, the pH controlled switch for this process and the varied response of PMV protein toward different nucleic acids make PMV assembly a worthwhile system for the study of protein-nucleic acid recognition mechanisms.

CHAPTER 7

THE FORMATION OF 25S PMV COAT PROTEIN IS ENTROPY-DRIVEN

7.1 Introduction

One of the better characterized parts of the PMV system presently available which may yield information about the general mechanism of protein polymerization is the interconversion between the 14S and 25S protein polymers (see Chapter 4). The protein is in a rapid equilibrium between 14S and 25S polymers under optimal reconstitution conditions (0.01 M tris buffer, pH 8.0, 25°C, 1 mg/ml protein). The formation of the 25S species from 14S protein can be brought about by raising the temperature from 4° to 25°C at pH 8.0. The conversion is complete in about 30 sec and is reversible. Overall, the protein equilibrium exhibits the temperature and concentration dependencies typical of entropy-driven systems. Lauffer (1975) proposed that the mechanism of entropy-drive for a variety of fundamental biological polymerization processes involving proteins, including the polymerization of TMV protein, is net water release by the protein upon polymerization. In this chapter, thermodynamic parameters for the 14S - 25S equilibrium of PMV protein are estimated and are found to be consistent with an entropy-driven water release mechanism for the polymerization of 14S to 25S polymer.

7.2 Theoretical analysis

The mass reaction for the equilibrium of PMV protein at pH 8.0 can be represented by



where x and y are defined by the stoichiometry of the equilibrium. The law of mass action gives the apparent equilibrium constant

$$K_{app} = \frac{[25S]^y}{[14S]^x} = \frac{f^y}{\left(\frac{x}{y}\right)^y m^{(x-y)} (1-f)^x} \quad (14).$$

Here, brackets represent concentration in molarity, f is the weight-fraction of protein present in the 25S form, m represents the molarity of total protein in terms of the 14S polymer. The dependence of the equilibrium constant upon temperature is given by the relationship

$$\ln K_{app} = \Delta S^{\circ}/R - (\Delta H^{\circ}/R) (1/T) \quad (15),$$

where ΔS° and ΔH° represent the entropy and enthalpy changes, respectively, for the standard condition of unit activity, R is the gas constant, T is the absolute temperature. In this analysis the standard state is defined as unit molarity. Equation (15) only holds for processes carried out at a constant temperature. If ΔH° is independent of temperature for a given process, then a plot of $\ln K_{app}$ versus $1/T$ should yield a straight line whose slope is $-\Delta H^{\circ}/R$ and whose inter-

cept is $\Delta S^0/R$.

We assumed the stoichiometry for the reaction is $2\ 14S \rightleftharpoons 25S$; that is, $x = 2$ and $y = 1$. This assumption arises from hydrodynamic and structural studies (unpublished) which showed that the 14S polymer is composed of about 16 subunits probably, by analogy to TMV protein (Durham et al., 1971), in the form of a two layer disc, with a molecular weight of approximately 350,000 daltons (see Chapter 3). Hydrodynamic considerations, similar to those used by Caspar (1963) to predict molecular weights from sedimentation coefficients for TMV protein, suggested that the 25S polymer consists of two 14S discs. This is a minimum estimate for the size of the larger polymer since the sedimentation coefficient of the faster species in a rapidly associating system is always greater than the maximum experimentally determined value (Cann, 1970, pg. 110).

The temperature and concentration dependencies of the 14S - 25S equilibrium at pH 8.0 were analyzed by analytical ultracentrifugation (see Chapter 4). The apparent proportions of the various polymers present at several protein concentrations and temperatures were estimated from these data by measuring the areas under the Schlieren peaks (Table 3). Although not strictly correct, this method gives a reasonable first approximation to the actual proportions of polymers (Gilbert, 1955). The assumption was made throughout that the extra material sedimenting

Table 3

Apparent percentages of polymorphic forms of PMV protein at different concentrations and temperatures at pH 8^{a,b}

Protein concentration (mg/ml)	Temperature (°C)												
	5			10			15			25			
	<14S	14S	<14S	14S	<14S	14S	81	15	85	<14S	14S	25S	
0.25	75	25	27	73	19	81	-	15	85	-	11	89	-
0.5	30	70	11	89	7	93	-	8	92	-	8	21	71
1.0	12	88	-	100	3	97	-	1	39	60	-	15	85
2.0	8	92	-	100	1	41	58	-	1.8	82	-	7	93

a Data for this analysis were taken from prior sedimentation experiments (Table 1, Chapter 4).

b Apparent percentages were obtained by measuring areas under the Schlicren peaks. Sedimentation profiles, on photographic glass plates, were enlarged about 11x and traced on graph paper, and the peak areas were measured by counting squares. Material sedimenting between adjacent peaks was assumed to be due to dissociation of the faster peak and so was apportioned appropriately.

between the 14S and 25S peaks was largely due to dissociation of the 25S protein at its sedimenting boundary. This behavior is typical for concentration dependent equilibrium systems whose rate constants are much larger than the sedimentation times. Using the data in Table 3 and equation (14), values for K_{app} were calculated for the equilibrium at several different temperatures and concentrations and are listed in Table 4. Only five of the sedimentation runs could be included in the analysis of this particular equilibrium; however, all the data are shown in Table 3 because they indicate clear trends for the protein to polymerize to larger forms with both increasing protein concentration and increasing temperature at pH 8.0.

$\ln K_{app}$ values were plotted versus $1/T$ for the protein equilibrium at two concentrations, 1 mg/ml and 2 mg/ml, and ΔH° and ΔS° values were determined according to equation (15) (Fig. 44 and Table 5). Both the enthalpy and the entropy changes for the formation of 25S polymer from 14S protein are large and positive, indicating that the conversion is both endothermic and, more importantly, entropy-driven.

7.3 Discussion

Considerations, similar to those for TMV protein polymerization (Lauffer, pg. 130ff, 1975), suggest that the entropy increase brought about by the 14S to 25S

Table 4

Calculated K_{app}^a values for the 14S - 25S equilibrium of PMV protein at various temperatures and concentrations at pH 8^b

Protein concentration (mg/ml)	Temperature (°C)
1.0	15
-	20
2.0	25
	$6.5 \pm 2.9 \times 10^5$
	$6.6 \pm 8.2 \times 10^6$
	$2.9 \pm 1.2 \times 10^5$
	$2.2 \pm 2.3 \times 10^6$
	$1.7 \pm 4.6 \times 10^7$

a K_{app} were calculated from equation (14) using the data in Table 3. Error propagation analysis was performed (see Appendix) and the estimated standard error $\lambda(K_{app})$ was computed and is listed along with the appropriate K_{app} .

b The equilibrium stoichiometry was assumed to be 2 14S \rightleftharpoons 25S.

Fig. 44. Dependence of K_{app} on temperature for the equilibrium $2\ 14S \rightleftharpoons 25S$. $\bullet-\bullet$, PMV protein at 2 mg/ml; $o-o$, PMV protein at 1 mg/ml. Vertical bars indicate the estimated standard error for K_{app} . Data were taken from Table 4.

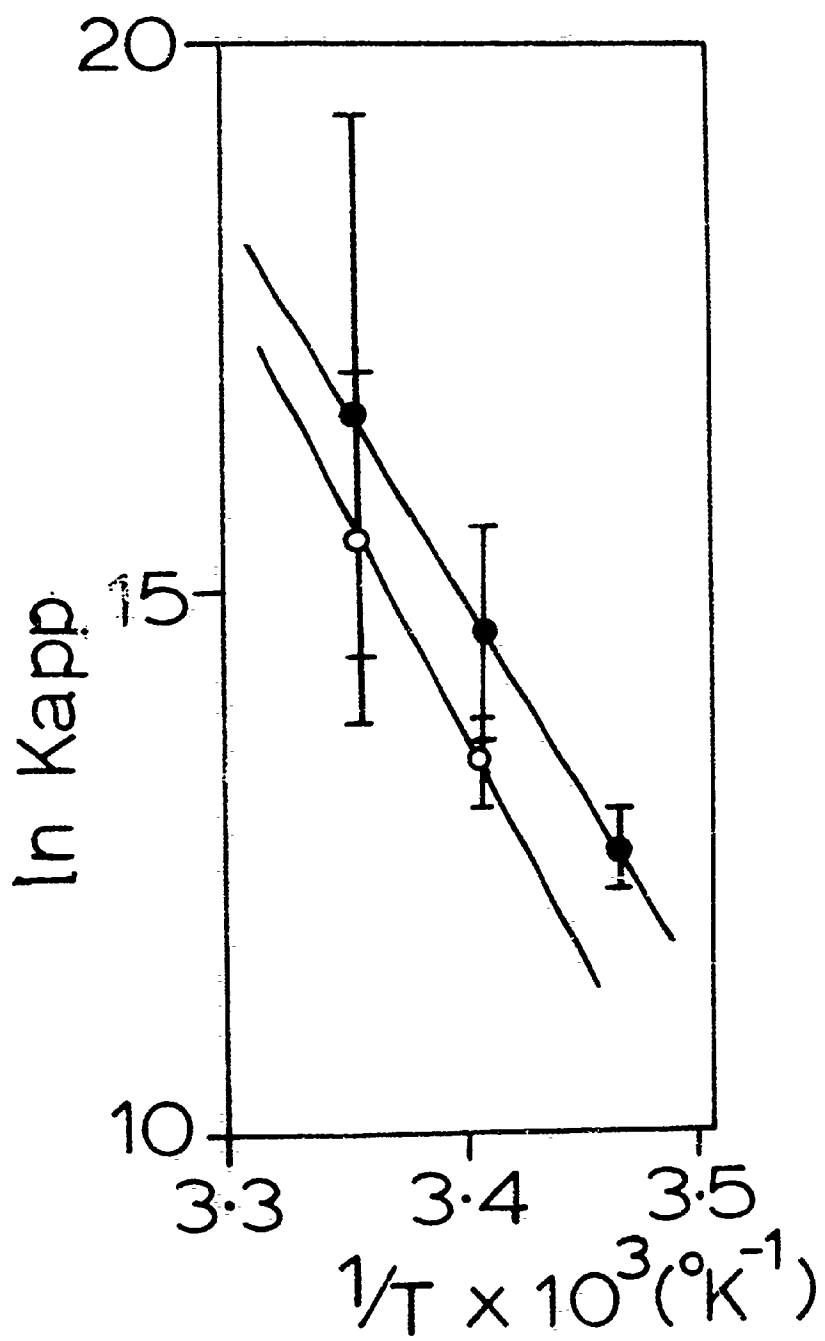


Table 5
 Thermodynamic parameters^a for the 14S - 25S equilibrium of PMV protein

<u>Protein concentration</u>	<u>ΔH° (kcal/mole 14S)</u>	<u>ΔS° (eu/mole 14S)</u>	<u>water released^b (moles/mole 14S)</u>
1 mg/ml	80 ± 45	300 ± 77	151 ± 39 - 641 ± 167
2 mg/ml	69 ± 30	265 ± 52	134 ± 27 - 566 ± 113

a ΔH° and ΔS° were calculated, using equation (15), from the slopes and intercepts, respectively, of the plots in Fig. 44. They are reported along with estimates of their standard errors. The latter were calculated by error propagation analysis and assume maximum errors of 10% in the estimates of the protein concentration, molecular weight of the monomer, number of subunits in the 14S polymer, and weight-fraction of the 25S polymer (see Appendix).

b The ranges given correspond to the range in Bull's data (1944) for the entropy losses incurred upon water uptake by various proteins. The estimated standard errors are based upon the estimated errors in the calculated ΔS° values (see Appendix).

polymerization comes from a net release of protein-bound water. The best estimates of entropy increases brought about by the dehydration of proteins come from Bull (1944), who measured water uptake by dry proteins in equilibrium with water vapor and then calculated corresponding entropy losses. His values range for +.468 to +1.98 cal per degree per mole H_2O for the release of protein-bound water. By using these values, the water released upon polymerization of PMV protein can be estimated as ranging anywhere from 107 to 808 moles water per mole 14S disc, or approximately 7 to 52 moles H_2O per mole protein subunit. These estimates take into account the variation in Bull's data as well as the estimated variation in the calculated ΔS^0 values for the present work (see Appendix for error analysis). Stevens and Lauffer (1965) measured the water released upon TMV protein polymerization as 0.027 g water/g protein or about 26 moles water per mole TMV protein subunit. The water release estimates for PMV protein, although speculative, nevertheless are within a reasonable range of values when compared with the more accurate estimates for TMV protein.

The idea that water release drives the formation of the 25S polymer from 14S discs suggests that the polymerization is basically a dehydration reaction. This being so, any substance which decreases the dehydration potential (i.e. potential water release per mole protein per ml

of solution) of the polymerization reaction should decrease the net free energy loss for the reaction and so inhibit 25S formation. Simple chloride salts are very effective as protein dehydrating agents (Bull and Breese, 1970; 1976) and NaCl decreases water binding by ovalbumin by about 70%. Hence, in the presence of NaCl net water loss by PMV protein during polymerization would be predictably diminished (thereby decreasing ΔS) and this could account for the NaCl-induced inhibition of 25S formation, and quite possibly as well for the deleterious effect of NaCl on PMV assembly.

The calculated enthalpy and entropy values at 1 and 2 mg/ml were not significantly different, probably owing to the large propagated error. However, it is clear from the data in Table 3 that the magnitude of the net free energy change for the polymerization reaction must decrease with decreasing protein concentration at constant temperature. This net free energy decrease is probably due to the decrease in total potential entropy gain at the lower protein concentrations, and is, in turn, most easily explained by invoking the release of protein bound water as the entropy drive for polymerization; that is, the potential entropy change for the 14S to 25S polymerization is proportional to the dehydration potential of the reaction which is dependent upon the total protein concentration. It is not improbable that the explanation of the properties of the 14S - 25S equilibrium

of PMV protein will be applicable to protein rod formation and to the reconstitution reaction.

APPENDIX

ERROR PROPAGATION ANALYSIS FOR THE CALCULATION OF THERMODYNAMIC PARAMETERS FOR THE 14S - 25S EQUILIBRIUM

Introduction

Chapter 7 described a theoretical analysis of the 14S - 25S equilibrium for PMV protein which allowed estimations to be made for the enthalpy ΔH° and entropy ΔS° terms for this reaction. A hypothesis was advanced in which the release of protein-bound water was proposed to contribute mainly to the gain in entropy upon conversion of 14S protein into the 25S aggregate. Estimates of the amount of water released in this reaction were made, and since these are fairly speculative values based on the calculated entropy change, it was necessary to determine the statistical reliabilities of these estimates. This appendix describes in detail the error propagation analysis from which was derived the standard errors and ranges for the thermodynamic parameters reported in Chapter 7.

Background

The basic approach employed for the error propagation analysis is that described by Shoemaker and Garland (1967). The linear regression error analysis was done following the procedure outlined by Draper and Smith (1966).

Assume that a quantity F is a function of several experimentally measurable variables x_i . One may write

$$F = f(x_1, x_2, \dots, x_n) \quad (1).$$

Small changes Δx_i in the experimentally determined values of x_i will produce a change ΔF in the calculated quantity F that is given by the approximation

$$\Delta F = \frac{\partial F}{\partial x_1} \Delta x_1 + \frac{\partial F}{\partial x_2} \Delta x_2 + \dots + \frac{\partial F}{\partial x_n} \Delta x_n \quad (2).$$

Let the Δx_i represent experimental errors $\epsilon(x_i)$ in the quantities x_i so that

$$\Delta x_i = \epsilon(x_i) \equiv x_i \text{ (measured)} - x_i \text{ (true)} \quad (3).$$

Similarly, the resulting error $\epsilon(F)$ in F

$$\Delta F = \epsilon(F) \equiv F \text{ (calculated)} - F \text{ (true)} \quad (4)$$

is given by

$$\epsilon(F) = \frac{\partial F}{\partial x_1} \epsilon(x_1) + \frac{\partial F}{\partial x_2} \epsilon(x_2) + \dots + \frac{\partial F}{\partial x_n} \epsilon(x_n) \quad (5).$$

The $\epsilon(x_i)$ are indeterminate; however, if magnitudes for these errors may reasonably be estimated then limits of error $\lambda(x_i)$ may be assigned such that

$$-\lambda(x_i) \leq \epsilon(x_i) \leq \lambda(x_i) \quad (6).$$

The aim of error propagation analysis is to calculate the limits of error $\lambda(F)$ of F based on the limits of error $\lambda(x_i)$ for the variables x_i ; that is, we want to know the maximum value of $\epsilon(F)$ which is allowed from the

error limits assigned to the x_i . This is found by setting the $\epsilon(x_i)$ in equation (5) equal to their respective limits $\lambda(x_i)$ and giving each term in equation (5) the same algebraic sign. The resulting equation is

$$\lambda(F) = \left| \frac{\partial F}{\partial x_1} \right| \lambda(x_1) + \left| \frac{\partial F}{\partial x_2} \right| \lambda(x_2) + \dots + \left| \frac{\partial F}{\partial x_n} \right| \lambda(x_n) \quad (7),$$

where $| |$ represents absolute value and all the $\lambda(x_i)$ are positive in sign. The expression for F is differentiated with respect to each of the variables x_i in turn, and the absolute magnitudes of the derivatives and the error limits of x_i are substituted back into equation (7) in order to calculate $\lambda(F)$.

A refinement of the calculation of $\lambda(F)$ results from the statistical likelihood that errors in the variables x_i will tend to cancel one another out. The final result is given by

$$\lambda(F) = \left\{ \left(\frac{\partial F}{\partial x_1} \right)^2 [\lambda(x_1)]^2 + \left(\frac{\partial F}{\partial x_2} \right)^2 [\lambda(x_2)]^2 + \dots + \left(\frac{\partial F}{\partial x_n} \right)^2 [\lambda(x_n)]^2 \right\}^{\frac{1}{2}} \quad (8).$$

This treatment gives a smaller value for $\lambda(F)$ than is given by equation (7) by a factor of approximately the square root of the number of variables x_i . For the complete derivation of equation (8) see Shoemaker and Garland (1967).

Error of K_{app}

The calculation of ΔS° and ΔH° values for the 14S - 25S equilibrium required the calculation of values for the apparent equilibrium constant K_{app} at various temperatures. The latter was given by equation (14) in Chapter 7:

$$K_{app} = \frac{f^y}{(x/y)^y m^{(x-y)} (1-f)^x}$$

where x , y , m , and f are defined in Chapter 7. Now K_{app} is obviously a function of x , y , m , and f . To find the limit of error $\lambda(K_{app})$ for K_{app} equation (8) is utilized to give

$$\lambda(K_{app}) = \left\{ \left(\frac{\partial K_{app}}{\partial m} \right)^2 [\lambda(m)]^2 + \left(\frac{\partial K_{app}}{\partial f} \right)^2 [\lambda(f)]^2 \right\}^{\frac{1}{2}} \quad (9).$$

The terms for x and y drop out since $\lambda(x)$ and $\lambda(y)$ are zero for a given stoichiometry. In order to calculate a value for $\lambda(K_{app})$ the partial derivative terms in equation (9) must be solved and values for $\lambda(m)$ and $\lambda(f)$ must be calculated.

 $\lambda(m)$

The total protein molarity m in terms of the 14S species is given by $m = w/NM$ where w is the weight-concentration of protein, M is the molecular weight of

monomer, and N is the number of monomers contained in the 14S polymer. From equation (8) an expression for $\lambda(m)$ can be derived:

$$\lambda(m) = \left\{ \left(\frac{\partial m}{\partial w} \right)^2 [\lambda(w)]^2 + \left(\frac{\partial w}{\partial N} \right)^2 [\lambda(N)]^2 + \left(\frac{\partial m}{\partial M} \right)^2 [\lambda(M)]^2 \right\}^{\frac{1}{2}} \quad (10).$$

The uncertainty of the extinction coefficient for PMV protein can reasonably be estimated as 10% and this gives $\lambda(w) = 0.1w$. The uncertainty of the molecular weight estimate for the protein monomer and of the number of subunits (16) in the 14S polymer are both of the order of 10% so that $\lambda(M) = 0.1M$ and $\lambda(N) = 0.1N$. Differentiating equation (10) and substituting the values for the error limits gives

$$\lambda(m) = \left\{ \left(\frac{.1w}{NM} \right)^2 + \left(\frac{.1w}{NM} \right)^2 + \left(\frac{.1w}{NM} \right)^2 \right\}^{\frac{1}{2}}$$

Since $m = w/NM$, then $\lambda(m)$ is $.17m$. Thus, the error limit for $\lambda(m)$ is approximately 17% of the estimated value.

$\lambda(f)$

The uncertainty in the estimate for the weight-fraction f of the 25S species derives from the errors involved in measuring the Schlieren peak areas. Certain assumptions were employed in making these measurements (see Chapter 7), however, an error limit assignment of 10% is probably not unreasonable. Let $\lambda(f) = 0.1f$.

$$\lambda(K_{\text{app}})$$

Differentiation and rearrangement of equation (9) yields

$$\lambda(K_{\text{app}}) = \left\{ \left(\frac{f^y}{(x/y)^y (y-x)^m (x-y+1) (1-f)^x} \right)^2 [\lambda(m)]^2 + \left(\frac{(x-y)f^y + yf^{(y-1)}}{(x/y)^y m^{(x-y)} (1-f)^{x+1}} \right)^2 [\lambda(f)]^2 \right\}^{\frac{1}{2}} \quad (11).$$

Assuming that the stoichiometry for the equilibrium is $2 \text{ 14S} \rightleftharpoons 1 \text{ 25S}$ gives $x = 2$ and $y = 1$. Substituting x , y , $\lambda(m)$, and $\lambda(f)$ into equation (11) results in

$$\lambda(K_{\text{app}}) = 0.1K_{\text{app}} \left\{ 1 + \left(\frac{1+f}{1-f} \right)^2 \right\}^{\frac{1}{2}}$$

Values for $\lambda(K_{\text{app}})$ were calculated for each K_{app} and are listed in Table 4 of Chapter 7.

Error of ΔH° and ΔS°

The values for ΔH° and ΔS° were obtained from the slopes and intercepts, respectively, of plots of $\ln K_{\text{app}}$ versus $1/T$ (absolute) for different protein concentrations (see Chapter 7). Therefore, calculating the limits of error of these parameters is equivalent to calculating confidence limits for the slopes and intercepts of each plot. Typical linear least-squares analysis yields values for slopes and intercepts along with their standard errors. It must be stressed, however, that such errors normally reflect

the deviations of the experimental points from the analytically fitted line and do not take into account any intrinsic variability of the points used in the fitting procedure. The ignorance of such variability can lead to highly erroneous confidence limits for the equation parameters. This variability can be taken into account rather easily. However, it is not often done so because the procedure is often considered to be complicated and its description is difficult to find in useful form in most of the popular statistical texts. Actually, it is no more complex than that used to solve for the best-fit line. The derivation of this procedure is presented in readable form in Draper and Smith (1966). It is somewhat complex and only the final result will be given here. The following two equations are used in calculating error limits for the slope and intercept of a fitted line taking into account both experimental errors and fitting errors:

$$\lambda(\text{slope}) = \left\{ \frac{\sum x_i^2 V(y_i) - (2/n) \sum x_i \sum x_i V(y_i) + (\sum x_i/n)^2 \sum V(y_i)}{(\sum x_i^2 - (\sum x_i)^2/n)^2} \right\}^{\frac{1}{2}} \quad (12)$$

$$\lambda(\text{intercept}) = \left\{ \frac{1}{n} \sum V(y_i) + V(\text{slope}) (\sum x_i)^2 \right\}^{\frac{1}{2}} \quad (13).$$

In these expressions V represents the variance and can be approximated by λ^2 . Thus, the calculation of $\lambda(\text{slope})$ and $\lambda(\text{intercept})$ is a straightforward procedure when this approximation is applied to the above equations.

In the present analysis, the x_i are replaced by $1/T_i$ and the y_i are substituted by $\ln K_{app_i}$. In order to solve equations (12) and (13) for the present example the error limits $\lambda(\ln K_{app})$ for $\ln K_{app}$ must be calculated. Now $\lambda(\ln K_{app})$ is simply $\frac{d \ln K_{app}}{d K_{app}} (= \frac{1}{K_{app}}) \lambda(K_{app})$ so that

$\lambda(\ln K_{app}) = \lambda(K_{app})/K_{app}$. Independent values for $\lambda(K_{app})$ were calculated for each temperature and equations (12) and (13) were solved for $\lambda(\text{slope})$ and $\lambda(\text{intercept})$. These values were employed to calculate $\lambda(\Delta H^\circ)$ and $\lambda(\Delta S^\circ)$ from the relations

$$\lambda(\Delta H^\circ) = \lambda(\text{slope})R \quad (14)$$

and

$$\lambda(\Delta S^\circ) = \lambda(\text{intercept})R \quad (15).$$

Equations (14) and (15) derive from error propagation analysis of the equations for ΔH° and ΔS° (see Chapter 7):

$$\text{slope} = -\Delta H^\circ/R \text{ and } \text{intercept} = \Delta S^\circ/R$$

Limits of error for ΔH° and ΔS° at the two different protein concentrations analyzed were calculated and are listed in Table 5 in Chapter 7.

It is worth pointing out that the major error involved in this entire analysis is that of the weight-fraction f of the 25S aggregate. $\lambda(K_{app})$ is equal to about 10% of the calculated value of K_{app} multiplied by a factor which is proportional to $(\frac{1+f}{1-f})^2$. This means that the error increases exponentially in relation to f . This can be seen immediately upon inspection of Table 4 in Chapter 7. In-

creasing f from .58 at 15° to .93 at 25° , at 2 mg/ml protein, resulted in a relative error increase for $\lambda(K_{app})$ from about $.4K_{app}$ to over $2.5K_{app}$. This ultimately leads to relatively large values for the error estimates of ΔS° and ΔH° and indicates that these error estimates are probably somewhat high.

Finally, this analysis does not take into account certain assumptions regarding the class and the stoichiometry of the 14S - 25S equilibrium (see Chapter 7). A 2:1 minimum stoichiometry was assumed to hold for this reaction, however, computer-modeling studies showed that higher ratios (3:1, 4:1, etc.) would give proportionately larger estimates for the ΔS° term, so that the qualitative aspects of the analysis presented in Chapter 7 are unchanged. The equilibrium was also assumed to be discrete, with no intermediate polymers or polymers larger than the 25S species being present.

REFERENCES

- AbouHaidar, M., and Bancroft, J. B. (1978). The initiation of papaya mosaic virus assembly. *Virology*. In press.
- AbouHaidar, M., Pfeiffer, P., Fritsch, C., and Hirth, L. (1973). Sequential reconstitution of tobacco rattle virus. *J. Gen. Virol.* 21, 83-97.
- Atabekov, J. G. (1972). Genetic information and the recognition of viral RNAs by virus-specific proteins. In: *The Generation of Subcellular Structures, Proceedings of the First John Innes Symposium*. Edited by R. Markham, J. B. Bancroft, D. R. Davies, D. A. Hopwood, and R. W. Horne. American Elsevier. New York. pp. 77-100.
- Atabekov, J. G., Novikov, V. K., Kiselev, N. A., Kaftanova, A. S., and Egarov, A. M. (1968). Stable intermediate aggregates formed by the polymerization of barley stripe mosaic virus protein. *Virology* 36, 620-638.
- Atabekov, J. G., Novikov, V. K., Vishnichenko, V. K., and Kaftanova, A. S. (1970). Some properties of hybrid viruses reassembled in vitro. *Virology* 41, 519-532.

- Bancroft, J. B. (1970). The assembly of spherical plant viruses. *Adv. Virus Res.* 16, 99-134.
- Bancroft, J. B., Hills, G. J., and Markham, R. (1967). A study of the self-assembly process in a small spherical virus. Formation of organized structures from protein subunits *in vitro*. *Virology* 31, 354-379.
- Berg, O. G., and Blomberg, C. (1976). Association kinetics with coupled diffusional flows. Special application to the lac repressor-operator system. *Biophys. Chem.* 4, 367-381.
- Bull, H. B. (1944). Absorption of water vapor by protein. *J. Am. Chem. Soc.* 66, 1499-1507.
- Bull, H. B., and Breese, K. (1970). Water and solute binding by proteins. 1. Electrolytes. *Arch. Biochem. Biophys.* 137, 299-305.
- Bull, H. B., and Breese, K. (1976). Binding of water and electrolytes to proteins. An equilibrium dialysis study. *Biopolymers* 15, 1573-1583.
- Butler, P. J. G. (1972). Structures and roles of the polymorphic forms of tobacco mosaic virus protein. VI. Assembly of the nucleoprotein rods of tobacco mosaic virus from the protein discs and RNA. *J. Mol. Biol.* 72, 25-35.

- Butler, P. J. G. (1974). Structures and roles of the polymorphic forms of tobacco mosaic virus protein. VIII. Elongation of nucleoprotein rods of the virus RNA and protein. *J. Mol. Biol.* 82, 333-341.
- Butler, P. J. G., and Durham, A. C. H. (1977). Tobacco mosaic virus protein aggregation and the virus assembly. *Adv. Prot. Chem.* 31, 187-251.
- Butler, P. J. G., and Finch, J. T. (1973). Structures and roles of the polymorphic forms of tobacco mosaic virus. VII. Lengths of the growing rods during assembly into nucleoprotein with the viral RNA. *J. Mol. Biol.* 78, 637-649.
- Butler, P. J. G., and Klug, A. (1971). Assembly of the particle of tobacco mosaic virus from RNA and discs of protein. *Nature New Biol.* 229, 47-50.
- Cann, J. R. (1970). *Interacting Macromolecules: The Theory and Practice of their Electrophoresis, Ultracentrifugation, and Chromatography.* Academic Press, New York. 249 pp.
- Casjens, S., and King, J. (1975). Virus assembly. *Ann. Rev. Biochem.* 44, 555-611.
- Caspar, D. L. D. (1963). Assembly and stability of the tobacco mosaic virus particle. *Adv. Prot. Chem.* 18, 37-121.

- Caspar, D. L. D., and Klug, A. (1962). Physical principles in the construction of regular viruses. Cold Spr. Harb. Symp. Quant. Biol. 27, 1-24.
- Chervenka, C. H. (1969). A Manual of Methods for the Analytical Ultracentrifuge. Spinco Division of Beckman Instruments. Palo Alto, California. 100 pp.
- Dandliker, W. B., and deSaussure, V. A. (1971). Stabilization of macromolecules by hydrophobic bonding: role of water structure and of chaotropic ions. In: The Chemistry of Biosurfaces, Vol. 1. Edited by M. L. Hair. Marcel Decker, New York. pp. 1-43.
- Draper, N. R., and Smith, H. (1966). Applied Regression Analysis. John Wiley & Sons. New York. pp. 18ff.
- Durham, A. C. H., Finch, J. T., and Klug, A. (1971). States of aggregation of tobacco mosaic virus protein. Nature New Biol. 229, 37-42.
- Durham, A. C. H., and Klug, A. (1971). Polymerization of tobacco mosaic virus protein and its control. Nature New Biol. 229, 42-46.
- Edsall, J. T., and Wyman, J. (1958). Biophysical Chemistry. Vol. 1: Thermodynamics, Electrostatics, and the Biological Significance of the Properties of Matter. Academic Press. New York.

- Erickson, J. W., Bancroft, J. B. and Horne, R. W. (1976).
The assembly of papaya mosaic virus protein. *Virology* 72, 514-517.
- Fraenkel-Conrat, H. (1957). Degradation of tobacco mosaic virus with acetic acid. *Virology* 4, 1-4.
- Fraenkel-Conrat, H., and Singer, B. (1964). Reconstitution of tobacco mosaic virus. IV. Inhibition by enzymes and other proteins, and use of polynucleotides. *Virology* 23, 354-362.
- Fraenkel-Conrat, H., and Williams, R. C. (1955). Reconstitution of active tobacco mosaic virus from its inactive protein and nucleic acid components. *Proc. Natl. Acad. Sci. U.S.A.* 41, 690-698.
- Francki, R. I. B., and McLean, G. D. (1968). Purification of potato virus X and preparation of infectious ribonucleic acid by degradation with lithium chloride. *Aust. J. Biol. Sci.* 21, 1311-1318.
- Franklin, R. E. (1955). Structural resemblances between Schramm's repolymerised A-protein and tobacco mosaic virus. *Biochem. Biophys. Acta* 18, 313-314.
- Franklin, R. E. and Commoner, B. (1955). X-ray diffraction by an abnormal protein (B8) associated with tobacco mosaic virus. *Nature* 175, 1076-1077.
- Fritsch, C., Stussi, C., Witz, J., and Hirth, L. (1973a). Specificity of TMV RNA encapsidation: in vitro

- coating of heterologous RNA by TMV protein.
Virology 56, 33-45.
- Fritsch, C., Witz, J., AbouHaidar, M., and Hirth, L. (1973b).
Polymerization of tobacco rattle virus protein.
FEBS Lett. 29, 211-214.
- Gilbert, G. A. (1955). *Disc. Farad. Soc.* 20, 68-71.
- Goodman, R. M. (1975). Reconstitution of potato virus X
in vitro. I. Properties of the dissociated protein structural subunits. *Virology* 68, 287-298.
- Goodman, R. M. (1977). Reconstitution of potato virus X
in vitro. III. Evidence for a role for hydrophobic interactions. *Virology* 76, 72-78.
- Goodman, R. M., Horne, R. W., and Hobart, J. M. (1975).
Reconstitution of potato virus X in vitro. II.
Characterization of the reconstituted product.
Virology 68, 299-308.
- Goodman, R. M., McDonald, J. G., Horne, R. W., and Bancroft,
J. B. (1976). Assembly of flexuous plant viruses
and their proteins. *Phil. Trans. Roy. Soc. Lond.*
Ser. B. 276, 173-179.
- Hague, D. N. (1971). *Fast Reactions*. Wiley-Interscience,
London. 159 pp.
- Harrison, B. D., Finch, J. T., Gibbs, A. J., Hollings, M.,
Shepherd, R. J., Valento, V., and Wetter, C. (1971).
Sixteen groups of plant viruses. *Virology* 45, 356-363.

- Hatefi, Y., and Hanstein, W. G. (1969). Solubilization of particulate proteins and non-electrolytes by chaotropic agents. *Proc. Natl. Acad. Sci. U.S.A.* 62, 1129-1136.
- Hayatsu, H., Wataya, Y., Kai, K., and Iida, S. (1970). Reaction of sodium bisulfite with uracil, cytosine and their derivatives. *Biochemistry* 9, 2858-2865.
- Hiebert, E. (1970). Some properties of papaya mosaic virus and its isolated constituents. *Phytopathology* 60, 1295.
- Horne, R. W., and Pasquali-Ronchetti, I. (1974). A negative staining-carbon technique for studying viruses. *J. Ultrastruct. Res.* 47, 361-383.
- Horne, R. W., Hobart, J. M., and Pasquali-Ronchetti, I. (1975). Applications of the negative staining-carbon technique to the study of virus particles and their components by electron microscopy. *Micron* 5, 233-261.
- Jencks, W. P. (1969). *Catalysis in Chemistry and Enzymology*. McGraw-Hill, New York. 644 pp.
- Jonard, G., Briand, J. P., Bouley, J. P., Witz, J., and Hirth, L. (1976). Nature and specificity of the RNA-protein interactions in the case of the tymoviruses. *Phil. Trans. Roy. Soc. Lond. Ser. B.* 276, 123-129.

- Kaftanova, A. S., Kiselev, N. A., Novokov, V. K., and Atabekov, J. G. (1975). Structure of products of protein reassembly and reconstruction of potato virus X. *Virology* 65, 283-287.
- Kaper, J. M. (1975). *The Chemical Basis of Virus Structure, Dissociation and Reassembly*. North-Holland Research Monographs, Frontiers of Biology, Vol. 39. Edited by A. Neuberger and E. L. Tatum. American Elsevier. New York. 485 pp.
- Kushner, D. (1969). Self-assembly of biological structures. *Bacteriol. Rev.* 33, 302-345.
- Lauffer, M. A. (1975). *Entropy-Driven Processes in Biology: Polymerization of Tobacco Mosaic Virus Protein and Similar Reactions*. Molecular Biology, Biochemistry and Biophysics series, Vol. 20. Edited by A. Kleinzeller, G. F. Springer, and H. G. Wittman. Springer-Verlag, New York. 264 pp.
- Lauffer, M. A., and Stevens, C. L. (1968). Structure of the tobacco mosaic virus particle; polymerization of tobacco mosaic virus protein. *Adv. Virus Res.* 13, 1-63.
- Matthews, R. E. F. (1966). Reconstitution of turnip yellow mosaic virus RNA with TMV protein subunits. *Virology* 30, 82-96.

- McDonald, J. G., and Bancroft, J. B. (1977). Assembly studies on potato virus Y and its coat protein. *J. Gen. Virol.* 35, 251-263.
- McDonald, J. G., Beveridge, T. J. and Bancroft, J. B. (1976). Self-assembly of protein from a flexuous virus. *Virology* 69, 327-331.
- Moore, W. J. (1962). *Physical Chemistry*. Prentice-Hall, Englewood Cliffs, N.J. 844 pp.
- Morris, T. J., and Semancik, J. S. (1973). In vitro protein polymerization and nucleoprotein reconstitution of tobacco rattle virus. *Virology* 53, 215-224.
- Novikov, V. K., Kimaev, V. Z., and Atabekov, J. G. (1972). Rekonstruktsiia nukleoproteida virusa X kartofelia. *Doklady Akademii Nauk SSSR* 204, 1259-1263.
- Ohno, T., Yamaura, R., Kuriyama, K., Inoue, H., and Okada, Y. (1972a). Structure of N-bromosuccinimide-modified tobacco mosaic virus protein and its function in the reconstitution process. *Virology* 50, 76-83.
- Ohno, T., Inoue, H., and Okada, Y. (1972b). Assembly of rod-shaped virus in vitro: reconstitution with cucumber green mottle mosaic virus protein and tobacco mosaic virus RNA. *Proc. Natl. Acad. Sci. U.S.A.* 69, 3680-3683.

- Ohno, T., Takahashi, M., and Okada, Y. (1977). Assembly of tobacco mosaic virus in vitro: elongation of partially reconstituted RNA. Proc. Natl. Acad. Sci. U.S.A. 74, 552-555.
- Okada, Y. (1975). Mechanism of assembly of tobacco mosaic virus in vitro. Adv. Biophys. 7, 1-41.
- Okada, Y., and Ohno, T. (1972). Assembly mechanism of tobacco mosaic virus particles from its ribonucleic acid and protein. Mol. Gen. Genet. 114, 205-213.
- Oosawa, F., and Asakura, S. (1975). Thermodynamics of the Polymerization of Protein. Academic Press, New York. 204 pp.
- Purcifull, D. E., and Hiebert, E. (1971). Papaya mosaic virus. C.M.I./A.A.B. Descriptions of Plant Viruses No. 56.
- Record, M. T. Jr., Lohman, T. M., and de Haseth, D. (1976). Ion effects on ligand-nucleic acid interactions. J. Mol. Biol. 107, 145-158.
- Reichmann, M. E., and Stace-Smith, R. (1959). Preparation of infectious ribonucleic acid from potato virus X by means of guanidine hydrochloride denaturation. Virology 9, 710-712.
- Richards, K. E., and Williams, R. C. (1972). Assembly of tobacco mosaic virus in vitro: Effect of state of polymerization of the protein component. Proc.

- Natl. Acad. Sci. U.S.A. 69, 1121-1124.
- Robinson, D. J., Hutcheson, A., Tollin, P., and Wilson, H. R. (1975). A double-helical structure for reaggregated protein of narcissus mosaic virus. *J. Gen. Virol.* 29, 325-330.
- Schrämm, G. (1947). Über die spaltung des tabakmosaikvirus und die wiedervereinigung der spaltstücke zu hönermolekularen proteinen. II. Versuch zur wiedervereinigung der spaltstücke. *Z. Naturforsch.* 2b, 249-257.
- Shoemaker, D. P., and Garland, C. W. (1962). *Experiments in Physical Chemistry*. McGraw-Hill, New York, pp. 30ff.
- Stevens, C. L., and Lauffer, M. A. (1965). Polymerization-depolymerization of tobacco mosaic virus protein IV. The role of water. *Biochemistry* 4, 31-37.
- Stubbs, G., Warren, S., and Holmes, K. (1977). Structure of RNA and RNA binding site in tobacco mosaic virus from 4-Å map calculated from X-ray fibre diagrams. *Nature* 267, 216-221.
- Stussi, C., Lebeurier, G., and Hirth, L. (1969). Partial reconstitution of tobacco mosaic virus. *Virology* 38, 16-25.
- Sugiyama, T. (1966). Tobacco mosaic viruslike rods formed by "mixed reconstitution" between MS2 bacteriophage ribonucleic acid and tobacco mosaic virus protein.

Virology 28, 82-96.

- Weber, K., and Osborne, M. (1969). The reliability of molecular weight determinations by dodecyl sulfate-polyacrylamide gel electrophoresis. *J. Biol. Chem.* 244, 4406-4412.
- Wilson, T. M. A., Perham, R. N., Finch, J. T. and Butler, P. J. G. (1976). Polarity of the RNA in the tobacco mosaic virus particle and the direction of protein stripping in sodium dodecyl sulphate. *FEBS Lett.* 64, 285-289.
- Zimmern, D. (1976). The region of tobacco mosaic virus RNA involved in the nucleation of assembly. *Phil. Trans. Roy. Soc. Lond. Ser. B.* 276, 189-204.
- Zimmern, D. (1977). The nucleotide sequence at the origin for assembly on tobacco mosaic virus RNA. *Cell* 11, 463-482.
- Zimmern, D., and Butler, P. J. G. (1977). The isolation of tobacco mosaic virus RNA fragments containing the origin for viral assembly. *Cell* 11, 455-462.